TECHNICAL REPORT TL-77-3

A MULTIPLE ROCKET LAUNCHER SIMULATION–REPORT II

U.S. ARMY
MISSILE
RESEARCH
AND
DEVELOPMENT
COMMAND

Ground Equipment and Missile Structures Directorate
Technology Laboratory

23 February 1977

Redstone Arsenal, Alabama 35809

DISPOSITION INSTRUCTIONS

DESTROY THIS REPORT WHEN IT IS NO LONGER NEEDED. DO NOT RETURN IT TO THE ORIGINATOR.

DISCLAIMER

THE FINDINGS IN THIS REPORT ARE NOT TO BE CONSTRUED AS AN OFFICIAL DEPARTMENT OF THE ARMY POSITION UNLESS SO DESIGNATED BY OTHER AUTHORIZED DOCUMENTS.

TRADE NAMES

USE OF TRADE NAMES OR MANUFACTURERS IN THIS REPORT DOES NOT CONSTITUTE AN OFFICIAL INDORSEMENT OR APPROVAL OF THE USE OF SUCH COMMERCIAL HARDWARE OR SOFTWARE.

REPORT DOCUMENTATION PAGE

READ INSTRUCTIONS BEFORE COMPLETING FORM

1. REPORT NUMBER: TL-77-3	2. GOVT ACCESSION NO.
3. RECIPIENT'S CATALOG NUMBER	
4. TITLE (and Subtitle): A MULTIPLE ROCKET LAUNCHER SIMULATION - REPORT II	5. TYPE OF REPORT & PERIOD COVERED: Technical Report
6. PERFORMING ORG. REPORT NUMBER: TL-77-3	
7. AUTHOR(s): Dean E. Christensen and Robert L. Richardson	8. CONTRACT OR GRANT NUMBER(s)
9. PERFORMING ORGANIZATION NAME AND ADDRESS: Commander, US Army Missile Research and Development Command, Attn: DRDMI-TL, Redstone Arsenal, Alabama 35809	10. PROGRAM ELEMENT, PROJECT, TASK AREA & WORK UNIT NUMBERS: (DA) 1W362303A214, AMCMS Code 63230321416.11
11. CONTROLLING OFFICE NAME AND ADDRESS: Commander, US Army Missile Research and Development Command, Attn: DRDMI-TI, Redstone Arsenal, Alabama 35809	12. REPORT DATE: 23 February 1977
	13. NUMBER OF PAGES: 99
14. MONITORING AGENCY NAME & ADDRESS (if different from Controlling Office)	15. SECURITY CLASS. (of this report): Unclassified
	15a. DECLASSIFICATION/DOWNGRADING SCHEDULE

16. DISTRIBUTION STATEMENT (of this Report)

Approved for public release; distribution unlimited.

17. DISTRIBUTION STATEMENT (of the abstract entered in Block 20, if different from Report)

18. SUPPLEMENTARY NOTES

19. KEY WORDS (Continue on reverse side if necessary and identify by block number)

General support rocket systems
Error budget inputs
Launch effects

20. ABSTRACT (Continue on reverse side if necessary and identify by block number)

A multiple-launching simulation program was devised which fires rockets in real time from a multiple launcher mounted on a transporter. This simulator was used to establish error budget inputs for general support rocket systems. Comparisons of the launch effects on system accuracies for various size rockets were conducted. This program has provided a means whereby a

ABSTRACT (Continued)

ABSTRACT (Concluded)

launcher concept may be developed which can effectively reduce the errors due to rocket unbalance and thrust misalignment. This is a follow-on report to Technical Report RL-76-11; "Multiple Launcher Characteristics and Simulation Technique," February 1976.

23 February 1977

TECHNICAL REPORT TL-77-3

A MULTIPLE ROCKET LAUNCHER SIMULATION - REPORT II

Dean E. Christensen
Robert L. Richardson

DA Project No. 1W362303A214
AMCMS Code No. 63230321416.11

Ground Equipment and Missile Structures Directorate
Technology Laboratory
US Army Missile Research and Development Command
Redstone Arsenal, Alabama 35809

CONTENTS

I. INTRODUCTION

In the earlier report [1], a rudimentary insight into the mallaunch associated with multiple firings of free flight rockets was presented. An analog computer technique was set forth to be used as a tool for researching launch errors associated with multiple launchings. This analog model exhibited a resonant condition between the firing rate and the launcher's structural frequency. The structural frequency of the launcher increases as the mass is reduced by rocket removal during a ripple.

This report presents the work performed in expanding the model and exercising it to better understand the system errors associated with multiple launchings. This model shows that some launchers exhibit the ability to reduce the impact dispersion of free rockets due to rocket abnormalities such as thrust misalignment and mass unbalance. This was demonstrated by comparing the errors from the simulation of the launcher to those computed by a closed-form solution to Euler's equations of motion using an assumed "rigid" launch platform. Launchers which exhibit the ability to reduce impact dispersion caused by rocket thrust misalignment and mass unbalance respond to these forcing functions in a manner which imparts corrective attitudes and rates to the rockets at launcher release. The program provides the designer a method for designating launchers which detract from free flight rocket errors rather than adding a mallaunch condition.

In this report, the effects of the more significant forcing functions and design parameters on the launch conditions are presented. The analog model was updated, improved, and completed. All of the important or nonnegligible actions and reactions are included. The model now includes yaw and two degrees of freedom in pitch for the launcher. Each rocket fired has six degrees of freedom. The simulation runs in real time on an analog computer. To verify and validate the approach, initial runs were made using surface launched unit fuel air explosive (SLUFAE) launcher characteristics. The resulting launcher pitch and yaw rates as functions of time were compared to test data obtained from a rate gyro package. The results compared well within the assumptions required to model the SLUFAE geometry.

In support to the development of a General Support Rocket System (GSRS), a parametric investigation was undertaken. Parameters were used which were similar to those being considered in a GSRS. A 6-in. diameter rocket concept with 42 rockets on the launcher was the baseline. It was followed by an 8 1/2-in. diameter rocket with a 12-round launcher. Plans to include a 12-in. diameter rocket system were curtailed due to time and funding constraints. The 12-in. diameter results were estimated by extrapolation. The major thrust of the parametric investigation was to establish launcher design guidelines for the free flight rocket technology program. These guidelines and the questions which were answered are presented in the next section of this report.

II. ACCOMPLISHMENTS

The free flight rocket technology program raised several questions concerning launcher effects on system accuracy. The multiple launcher simulation program was established to assist in answering these questions. The more significant questions are:

a) What type of firing platform is best, a truck or a tracked vehicle?

b) Are outriggers or suspension lockouts required?

c) What effect does rocket spin rate at launch have on system accuracy?

d) Is a nontipoff launcher more desirable than a tipoff launcher?

e) How does the firing rate affect accuracy?

f) Is an active control system required for maintenance of aim?

g) What effect does thrust misalignment and rocket mass unbalance have on launch accuracies?

h) How does missile exhaust gas impingement on the launcher affect accuracy of ripple firings?

This investigation begins to answer most of these questions. Additional verification is required in some areas. The answers, at this time, are as follows:

a) Without suspension lockout or outriggers, a truck is a better launching platform than a tracked vehicle. Five-ton trucks have higher natural frequencies and larger sprung moments of inertia than tracked vehicles of similar payload capacities.

b) Suspension lockouts and/or outriggers are not required on the M811 truck series when launching large quantities of rockets from a single platform. Lockout is required to achieve similar accuracies from a tracked vehicle suspension. Outriggers are needed for concepts which have smaller quantities of larger rockets.

c) Selection of the proper rocket spin rate at launch can be very effective in controlling system dispersion. In general, higher spin rates reduce the dispersion caused by thrust misalignment, especially for nontipoff launchers. Lower spin rates reduce the effects of rocket mass unbalance. A parallel effort is being conducted to determine the effects of rocket flexibility on launch attitude and rate errors. Higher spin rates appear to produce errors caused by the bending of long slender rockets while constrained on the launcher.

d) Tipoff launchers show a large reduction in the initial flight dispersion errors if the spin rate at launch is low (below 9 rps). This is due to longer launcher guidance periods where the rockets are forced to rotate about their rear support points rather than their centers of mass. The rocket's inertia is greater about the rear supports which reduces the dispersion due to thrust misalignment. At low spin rates the effects of rocket mass unbalance is reduced. The attitude rates and dispersions induced by tipoff are reproducible and can be nullified by initial aim changes. The possibility of a simple, low cost, smooth bore tube, tipoff launcher achieving low dispersions appears achievable if low spin rates at launch are acceptable.

e) Firing rates are critical in the reduction of dispersion. Optimum rates can be achieved in excess of one rocket per second. The present technique of establishing a firing rate is to have it sufficiently low to allow structural damping to occur. Results of the simulation show that the rate can be increased if resonance with the launcher's structure is avoided. The analog simulation program is a design tool which can be used to avoid resonant conditions between spin rate, structural frequencies and firing rates. This problem is complex for multiple rocket launchers where the structural frequencies are changing during a ripple sequence due to mass reduction.

f) The simulation program demonstrates that an active control system is not necessary for maintenance of launcher stability. Proper selection of launcher geometry and stiffness will produce a launcher which is a passive control system for the rockets. The launcher can be made to reduce the errors due to thrust misalignment and rocket mass unbalance.

g) Thrust misalignment and rocket mass unbalance are the random forcing functions which produce random launch accuracies. A properly designed launcher can sense these conditions and respond to them in a manner which will induce rocket motions at release, which are out of phase, and, hence, provide corrective action.

h) The program includes the effect of rocket exhaust gas impingement on the launcher and transporter. Preliminary results show that this problem is not as great as it was once thought to have been. This forcing function is reproducible and can be utilized to control launcher motions. It is one of the main considerations in the selection of a firing order.

The major accomplishment of this portion of the free flight rocket technology effort is that it has provided a tool for use in defining the launcher's effect on system dispersion. By comparing the simulation results to the closed-form solutions for a rigid launcher, the added or subtracted dispersion due to the launcher can be obtained. The curves showing the results of the simulation include the results from the closed-form solutions for a rigid launcher. The rigid launcher solutions provide the attitude and rate errors at tube exit due to the

rocket effects caused by thrust misalignment and mass unbalance. Other launcher errors such as tube or rail clearances and straightnesses, round to round alignment, and aiming inaccuracies must be superimposed into overall error budgets. An example of this is presented in Table 4. This table presents the errors which are associated with the concepts which have been analyzed to date.

The limited sample size of two concepts with some data from a 12.2-in. diameter rocket simulation, SLUFAE, and the multirail test programs should be considered when determining the confidence of the answers presented. As additional work is performed, the confidence will increase. It is recommended that the effort on flexible rocket work be incorporated along with additional simulations of other multiple rocket launcher concepts. Any test results and future test programs should be utilized for verification and understanding of the simulation results.

III. MODEL DESCRIPTION

The simulation program is based on a mathematical model which has evolved over a period of several years. More complex models have been tried whose results did not merit their added complexity. The model and its equations used for this study provide for all the major or gross motions involved in a rocket launcher which affect the rocket's accuracy.

Figure 1 is a description of the model. Each rocket has six degrees of freedom. In Figure 1, x is the down range distance along the flight path and y and z are the normal or transverse displacements of the rocket. θ is the rocket's pitch attitude, ψ is the yaw attitude, and γ is the roll angle. Small angle theory has been applied to θ and ψ.

The launcher has two degrees of angular freedom about an assumed instantaneous center of rotation; η is the pitch attitude of the vehicle or base structure and λ is its yaw attitude. The instantaneous center of rotation is located at the vehicle's pitch center.

A third degree of angular freedom is required for the launcher to account for the relative motion in pitch between the base and the tipping parts or pod. This angle is defined as ϕ; the rotation is with respect to the elevation trunnion.

For a multiple launching program where several rockets are launched in one sequence, a real time simulation is necessary. Ripple firing durations of 1 minute in length are not uncommon. To keep track of the various motions which have frequencies in cycles per second by numerical methods would be expensive in terms of computer time. The rapid output of large quantities of data is required. These considerations dictated the use of an analog computer for solving the equations. An EAI 681 analog system was available, and the problem and model were sized to fit on this system. Considerable digital logic was involved in the simulation

of the intervalometer (sequence timer) and in varying the parameters for each rocket. The launcher's mass and inertia characteristics had to change continuously. Exhaust impingement forces and their moment arms change as a function of the firing order. The program was configured to allow the firing rate to be readily changed. It is more difficult to change the firing order. Various launcher concepts can be handled; however, differences in concepts require modifications to the model. Fast turnaround time from one concept to another is not available. It may take hours or days to change concepts. The big advantage in the approach is its real time capability after it has been implemented. Parameters can be varied within limits by changing potentiometer settings. Parametric studies involving the firing of several thousand rockets per day can be achieved. Any of the time-varying functions and their derivatives can be monitored. Data can also be reduced in real time by analog means prior to recording.

Many simulation programs have been developed which were never used to perform parametric studies. They are too complex and require lengthy computer runs and time-consuming data reduction. The model developed for multiple launchers was a tradeoff between complexity and operational versatility. To achieve a simulation program which could be used for parametric analyses with the computing equipment available, some limitations were imposed. These limitations and assumptions will now be discussed.

Launcher roll has not been incorporated into the model. Roll effects are not directly effective in downrange dispersion. Roll must be coupled into pitch and yaw to be effective. The small pitch and yaw rates associated with a relatively massive multiple launcher restrict this coupling to a minimum. Its effects are lost in the gross motion associated with the rocket's flight.

Cross products of launcher inertia produce a pitch-yaw coupling of the launcher motion. The cross products of inertia have been assumed to be zero for this model. This assumption is valid only for symmetric firing positions and orders. Rockets are fired from the pod in a preselected manner to maintain pod balance. In the design of a system this would be accomplished for the purpose of reducing the launcher motions due to coupling. The other symmetric condition imposed is not readily dismissed. The system must be fired from a symmetric base. In the case of a vehicle-mounted launcher the simulation is more exact for firing directly over the vehicle centerline, probably over the cab. To remove this restriction, more analog equipment would be needed. The increased launch errors caused by various azimuth positions have not been determined. The restriction of over-the-cab firing is not a major limitation. Each concept simulated has been compared on a relative basis. Azimuth settings off the vehicle centerlines should have equivalent effects for each concept. Future effort should be directed towards the addition of off-center firing positions. Results from the simulation are without this coupling and represent over-the-cab firings.

Rocket dynamic unbalance produces a rocket fixed torque proportional to the spin rate. Thrust misalignment also produces a rocket fixed torque; it is proportional to the thrust. Sufficient analog equipment was not available to include both effects simultaneously. The closed-form solutions obtained from Euler's equations show that the thrust misalignment term is the larger term during the phase when the rocket is thrusting and spin is being induced. All of the results obtained from the simulation are for thrust misalignment only. On curves where comparisons are made, the same values for thrust misalignment were used for the simulated results and the Euler's solutions. This allows meaningful comparisons to be made. The analog techniques are described in a report by Christensen [1]. A complete analog diagram is included as an enclosure. The equations of motion are presented in Appendix A.

In summary, the model was established to answer specific questions concerning multiple launchers. It was configured to accomplish this end with the equipment available. The accomplishments achieved were presented in Section II. More detailed results are included in Section VI.

IV. A CLOSED-FORM SOLUTION

To determine if a launcher is contributing to system dispersion or detracting from the rocket-induced dispersion, a method of measure or comparison was required. The following equations were derived by Dr. John Cochran, Auburn University, for this purpose. These equations represent the solution to Euler's equations for a free flight rocket. These simplified equations were derived from work accomplished previously by Dr. Cochran under an Army contract with the US Army Research Office, Grant DAHC04-75-0034 [2].

The solution is valid for rockets in free flight prior to the time aerodynamic forces become significant. They are valid only for nontipoff rigid launchers where zero launch attitudes and rates are assumed. It is also assumed that no interference occurs between the rocket and the launcher after release. Free flight time in the tube for the 6-in. rocket is 0.0339 sec. The parameters are defined and the equations are presented in this section for the closed-form solution. Phi and its derivative with respect to time are the angular attitude and rate, respectively, of the rocket relative to its initial aim axis. These equations were programmed on a calculator-plotter. Values were used as presented in Section V and typical results were plotted. These plotted curves are presented in Figures 2 through 7. The relative effects of thrust misalignment and rocket dynamic unbalance on rocket motions during the initial phase of the trajectory are shown.

For the rocket parameters used, Figure 4 indicates that an optimum spin rate at launcher release would be nearly 30 rps. The actual rate used for design of a real system would be considerably less due to the addition of other effects such as launcher deflections and rocket bending. Many other items also enter into this determination. They include aerodynamic effects and propulsion characteristics such as burn times and thrust profiles. The time of release and time of flight are very significant. The entire system from ignition to impact must be studied as a unit in order to select an optimum spin rate.

The last two figures in this section (Figures 6 and 7) show the comparisons of the 6- and 8.5-in. concepts. The thrust misalignment and dynamic unbalance effects have been separated. Rockets currently manufactured have thrust misalignments on the order of 1 mil. Rockets can be dynamically balanced to less than 0.1 mil which would reduce the values shown on the curves. The dispersions presented are angular and could apply to pitch or yaw.

p	Spin rate (rad/sec)
I_A	Rocket's axial moment of inertia (slug-ft^2)
I_T	Rocket's transverse moment of inertia (slug-ft^2)
T	Thrust
d	Distance from CG to nozzle (ft)
$t(\Delta t)$	Time from perfect release to handover (sec)
α	Angular thrust misalignment (rad)
μ	Angular misalignment of the principal longitudinal axis of inertia (rad)*
2Φ	Total transverse angular dispersion (rad)
$2\dot{\Phi}$	Total transverse angular rate dispersion (rad/sec)

*Dynamic unbalance

Note: these solutions are not valid for zero spin rates.

$$n = \frac{I_T - I_A}{I_T} p$$

$$\Phi = \left[\propto \frac{Td}{pnI_T} + \mu \right] \sqrt{(\sin pt - pt)^2 + (\cos pt - 1)^2}$$

$$\dot{\Phi} = \left[\propto \frac{Td}{nI_T} + \mu p \right] \sqrt{2(1 - \cos pt)}$$

V. PHYSICAL PARAMETERS

This section describes the systems which were simulated and the values used to compute the closed-form solutions. The input data presented were used to scale the analog equations and obtain the potentiometer settings contained in Appendix B. The 6-in. diameter rocket and the corresponding 42-round launcher were used as the baseline and are depicted on the analog schematic.

Table 1 presents the rocket parameters which were used along with the range of spin rates considered. Table 2 presents the basic launcher parameters which were considered. The firing rates were varied as shown on the curves in the results section. The nominal firing rate for the 6-in. diameter rocket system was two rockets per second. For the 8.5-in. diameter rocket system, the nominal rate was one rocket per second.

Table 3 lists the transport vehicle characteristics. Data were readily available for the 5-ton truck and were used as the baseline. The vehicle's natural frequencies were varied to make it possible to determine how any type vehicle would react. Known frequencies for various vehicles are indicated and are presented in Section VI.

The 12-in. diameter rocket was not simulated in detail. Estimates for the performance of the 12-in. rocket were obtained by interpolation. The 12-in. input data are presented and included as a reference for future investigations.

Figure 8 shows the definitions of important dimensions and forces for a typical rocket in the simulation. Figure 9 gives the definitions of relevant dimensions, forces, and natural frequency values for the launcher, launcher base or transport vehicle, and the rocket in its initial launch position.

An n-dimensional parametric study was undertaken. Figure 10 shows the parameters which had a major contributing effect on the launching system. Each of these parameters was varied independently in a systematic manner around the nominal value to assess its effect on performance. The performance was measured by recording the rockets' attitudes and angular rates as they left the launcher. Each of these parameters was varied over practical ranges for which a system would be designed.

The quadrant elevation (QE) of the firings was held constant at 45 deg. During the design of elevation drive systems, a flat curve of elevation stiffness versus QE is desired. If the stiffness of the elevation drive system varies with QE, this effect on dispersion will be related to the effects presented as a function of the pod-to-launcher frequency or stiffness. This parameter was varied and the results are presented. Figure 11 is a graph showing the exhaust impingement forces on the launcher as a function of rocket travel. These forces were estimated from thrust levels and experience from measurements made on other systems. Curve A was the nominal curve used for the 6-in. diameter rocket simulation. For the 8.5-in. diameter rocket, all four force curves were used and the results were compared to find the effect of variations in exhaust gas impingement levels. The exhaust force was labeled F_E, and it represents the effective force applied at the centroid of the exhaust impingement with a corresponding moment arm R_E as shown on Figure 9.

Figure 12 shows how thrust misalignment and mass offset were incorporated in the simulation. Only one random number generator was available. It was used to generate random values for r_1. The initial location for the thrust misalignment plane (γ_0) was also randomly selected. The magnitudes of r_1 and r_2 which were used, represent the present state-of-the-art in rocket manufacture. The nominal values for the 6-in. diameter rocket are shown on the figure: $r_1 = \pm 0.009$ ft, $r_2 = 0.01$ ft. For the 8.5-in. rocket, the nominal values are: $r_1 = \pm 0.013$ ft, $r_2 = 0.011$ ft.

This section of the report has presented the nominal parameters which were used and has provided a description of those parameters. The next section will present the results obtained from the parametric investigation.

VI. RESULTS

The results presented in this section are in the form of parametric curves. These curves were used to obtain the information discussed in Section II. The curves exhibit the resonant conditions occurring between various parts of the structure and rocket spin.

To obtain the effectiveness of a given launcher, data points from the closed-form solution (Section IV) were placed on each set of curves. These data points are described by a circular symbol. The simulated results for nontipoff launchers are indicated by square symbols. The data points simulated for the tipoff launchers are indicated by triangular symbols. Curves on the same graph are for the same system parameters unless otherwise indicated. Parameters which are not labeled on the curves are the nominal values as presented in Section V.

The X-marked symbols, obtained from the closed-form solutions, represent rocket-induced launch dispersion at tube exit. This solution assumes no launcher motion and a nontipoff launch condition. The errors are a result of the rocket's flight between release and exit from the launcher. During this portion of the flight, the rocket's velocity is low and aerodynamic effects can be neglected. It has been assumed that the launcher has been properly designed and that "blow-by" exhaust effects are not present. An additional assumption of no launcher-rocket interference has been made. Launchers should always be designed such that no rocket interference occurs during this portion of the flight.

The results obtained from the simulation include the effects of launcher motion caused by launcher-rocket interactions and exhaust impingement on the structure. The motion was tracked in real time for ripple firings. Attitudes and angular rates for each rocket were recorded as the rear of the rocket passed the forward edge of the launcher structure. Several ripples were repeated and superimposed to obtain a maximum dispersion for each data point.

Sufficient runs were made in an attempt to obtain the maximum dispersion. It has been assumed that this approximates a 3σ value. It is the total amplitude of the dispersion. These values were divided by two to obtain the half amplitude data. Assuming that the dispersion errors have a normal distribution, a 1σ value was estimated by dividing by three. These estimated 1σ half amplitude values are shown as ordinate scales on the right side of most curves.

Examples of the raw data, as recorded directly from the simulation, are shown in Appendix C. The spread on total dispersion was recorded in a laboratory notebook. These tables are reproduced and recorded in Appendix C. A calculator-plotter combination was then used to plot the data points on the curves presented in this section. Lines connecting these data points were added.

On some of the original attitude curves there was a bias due to rocket weight removal from the launcher. This bias can be controlled by proper geometric considerations. Runs were made with changes in launcher geometry and the direction and slope of the bias was changed. To expedite the parametric study, no attempt was made to optimize the launcher geometry. The bias was stripped from the data. Resonant points

can be seen on many of the curves. All possible combinations of parameters were not used in the parametric study. Specific needs can be addressed in future efforts for particular concept investigations aimed at given system requirements.

If the simulated curves fall below the computed curves, then the launcher is detracting from the rocket-induced errors and the launcher is performing its intended function. If the simulated data are above the computed data, then the launcher is adding to the rocket-induced errors and a mallaunch condition exists. The simulated curves contain the total system dispersion at launcher exit for an assumed rigid rocket.

Table 4 presents an error budget for the systems which were investigated. The errors were computed for the nominal sets of parameters. The simulation results which were used are for nontipoff launchers. The errors are approximately the same for tipoff launchers at the nominal 9-rps spin rate which was used. The first sheet of the table presents the conditions and times involved. The rocket velocities at launcher exit are presented. The second sheet shows all the error sources including launcher manufacturing tolerance effects caused by rocket-to-rocket initial alignment, tube or rail straightness, and rocket-to-launcher clearances. Initial aiming and target location errors are not included. For the smaller diameter rockets, the launchers are detracting from the rocket-induced errors. For the 12.2-in. diameter rockets, the launcher is adding a mallaunch error. The errors presented are the angular deviations and rates from the intended initial aim axis for a ripple launch. The launcher control values are half amplitude 1σ values. If the input values of 0.2 mil for dynamic unbalance and 1 mil for thrust misalignment are realistic 1σ values, then the total errors are realistic.

For the 6-in. diameter rocket results shown on Figures 13 through 27, the nominal value for the maximum mass offset (r_1) is ± 0.009 ft and the nominal thrust misalignment (r_2) is 0.01 ft. To obtain the 3.45 mils for the maximum thrust misalignment, r_1 and r_2 were added and divided by the distance from the nozzle to the rocket CG (5.5 ft). For the 8.5-in. rocket, the maximum value was ± 0.013 ft for r_1 and 0.011 ft for r_2. These values made the maximum nominal value of angular thrust misalignment for the 8.5-in. diameter rocket 3.45 mils. This angular value was the same for both rockets to allow comparisons to be made. Assuming a normal distribution for the thrust misalignment, its 1σ value would be approximately 1.15 mils. Parametric curves are included which show the effects of varying the maximum angular thrust misalignment (Figures 26 through 35).

Figures 13 through 16 show the rockets' pitch and yaw attitudes and rate dispersions for the 6-in. and 8.5-in. rocket systems versus rocket spin rate at release. In general, the 8.5-in. rocket dispersion is greater than that of the 6-in. rocket. The tipoff launcher provides the smallest errors at low spin rates. Resonant conditions can be seen on the curves.

Figures 17 and 18 show the effects of the launcher's structural stiffness in pitch of its elevating system. This stiffness is represented by the loaded natural frequency of the pod with respect to the base. For the 6-in. diameter rocket system, a 5-Hz loaded pod natural frequency corresponds to the same stiffness as a 9.1-Hz empty pod natural frequency. For the 8.5-in. rocket system, the 5-Hz loaded natural frequency corresponds to a 7.55-Hz empty frequency. The loaded pod natural frequency for the SLUFAE launcher is indicated on the graphs. It represents the highest practical value which can be obtained for a mobile field army system with current technology in structural design.

Figures 19 and 20 show the effect of the transport vehicle's pitch frequency. The 8.5-in. diameter system has higher dispersion than the 6-in. diameter system. The frequencies of three army transport vehicles are indicated.

Figure 21 shows the effect of the system's yaw natural frequency for the 6-in. diameter system. A 6-Hz loaded pod natural frequency corresponds to a 6.62-Hz empty pod natural frequency. The vehicle and launcher are rigidly attached in yaw by a wide elevation trunnion. Both bodies act as unit, and only only one degree of freedom is required to describe the yaw motion.

Figures 22 and 23 show the effects of guidance length on dispersion for the 8.5-in. diameter system using exhaust configuration D. The dispersion decreases as the guidance length increases. It must be remembered that there is a practical limit placed on guidance length by system geometrical considerations. The nominal values used (4 ft for the 6-in. diameter, 5 ft for the 8.5-in. diameter rocket) are approaching the upper practical limits for the systems simulated.

Figures 24 and 25 show that the firing interval has little effect on dispersion for attitudes except at resonance points. The curves for rate dispersions are flat. Figures 26 and 27 indicate how thrust misalignment affects dispersion. The angular values for the thrust misalignment are a result of combining r_1 and r_2.

Figures 28 through 35 were plotted with a more realistic value for mass offset of 0.0013 ft. The maximum random thrust misalignment (r_2) was varied to obtain these curves. These curves were run for a nontipoff ripple launching of twelve 8.5-in. diameter rockets launched at various spin rates. The highest or worst case of exhaust gas impingement was used. The bias on pitch attitudes caused by launcher relaxation producing an aim change was not stripped from the data. Its effects can be seen by the large values of pitch attitudes which result from the simulation. These values can be reduced by proper geometric considerations during design. The effects of launcher relaxation can also be compensated for by aim changes or boresight considerations. The slope of these pitch attitude curves is significant and it is less than the rocket-only data.

Also, on Figures 28 through 35, the rocket only data were obtained from the closed-form solution, and these can be considered to be either pitch or yaw data because the launcher is assumed to be rigid. The ordinate intercepts show the residual errors contributed by the launcher when a perfect rocket is used with zero thrust misalignment and only 0.0013 ft of mass offset. These particular curves were requested by and presented to the GSRS office.

Figures 36 and 37 show how various exhaust gas impingement profiles effect dispersions in pitch and yaw for the 8.5-in. diameter rocket system. (For the profiles, see Figure 11.) The worst case was considered to be profile D. A realistic profile is considered to be C. The 6-in. diameter rocket system would exhibit the same general characteristics as the 8.5-in. data. The variations in exhaust profiles have little effect except for pitch attitude dispersions. These results are based on a preselected firing order. Rockets were fired alternately from each side of the pod, from outboard to inboard, and from top to bottom of the pod.

The data presented have been limited. Due to the large number of parameters involved, all possible comparisons are not shown. Only the more significant findings to date were presented. Other data were gathered during the establishment of the simulation. Future efforts can be established to generate data for answering specific questions and obtaining trends for various effects. The conclusions made from the data are presented in Section II.

VII. RECOMMENDATIONS

The work presented in this report is one portion of the work required for a complete simulation of a multiple free-flight rocket system. Ongoing parallel efforts on the flexible rocket effects on launch accuracies of free flight rockets can be coupled to this work. Additional programs covering the trajectories of free-flight rockets are available and can be updated to include multiple firings. Existing equipment in the Advanced Simulation Center of the Technology Laboratory of the US Army Missile Research and Development Command could then be used for a complete simulation of multiple rocket systems from ignition to impact. This would provide a means for accurately predicting impact dispersions and a method for conceiving systems with desired impact patterns. Real time simulations of this nature would result in considerable savings in development time and dollars. It would minimize the number of hardware trials and modifications.

A complete real time simulation of a multiple free-flight rocket system would benefit the current developmental effort of the GSRS. Another program which would benefit is the Armor Defeating Aerial Rockets System. For this system an additional simulation would be required for

the helicopter. Present work in the Ground Equipment and Missile Structures Directorate includes analog simulation of launcher motion on the external stores of a helicopter. This program could be modified and mated with the multiple launching simulation effort.

The Ground Equipment and Missile Structures Directorate is currently ready to undertake a program of this scope. It is recommended that a systems approach be taken and that a complete simulation be devised. The benefits to be gained from such an endeavor are numerous.

TABLE 1. ROCKET CHARACTERISTICS

Diameter (in.)	6	8.5	12.2
Weight (lb)	175	450	1170
Length (in.)	96	150	177
Support (CG to forward support - d_1, in.)	6	12	-6
Locations (CG to aft support - d_2, in.)	66	84	84
Nozzle to CG - d_4 (in.)	66	84	84
Maximum thrust - τ_{max} (lb)	9500	34,000	83,000
Thrust rise time - t_1 (sec)	0.010	0.025	0.025
Transverse moment of inertia - I_T (slug-ft^2)	37	180	592
Roll moment of inertia - I_R (slug-ft^2)	0.175	1.0	5.62
Maximum thrust misalignment - r_2 (ft)	0.01	0.011	0.011
Maximum mass unbalance - r_1 (ft)	0.01	0.013	0.013
Spin rate ranges (rps)	0 to 15	0 to 15	0 to 15

TABLE 2. LAUNCHER CHARACTERISTICS

Rocket diameter (in.)	6	8.5	12.2
Number of rockets/number of pods	42/1	12/2	4/1
Natural frequency of the tipping parts with respect to the base (Hz)			
Loaded	3.7	3.5	3.4
Empty	8	5.3	6.0
Total launcher weight/weight of tipping parts - loaded (lb)	12,000/9100	16,000/10,000	
Pitch inertia of the tipping parts with respect to the trunnion (slug-ft^2)			
Loaded	14,000	16,000	15,000
Empty	3000	7000	7000
Yaw inertia of the tipping parts with respect to the CG at 0 deg QE (slug-ft^2)			
Loaded	4400	5200	5600
Empty	1000	2600	2900
Launcher geometry (in.) start/increment/end			
a_1	72	72	72
b_1	12	27	36
a_2	60	72	80
b_2	48	16	22
d_5	48	60	102
d_6	72/12/12	23/12/11	36/26/10
d_7	0	0	0
d_8	1080	960	960
d_9	±36/12/0	±35/12/11	±30
Time-Δt-end of guidance to tube exit (sec)	0.034	0.039	0.029
Stiffness-K (ft-lb/rad)	7.58×10^6	7.74×10^6	7.70×10^6
Damping-C (ft-lb-sec/rad)	6.5×10^4	7.04×10^4	7.06×10^4

TABLE 3. TRANSPORT VEHICLE CHARACTERISTICS

Vehicle		M811 5-Ton Truck	M548 Tracks	MICV Cargo Tracks
Maximum off road payload (lb)		15,000	12,000	23,000
Sprung mass natural frequencies about the sprung CG without the payload (Hz)				
Pitch		3.52	1.91	1.59
Yaw		5.00	4.00	2.60
Roll			4.00	1.95
Heave		2.90	2.74	1.75
Pitch about the pivot		2.75	1.78	1.48
Sprung mass (slug)		435		690
Sprung mass moments of inertia without the payload about the sprung CG (slug-ft^2)				
Pitch		12,000	8825	16,000
Yaw		14,000	10,100	18,000
Roll			2367	
Pitch about the pivot		19,700		18,500
Suspension system's damping factor ($\xi = C/C_c$)				
Pitch		0.1	0.083	
Yaw				
Roll				
Heave				
Dimensions or locations (ft) X - longitudinal Y - vertical Z - lateral (on centerline)				
From the centerline of the front road wheel to the unloaded sprung CG	X	81.4		54
	Y			15
From the unloaded sprung CG to the probable trunnion centerline	X	120		114
	Y			48
From the unloaded sprung CG to the estimated pivot	X	46		42
	Y			15
	K_B	5.867×10^6		1.60×10^6
	C_B	6.8×10^4		
	K_Y	1.974×10^7		
	C_Y	1.25×10^5		

TABLE 4. ERROR BUDGETS AT LAUNCHER EXIT FOR MULTIPLE LAUNCHING SYSTEMS

Inputs									
Rocket Diameter (in.)	No. of Rockets	Weight (lb)	Thrust Level (lb)	G's	Thrust Rise Time	Guidance Length (ft)	Tube Length (ft)	Time at EOG (sec)	Time at Tube Exit (sec)
6	42	175	9500	54	0.01	4.0	9.0	0.0725	0.1064
8.5	12	450	34,000	75.5	0.025	5.0	13.0	0.0777	0.1165
12.2	4	1170	83,000	71	0.025	8.5	15.0	0.096	0.1250

Rocket Diameter (in.)	Rocket Velocity (ft/sec)	Rocket Velocity (ft/sec)	Spin Rate at EOG (rps)	Spin Rate at Tube Exit (rps)	Rockets Axial I ($slug\text{-}ft^2$)	Rockets Transverse I ($slug\text{-}ft^2$)
6	118	177	9	9.0	0.175	37
8.5	159	253	9	9	1.0	180
12.2	190	280	10	10	5.62	592

Rocket Diameter (in.)	Distance Nozzle to CG (ft)	Distance Front Support (ft)	Distance Rear Support (ft)	Length to Diameter Ratio
6	5.5	0.5	5.5	16.0
8.5	7.0	1.0	7.0	17.6
12.2	7.0	-0.5	7.0	14.5

TABLE 4. (Concluded)

Results						
Attitudes (mils)						
Rocket Diameter (in.)	Launcher Tolerances	0.2-mil Dynamic Unbalance	1-mil Thrust Misalignment	RSS	Launcher Control	Total Error (1σ)
6.0	0.083	0.331	0.735	0.810	-0.129	0.681
8.5	0.100	0.421	0.875	0.976	0.421	1.40
12.2	0.117	0.303	0.380	0.500	1.50*	2.00
Rates (mils/sec)						
6.0	6.57	18.51	41.07	45.52	-9.18	36.35
8.5	6.67	20.13	41.86	46.93	-3.01	43.92
12.2	9.74	19.86	24.92	33.32	10.0*	43.32

*These values have been estimated by extrapolation and a minimum number of analog runs.

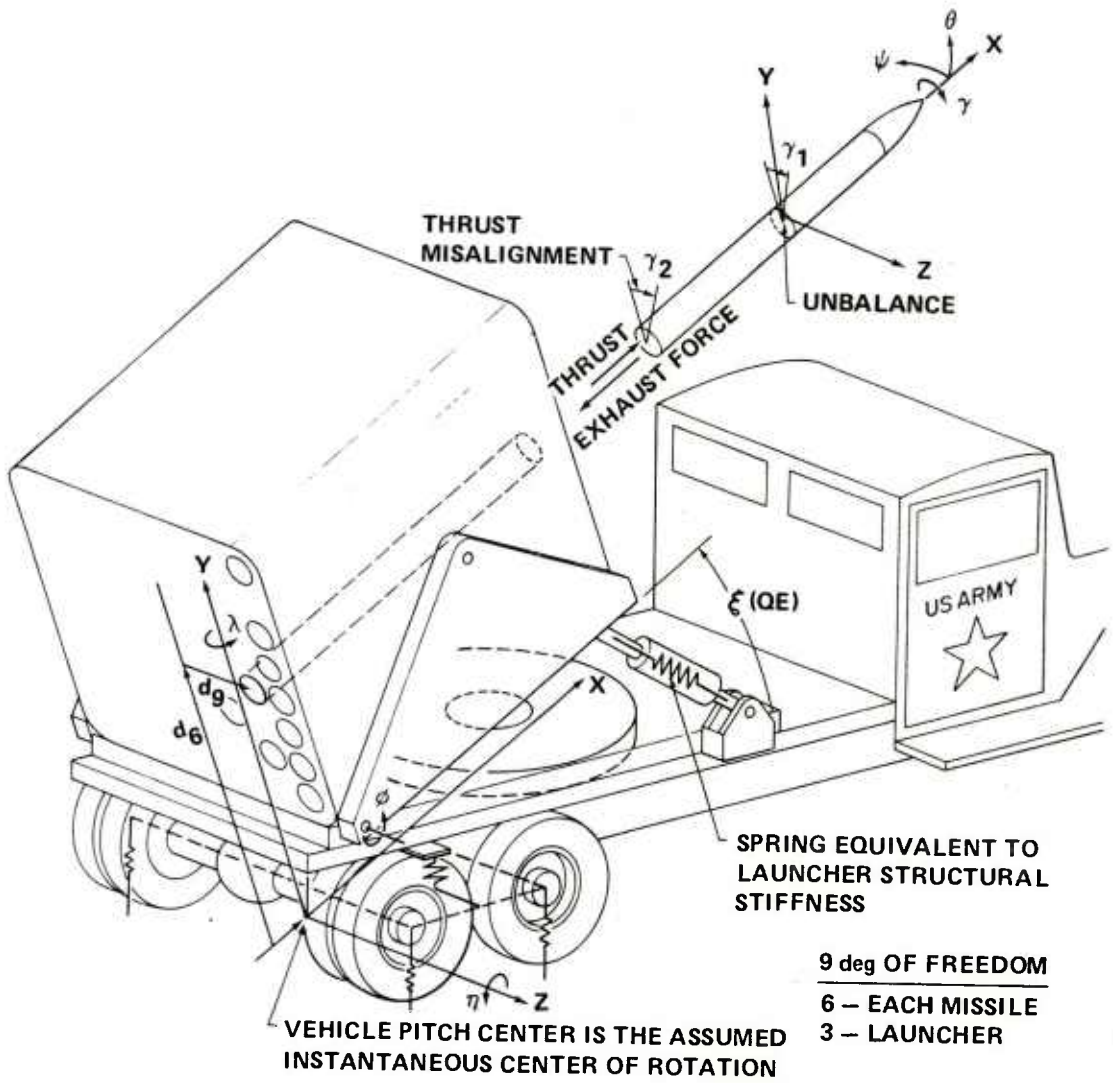

Figure 1. Multiple launcher simulation (real time).

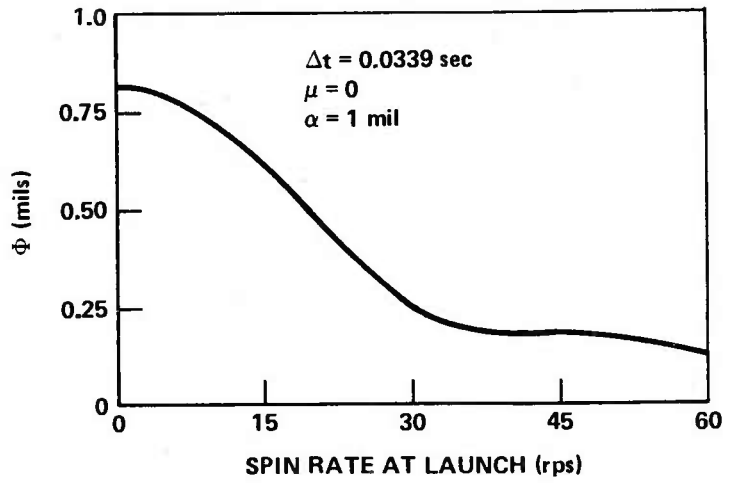

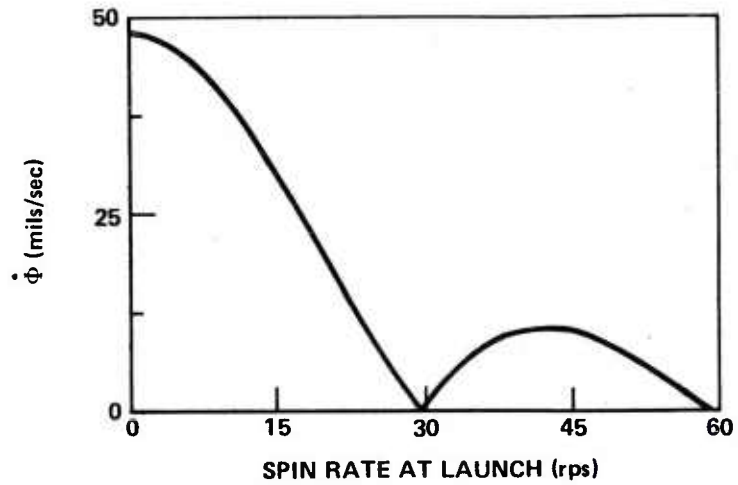

Figure 2. Angular motion versus spin rate for thrust misalignment for a 6-in-diameter rocket.

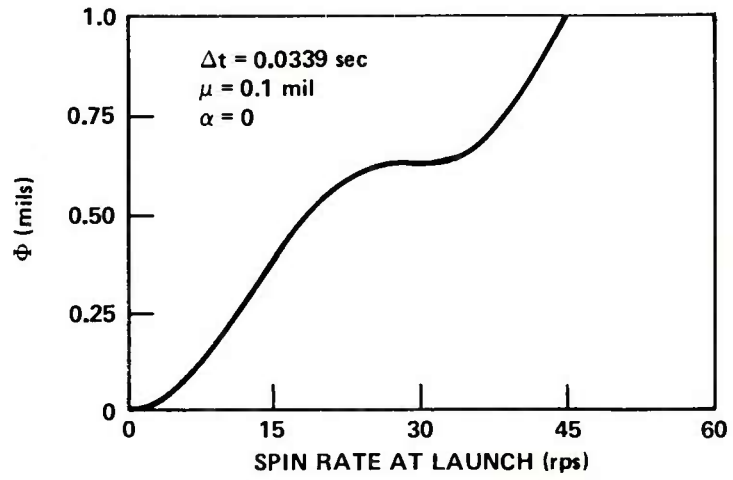

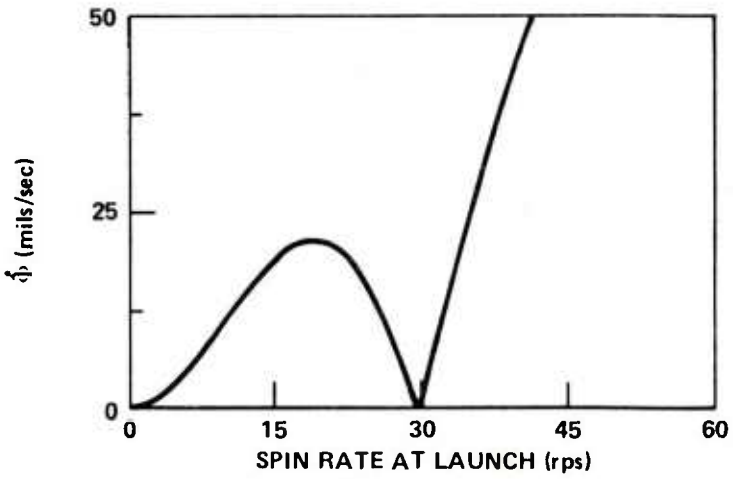

Figure 3. Angular motion versus spin rate for dynamic unbalance for a 6-in.-diameter rocket.

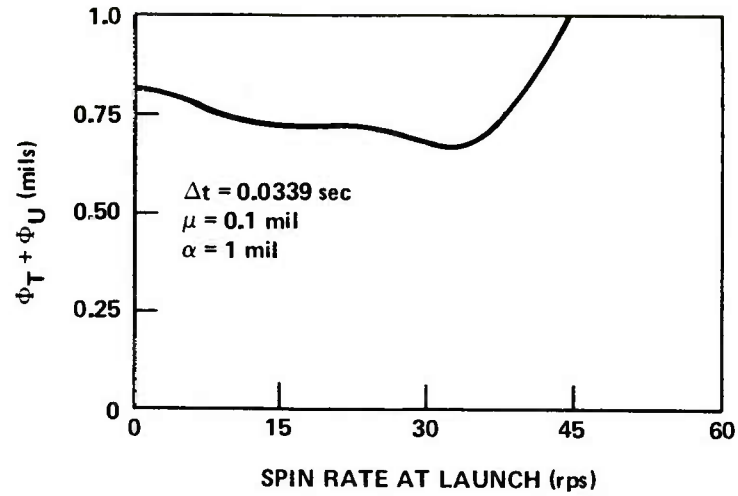

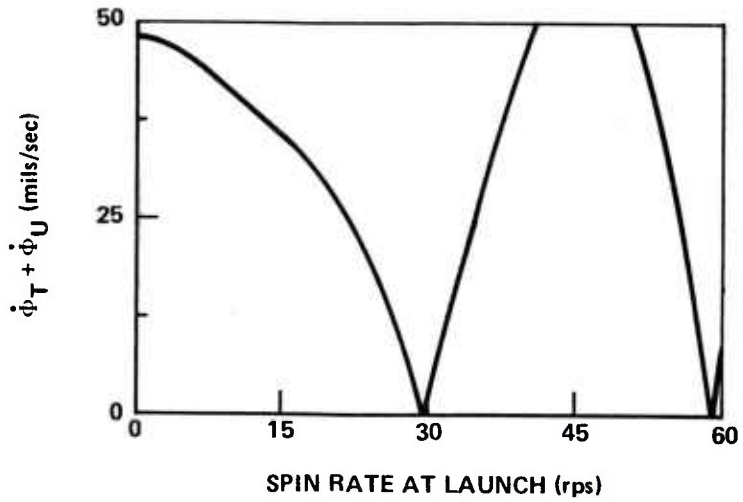

Figure 4. Angular motion versus spin rate for thrust misalignment and dynamic unbalance for a 6-in.-diameter rocket.

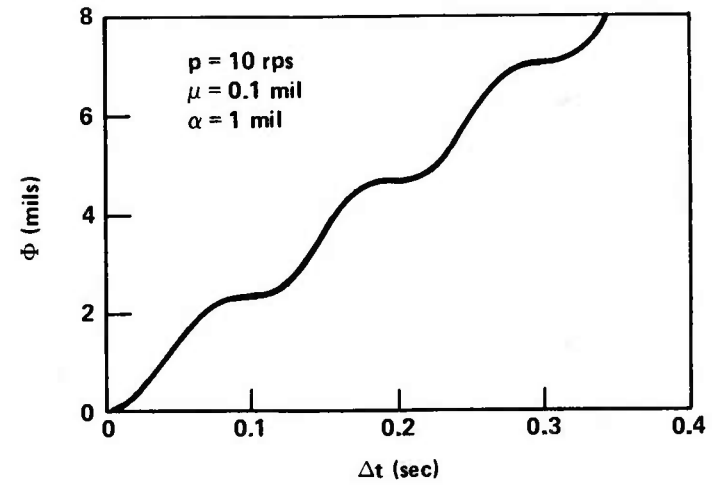

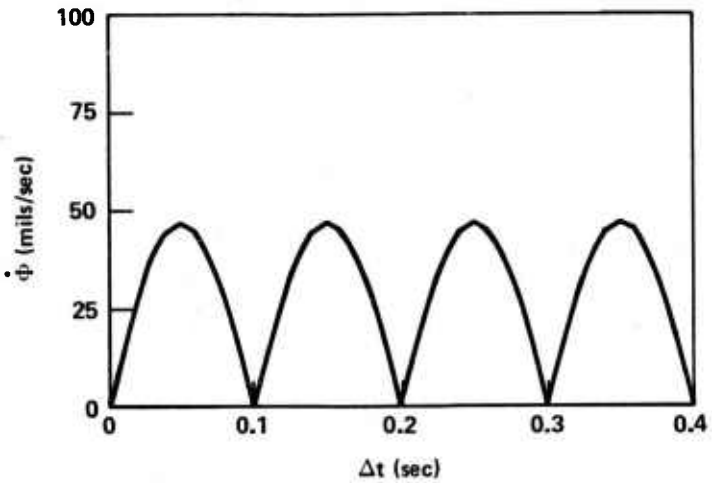

Figure 5. Angular motion versus time for dynamic unbalance and thrust misalignment for a 6-in.-diameter rocket.

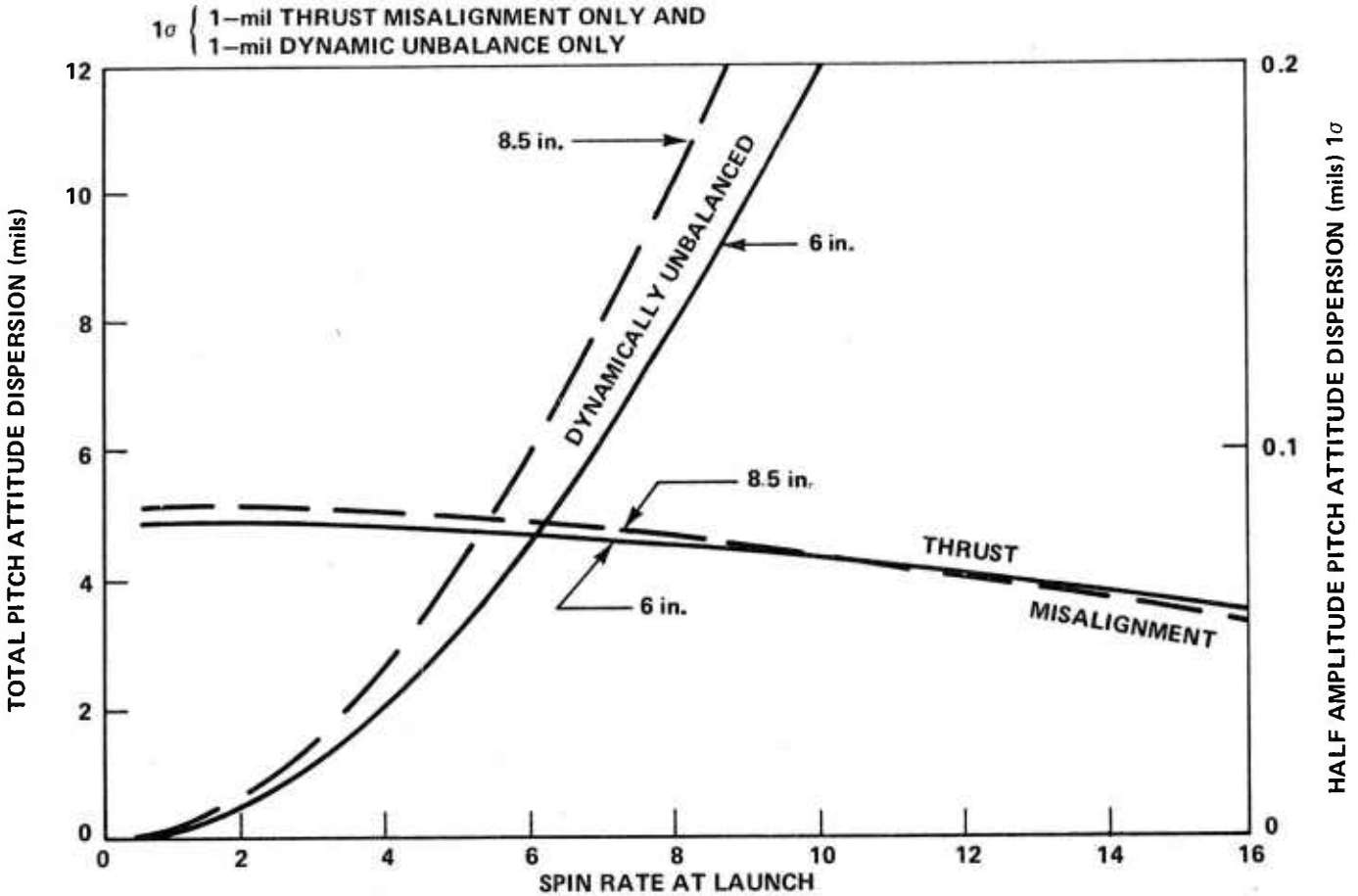

Figure 6. Rocket-induced launch errors at launch tube exit infinitely rigid launcher.

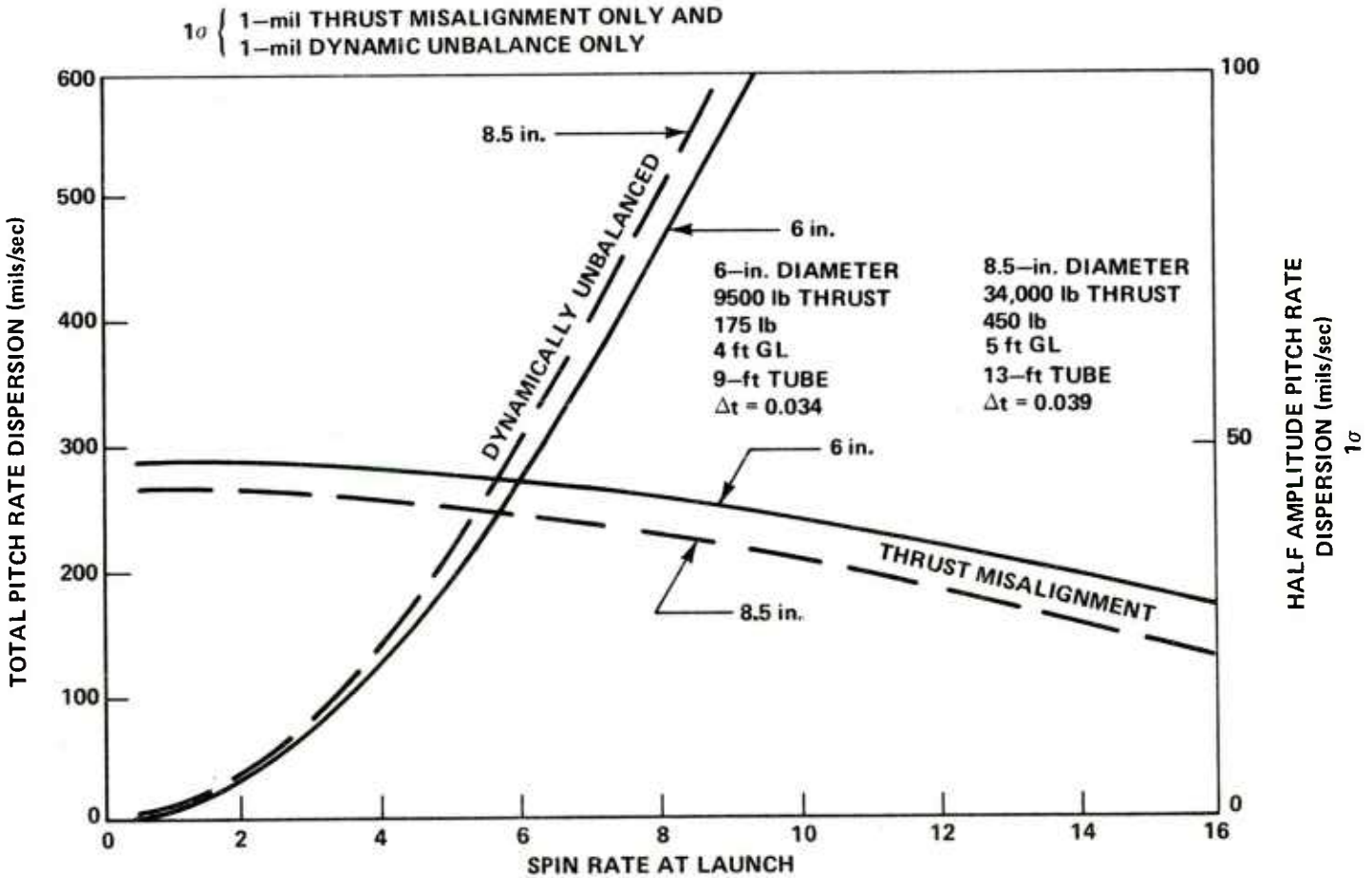

Figure 7. Rocket-induced launch errors at launch tube exit infinitely rigid launcher.

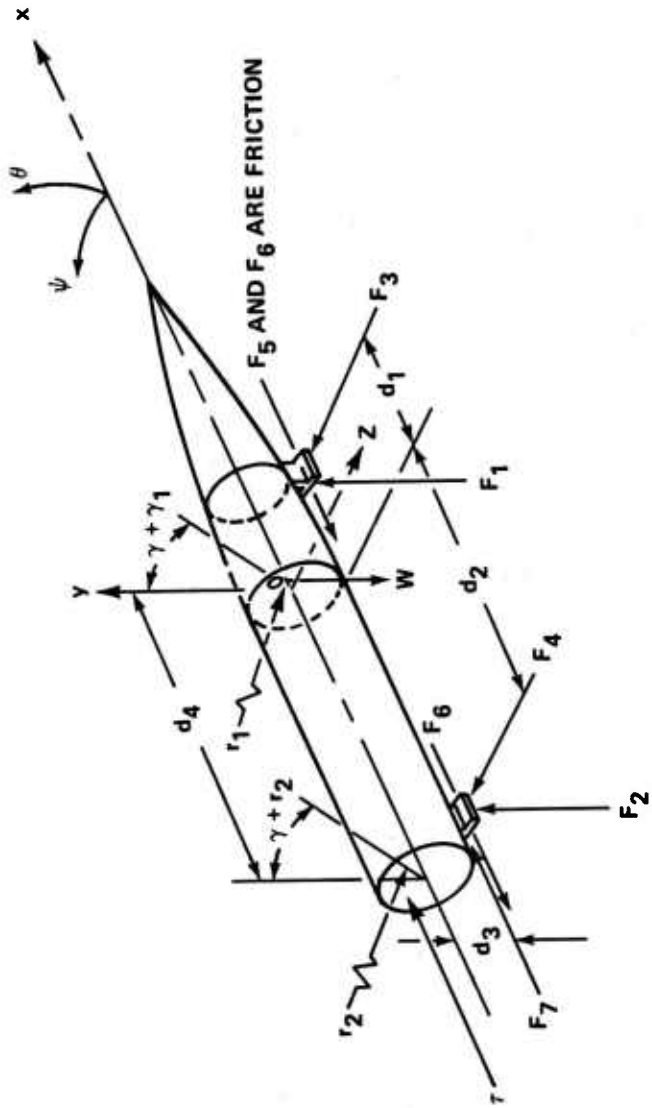

Figure 8. Definition of rocket dimensions.

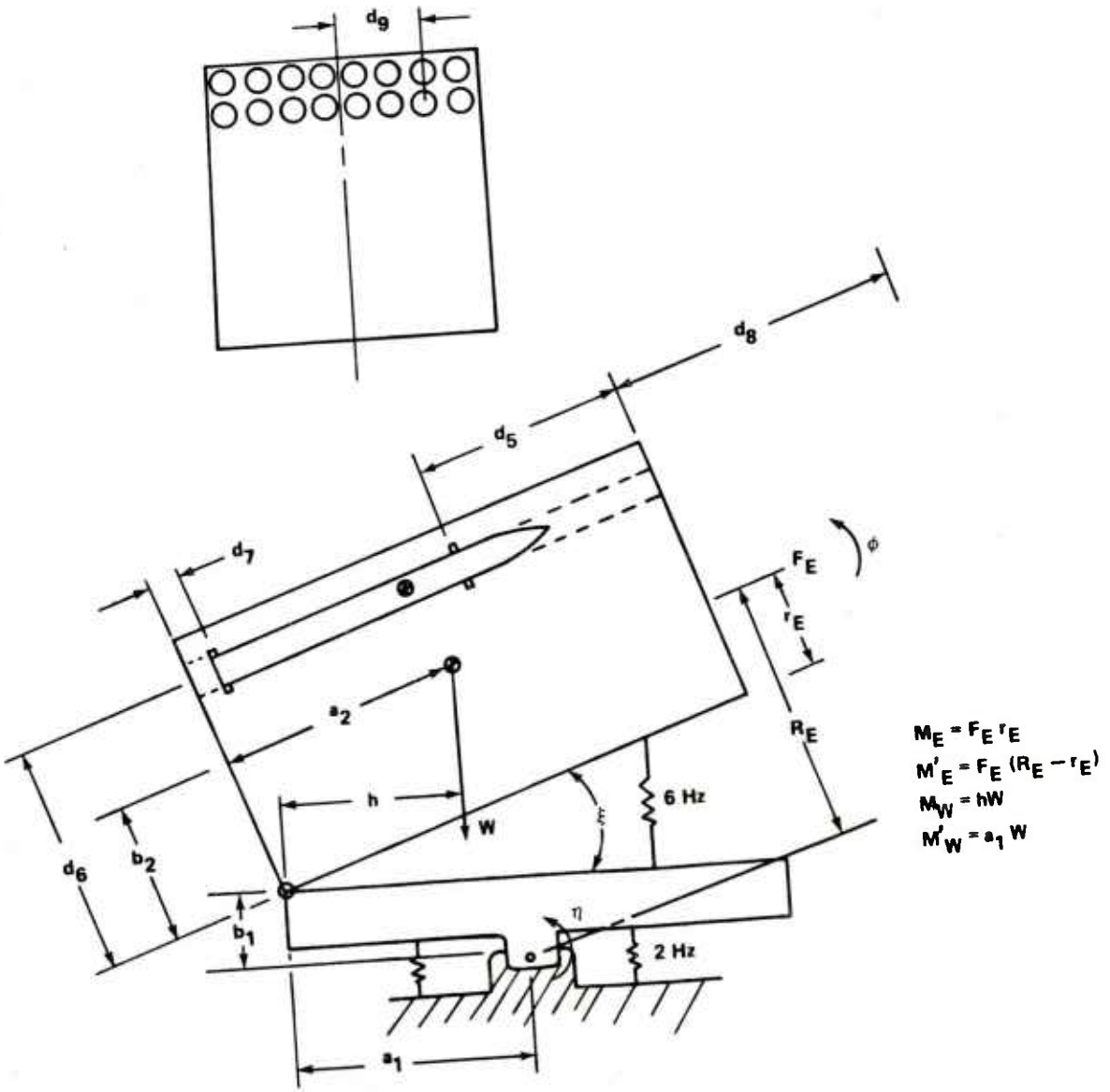

Figure 9. Definition of launcher dimensions.

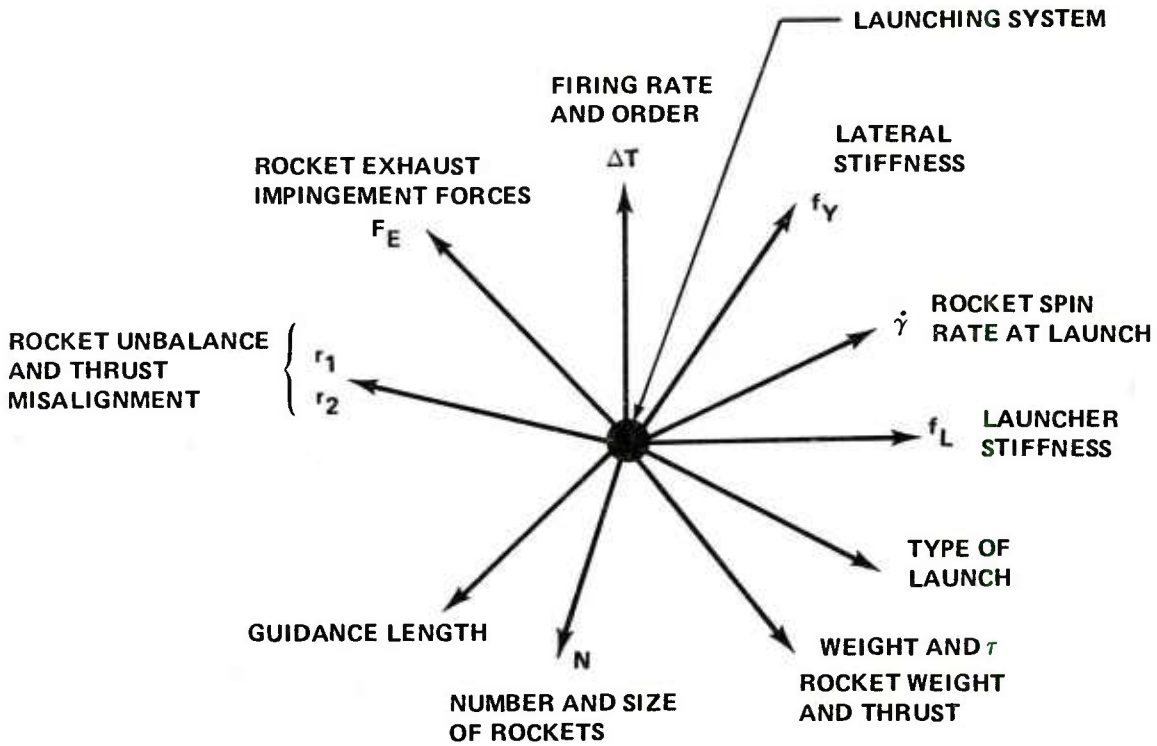

Figure 10. Launch system parametrics.

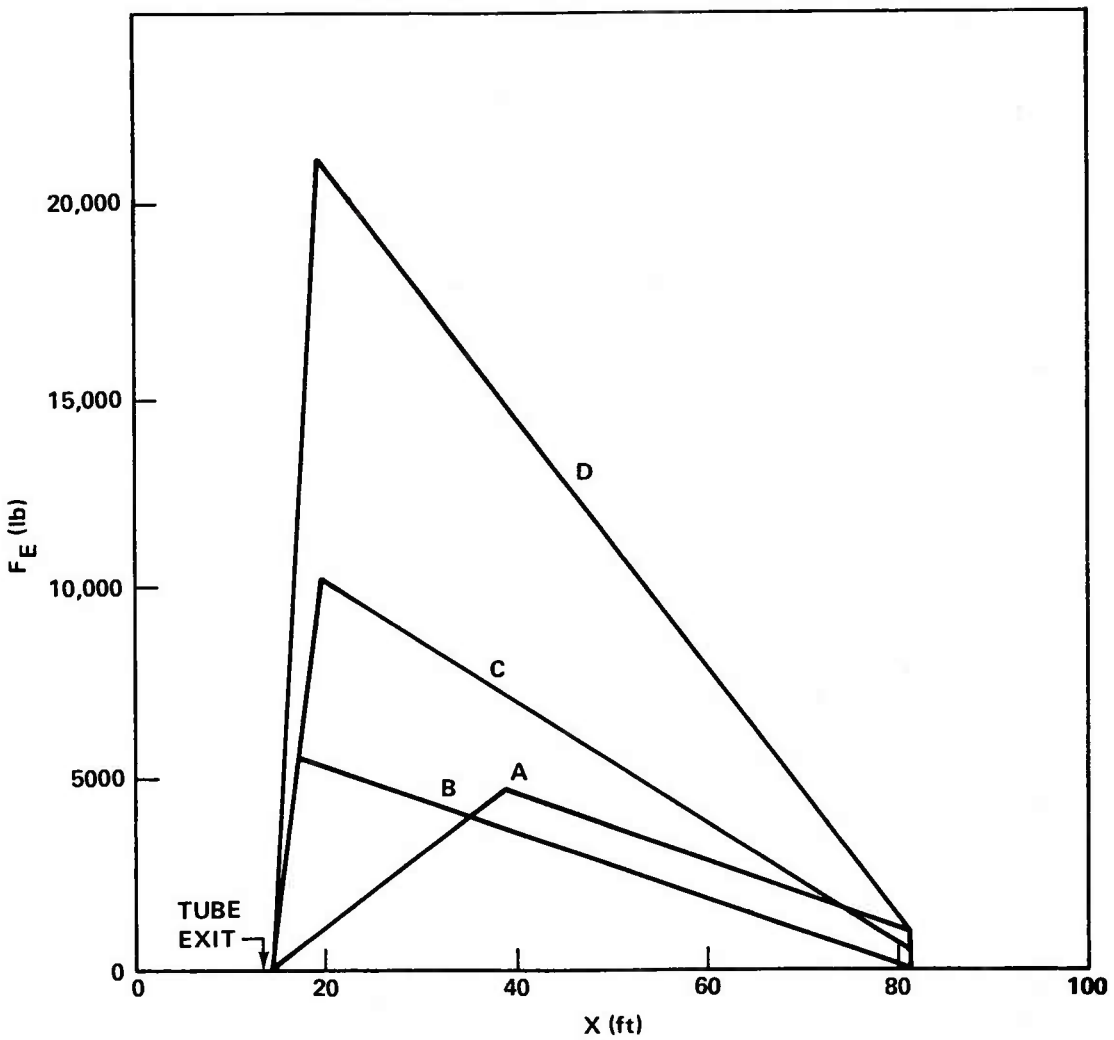

Figure 11. Exhaust field configurations.

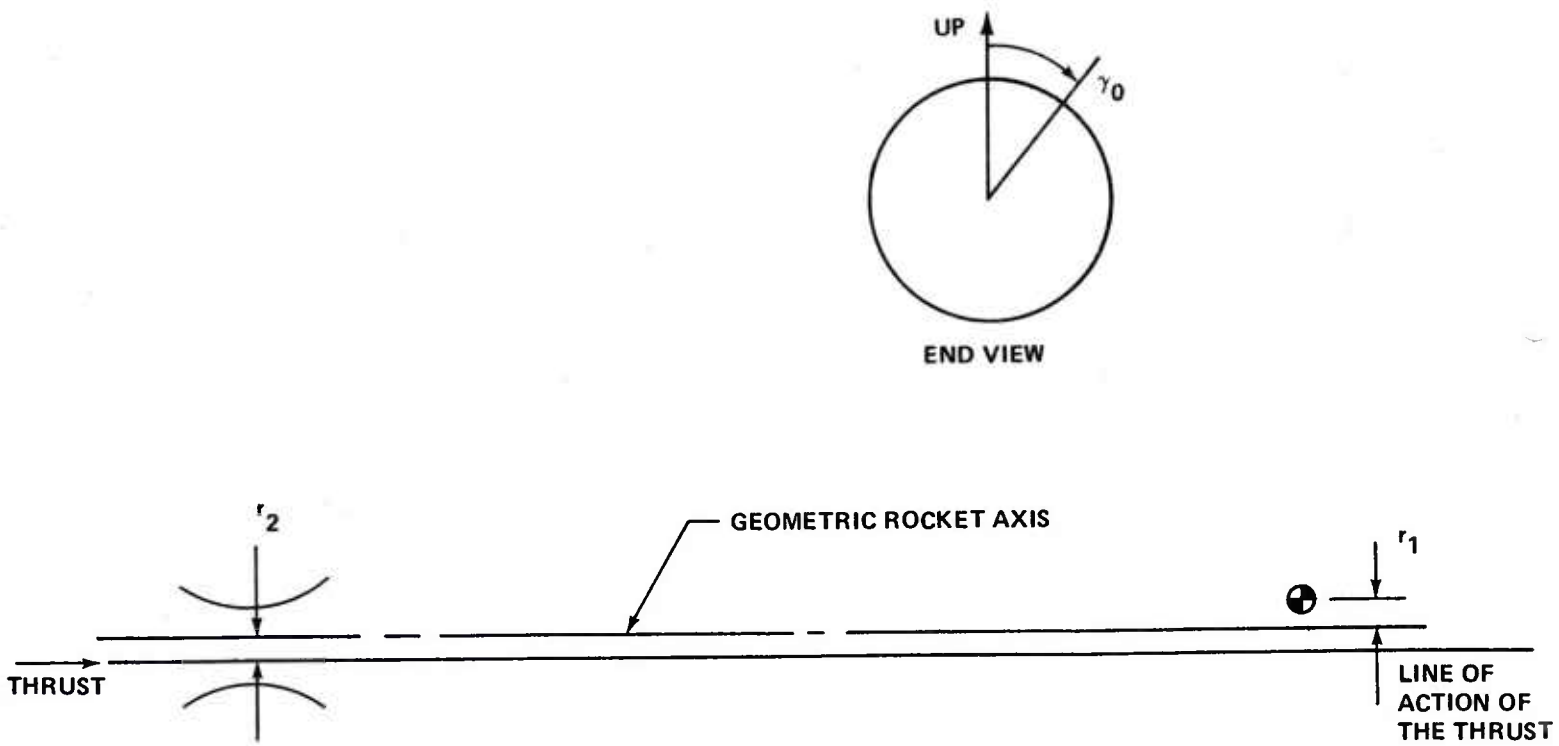

NOTES: 1. γ_o LOCATES THE INITIAL ORIENTATION OF THE PLANE OF THE THRUST VECTOR AND THE CENTER OF MASS. IT IS RANDOM BETWEEN ±180 deg.

2. r_1 = ±0.009 ft (RANDOM BETWEEN LIMITS OF 0.009 ft)
3. r_2 = +0.01 ft (CONSTANT)
4. TORQUE DUE TO THRUST OFFSET = THRUST x $(r_2 - r_1)$,

   HENCE, MAXIMUM TORQUE = 0.019 x THRUST (ft–lb)
   AND MINIMUM TORQUE = 0.001 x THRUST (ft–lb)

Figure 12. Mass offset and thrust misalignment diagram for the 6-in.-diameter rocket.

LAUNCH PITCH DISPERSION
FORTY–TWO 6–in. DIAMETER ROCKETS

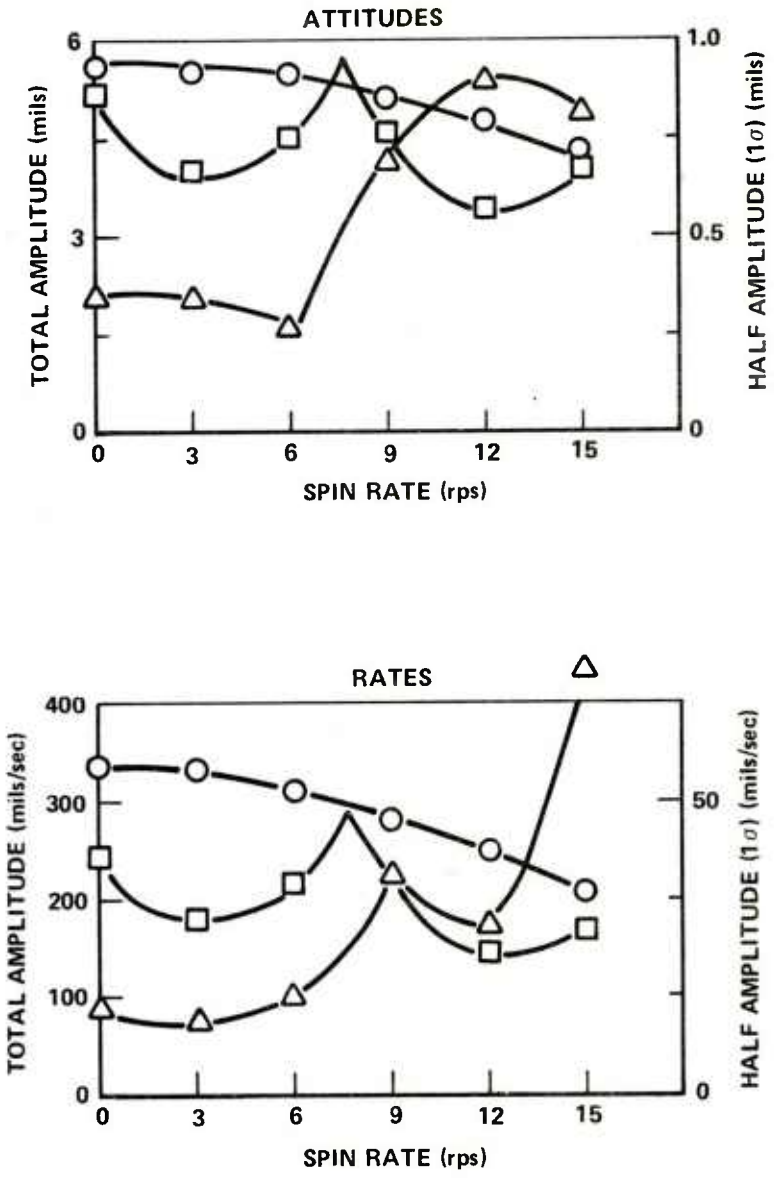

LAUNCHER TYPE

○ RIGID NONTIPOFF
△ FLEXIBLE TIPOFF
□ FLEXIBLE NONTIPOFF

Figure 13. Rocket pitch motion at tube exit versus spin rate at launch.

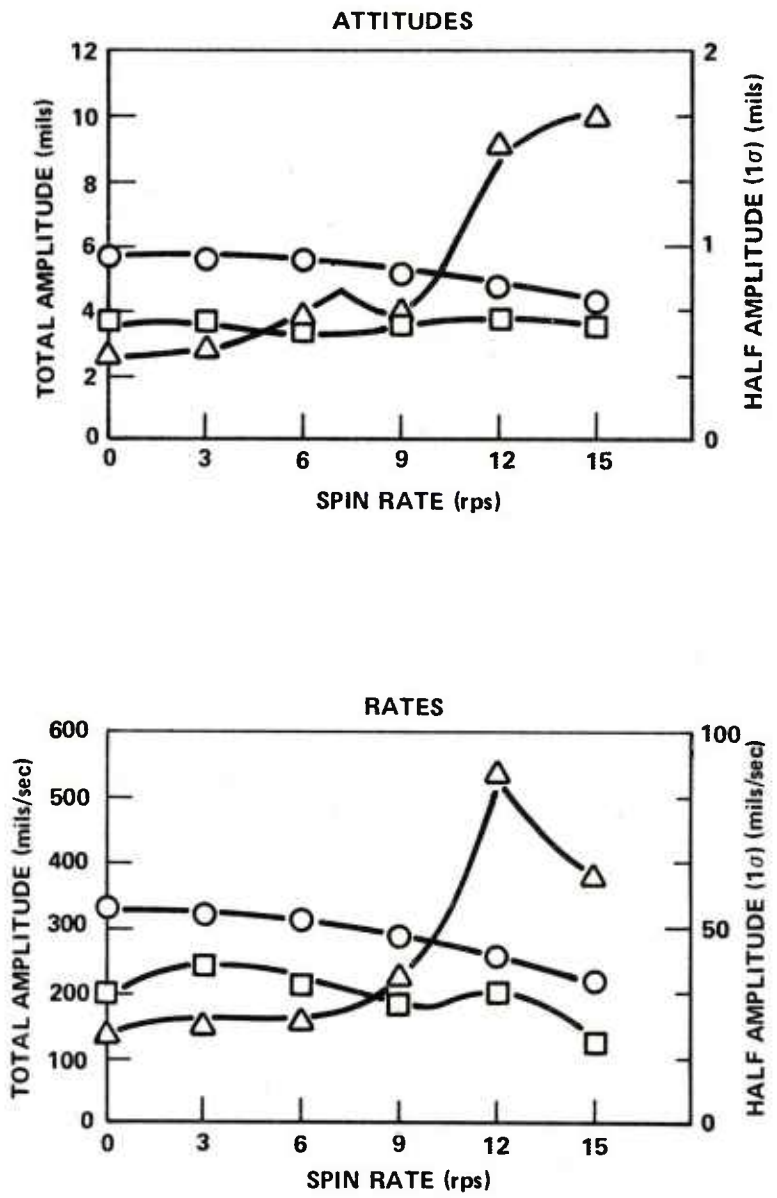

Figure 14. Rocket yaw motion at tube exit versus spin rate at launch.

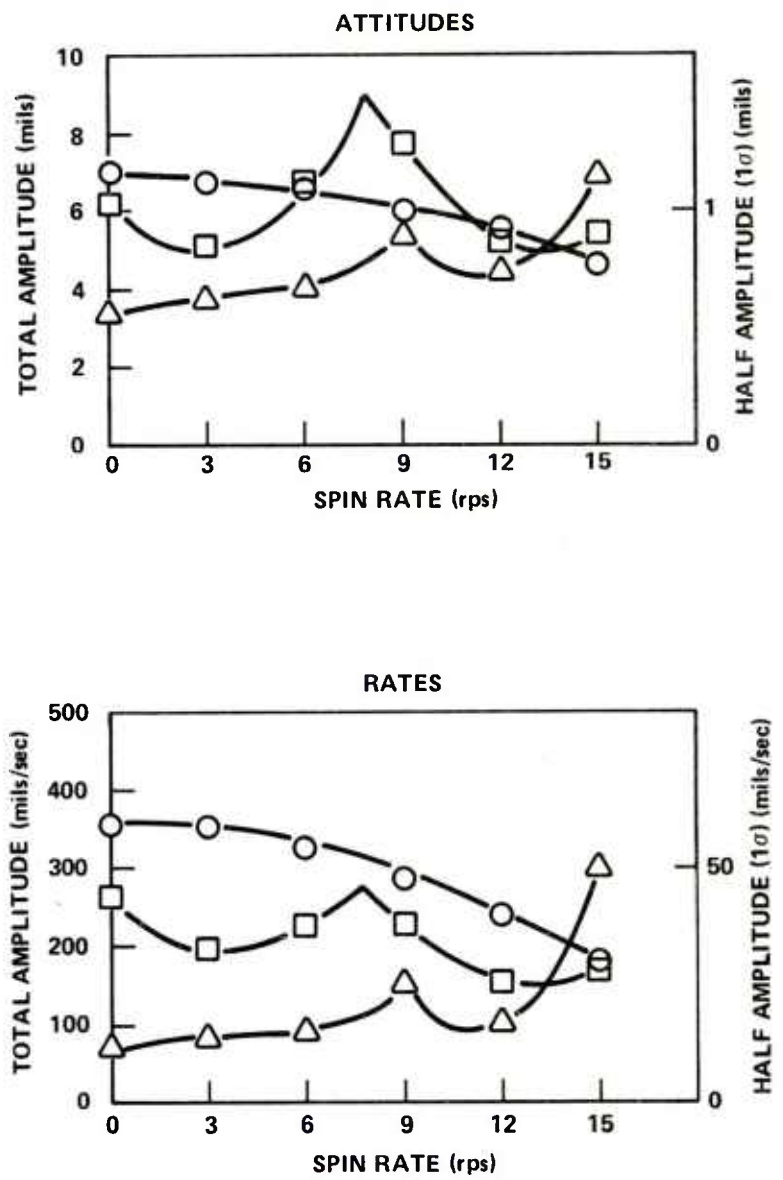

Figure 15. Rocket pitch motion at tube exit versus spin rate at launch.

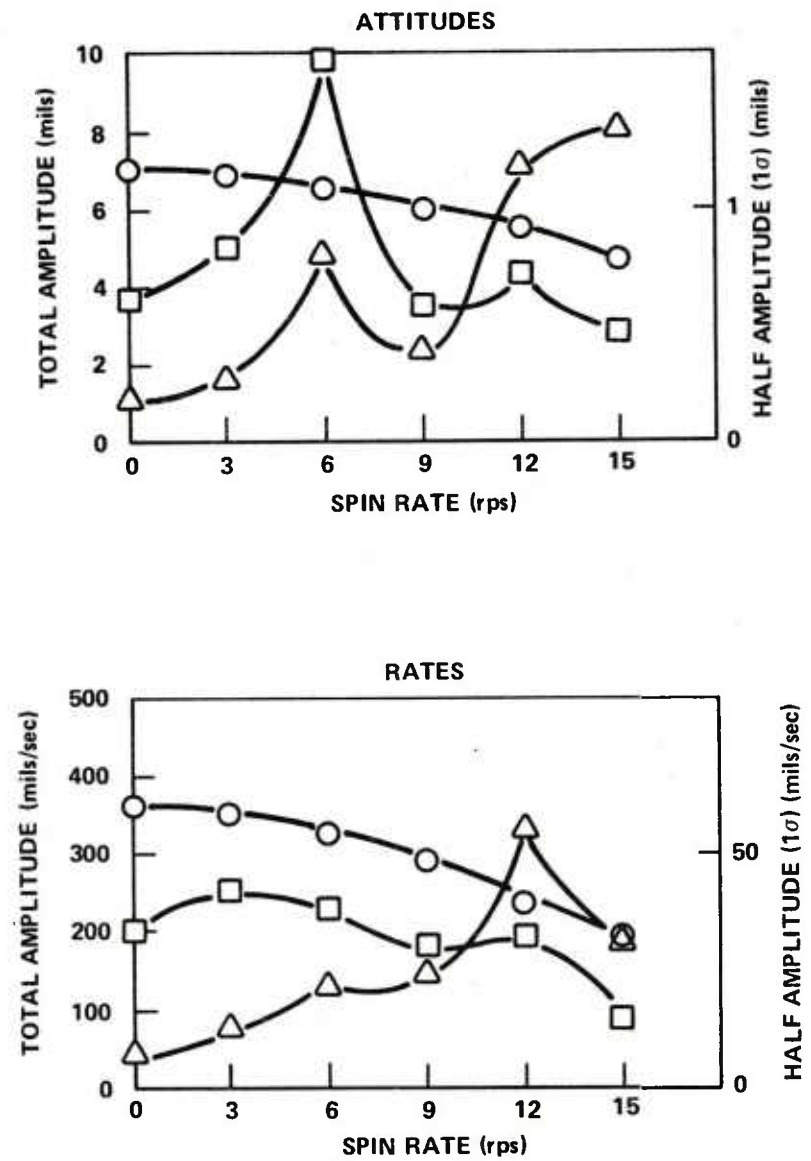

Figure 16. Rocket yaw motion at tube exit versus spin rate at launch.

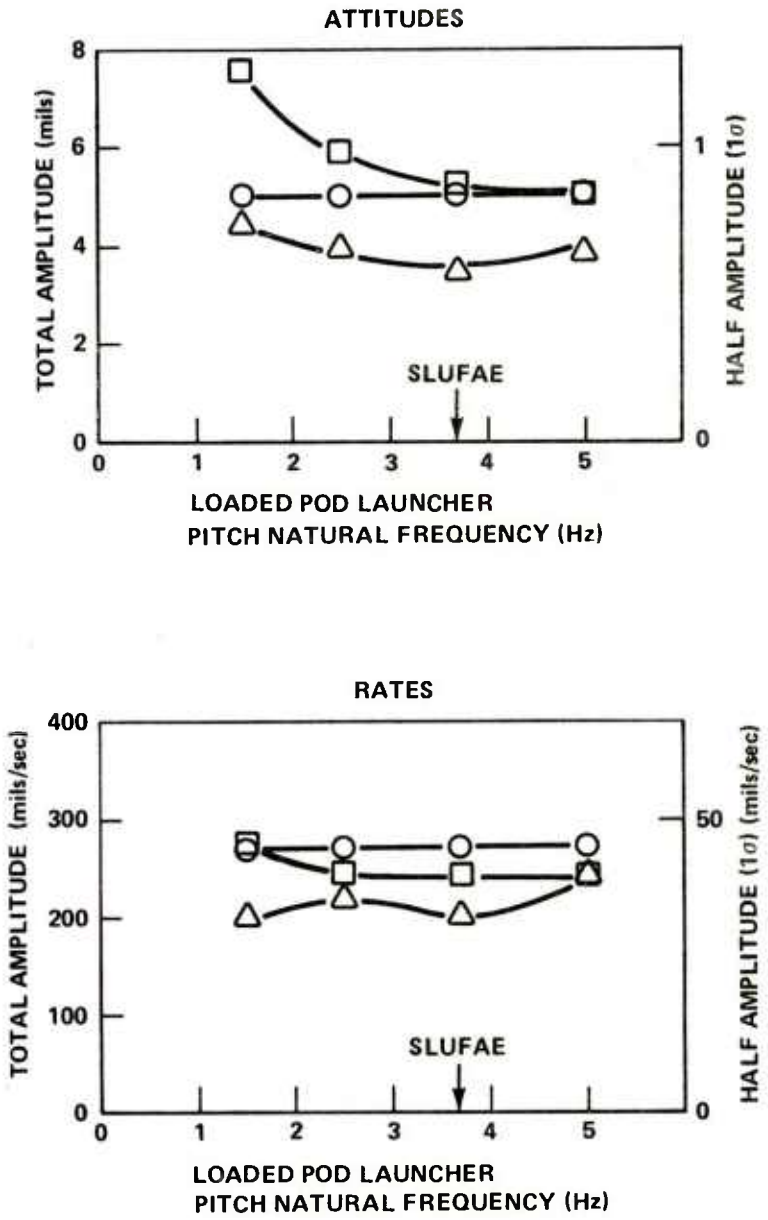

Figure 17. Rocket pitch motion at tube exit versus launcher pitch natural frequency.

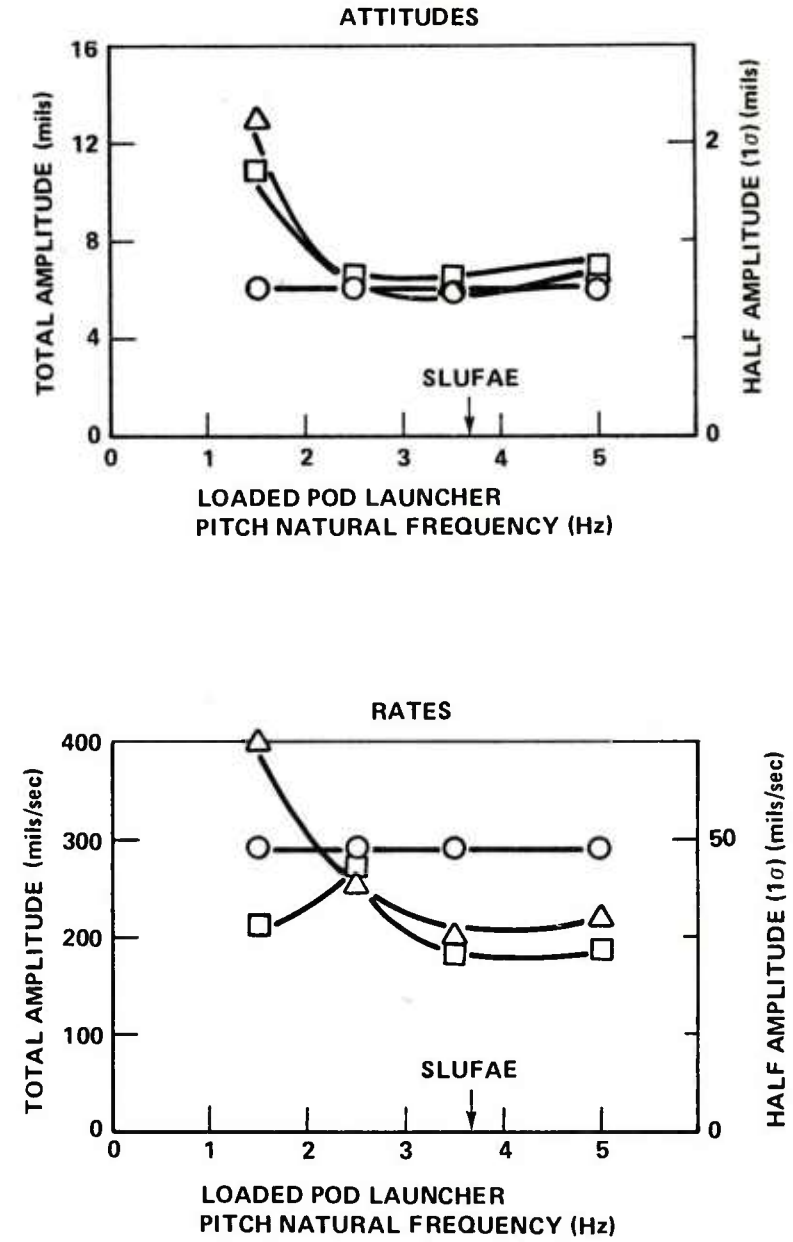

Figure 18. Rocket pitch motion at tube exit versus launcher pitch natural frequency.

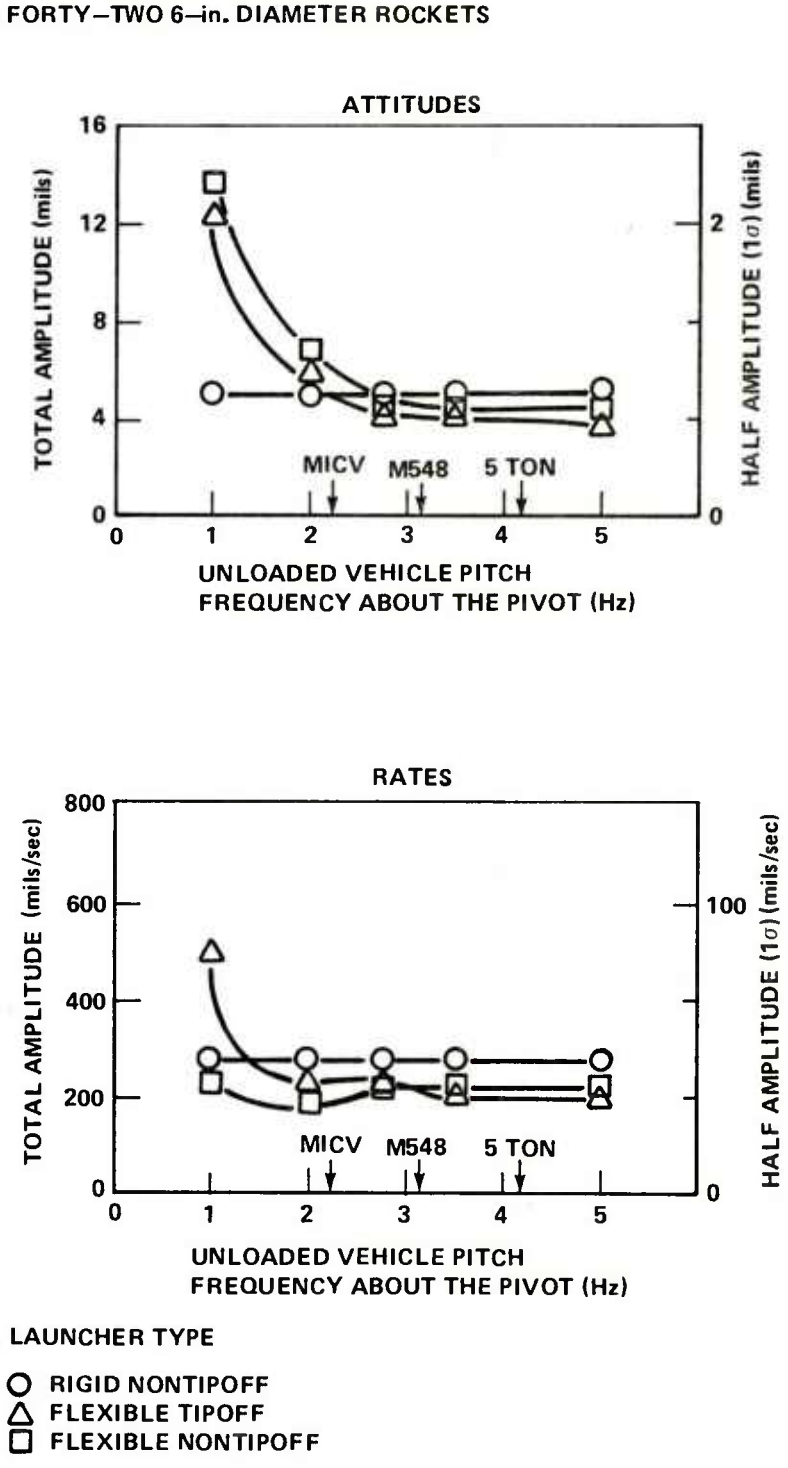

Figure 19. Rocket pitch motion at tube exit versus vehicle pitch frequency about the pivot.

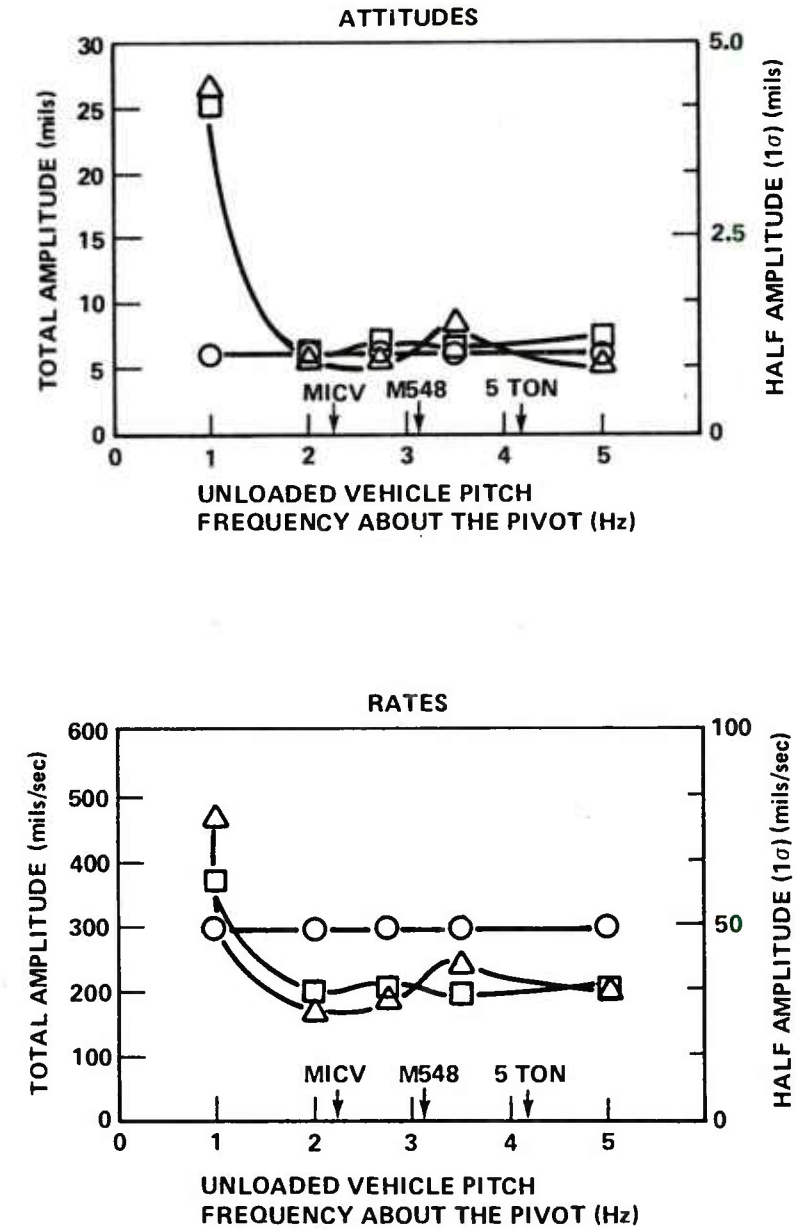

Figure 20. Rocket pitch motion at tube exit versus vehicle pitch frequency about the pivot.

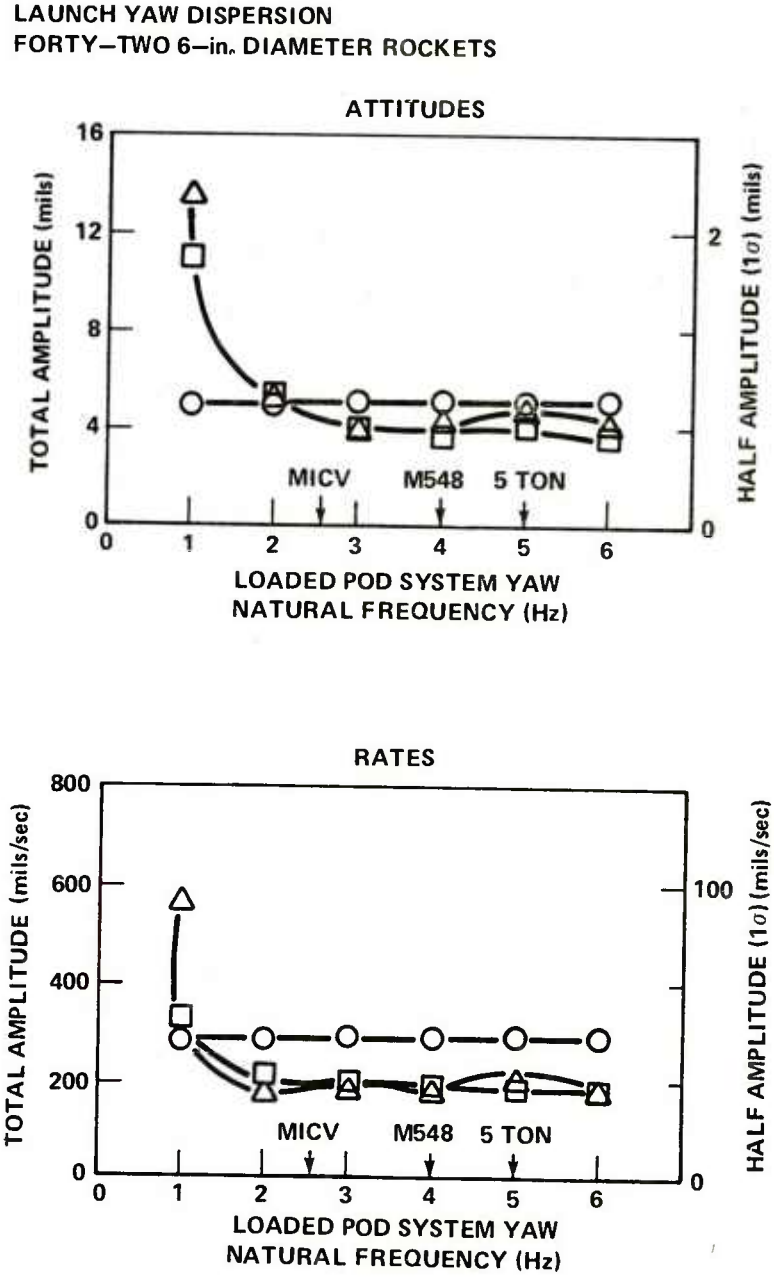

Figure 21. Rocket yaw motion at tube exit versus system yaw natural frequency.

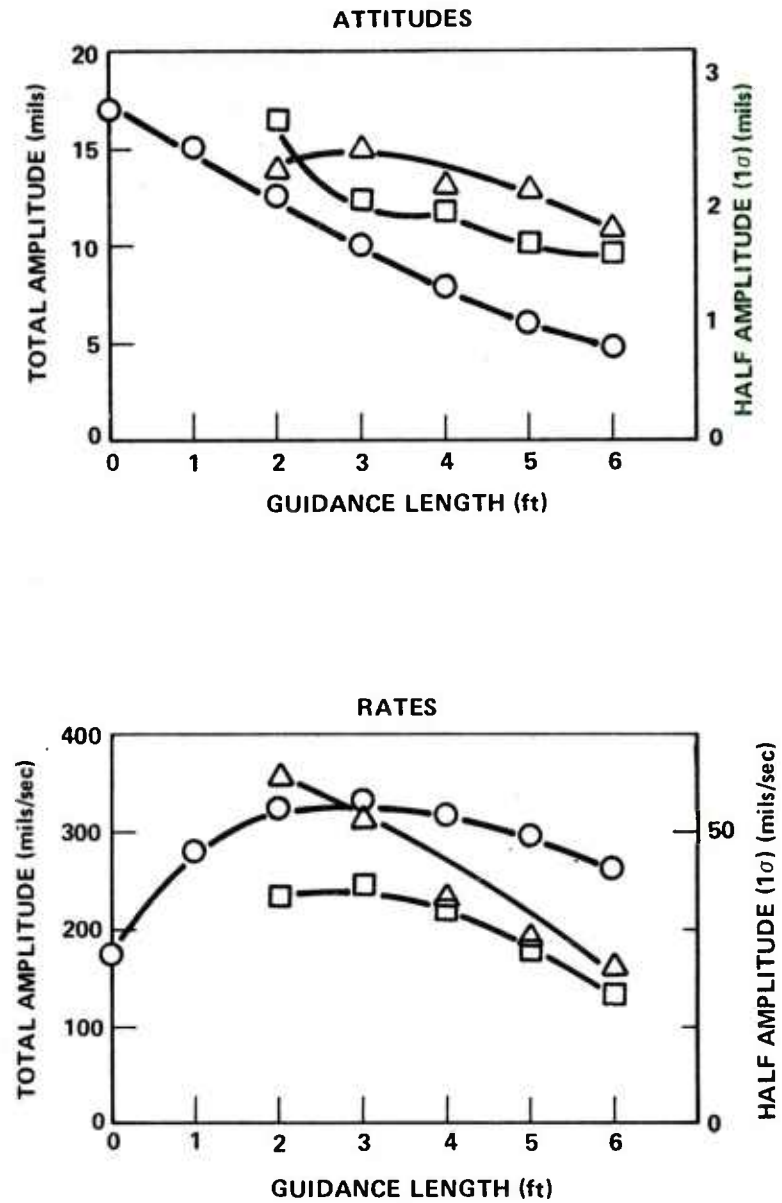

Figure 22. Rocket pitch motion at tube exit versus guidance length using exhaust pattern D.

LAUNCH YAW DISPERSION
TWELVE 8.5–in. DIAMETER ROCKETS

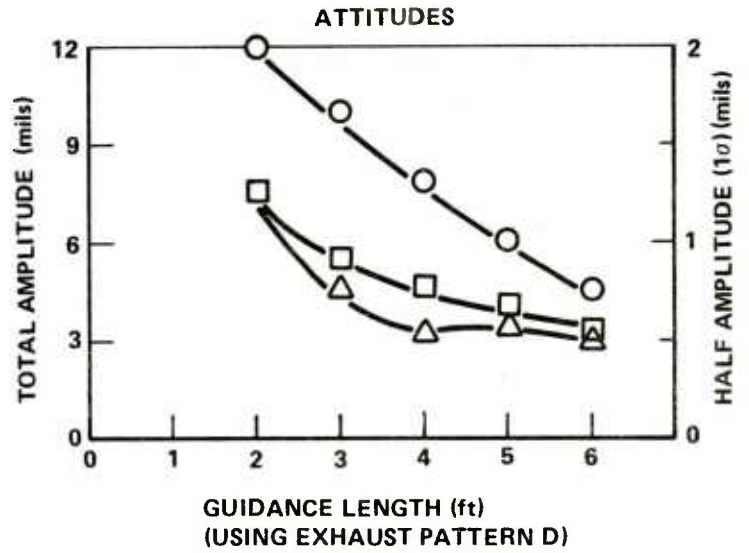

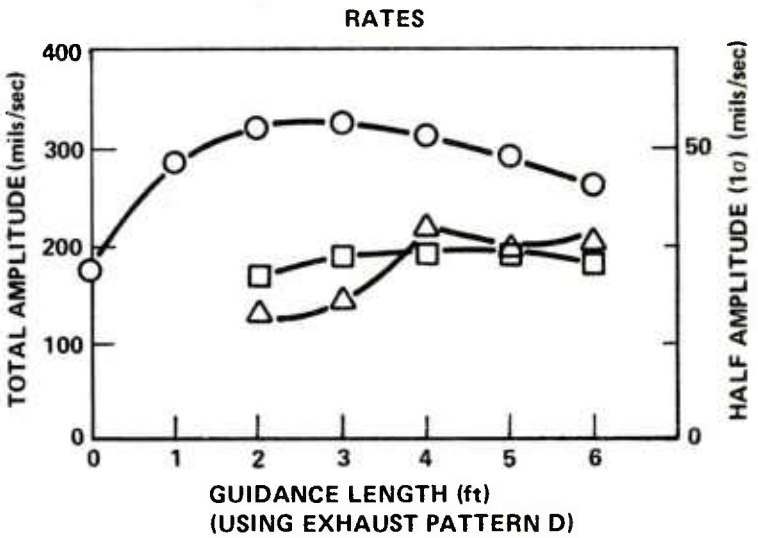

LAUNCHER TYPE

○ RIGID NONTIPOFF
△ FLEXIBLE TIPOFF
□ FLEXIBLE NONTIPOFF

Figure 23. Rocket yaw motion at tube exit versus guidance length.

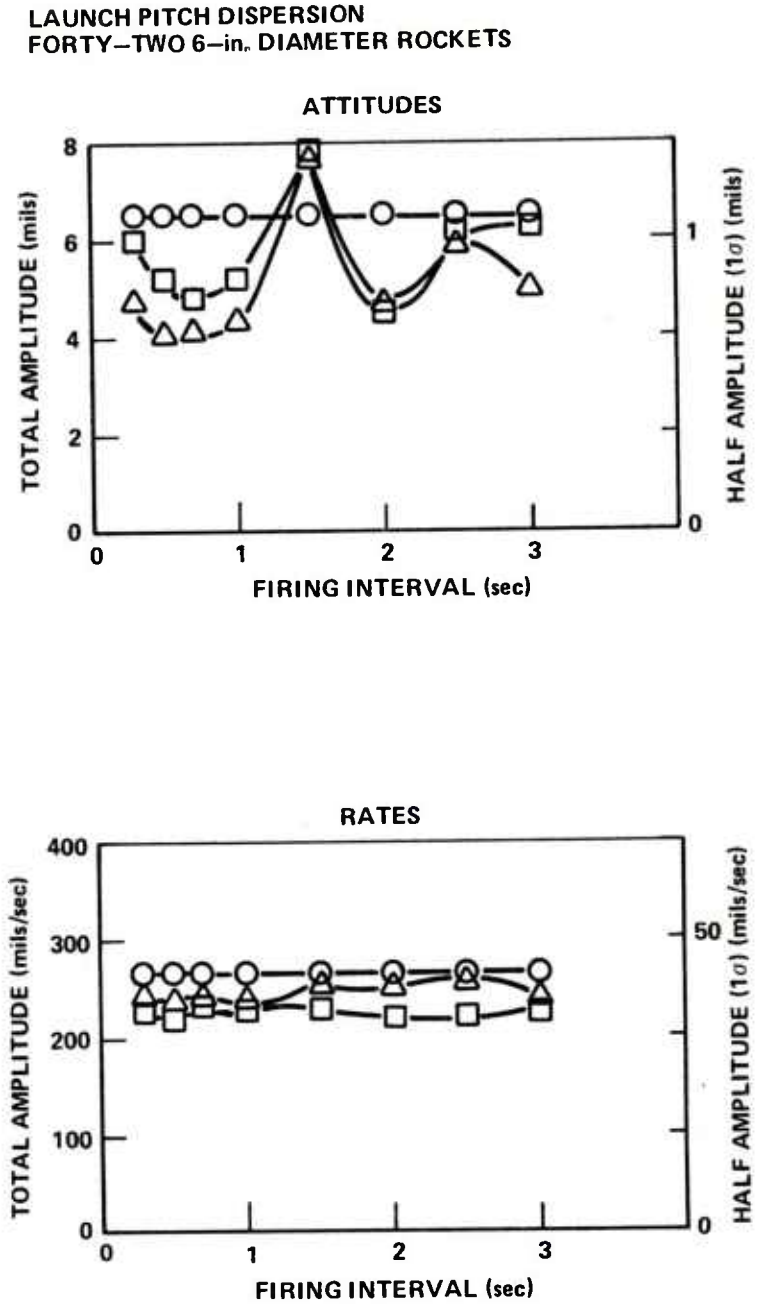

Figure 24. Rocket pitch motion at tube exit versus firing interval.

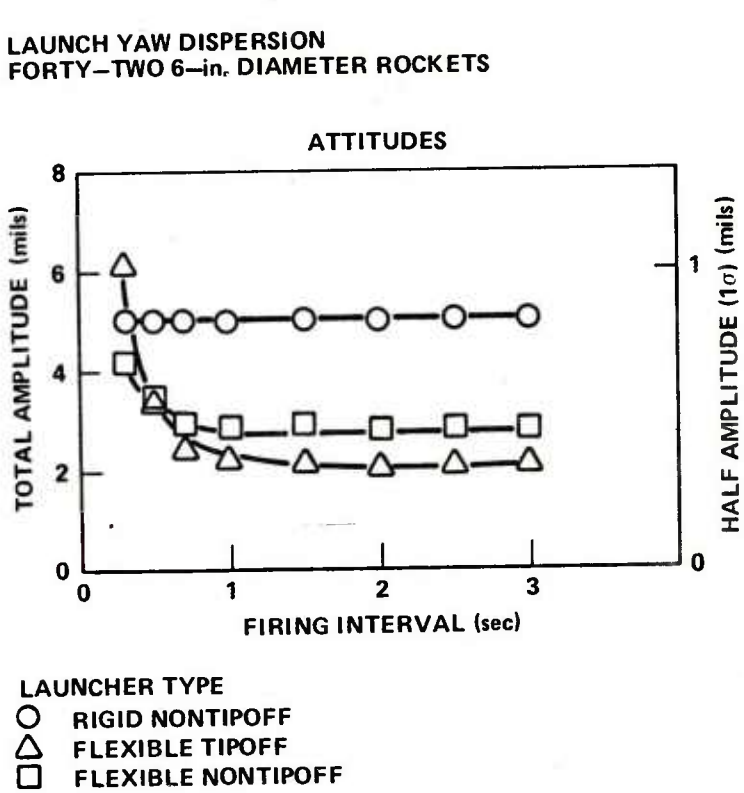

Figure 25. Rocket yaw motion at tube exit versus firing interval.

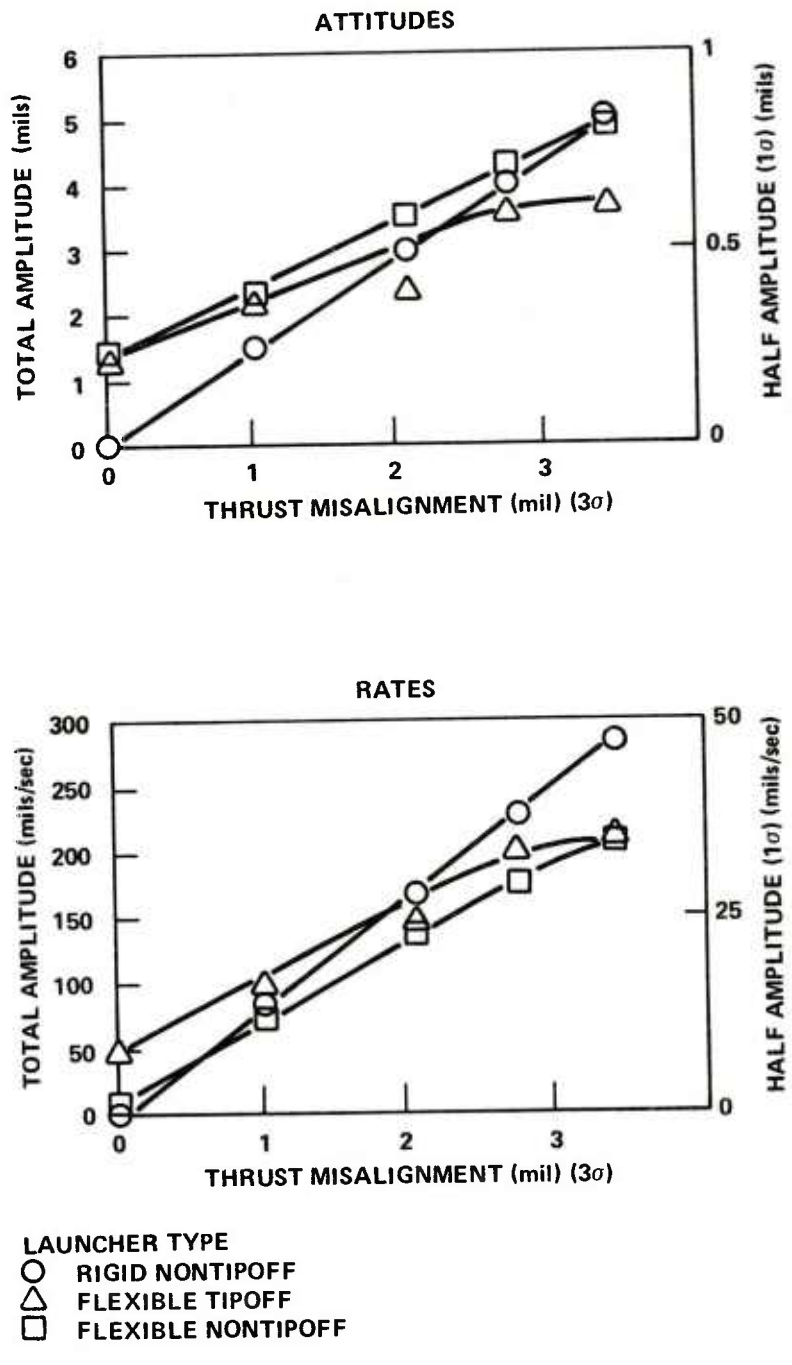

Figure 26. Rocket pitch motion at tube exit versus mass offset and thrust misalignment.

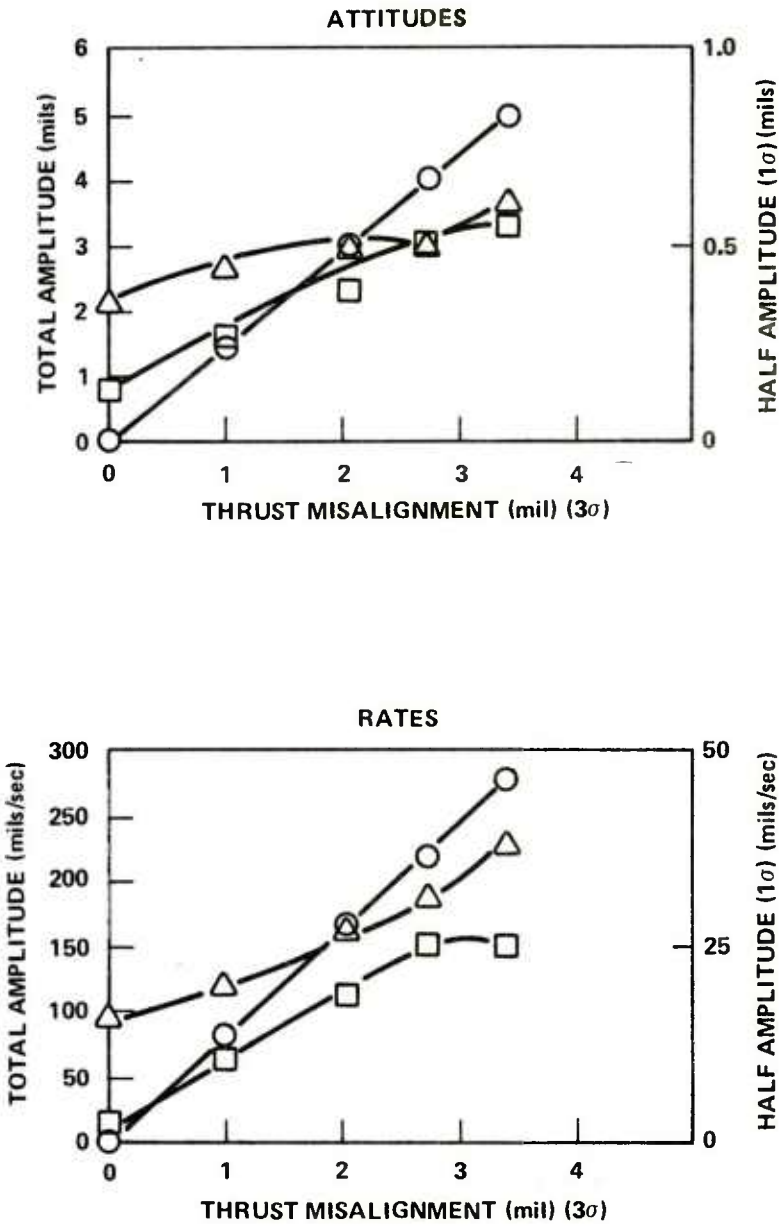

Figure 27. Rocket yaw motion at tube exit versus mass offset and thrust misalignment.

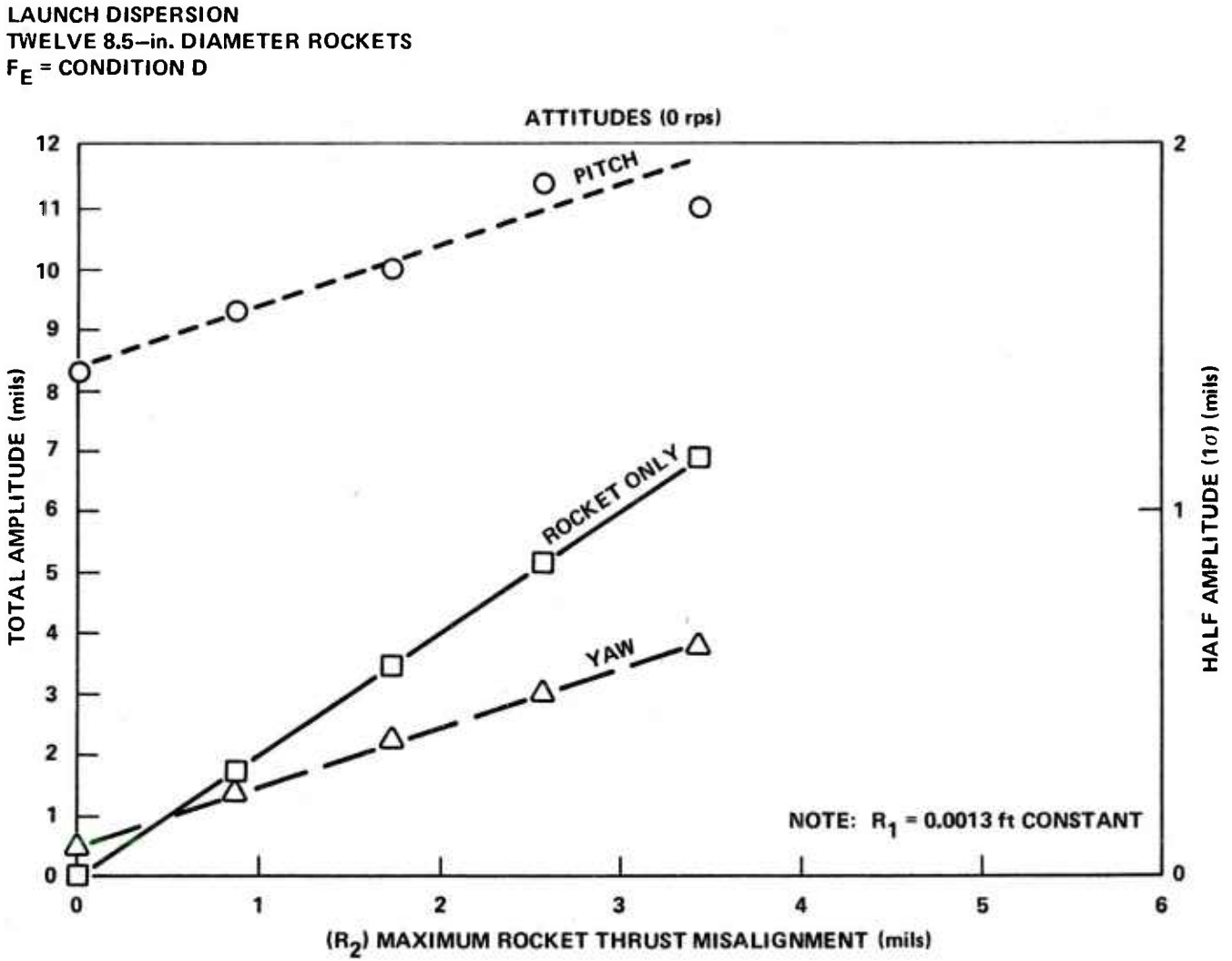

Figure 28. Rocket attitude motion at tube exit versus maximum rocket thrust misalignment.

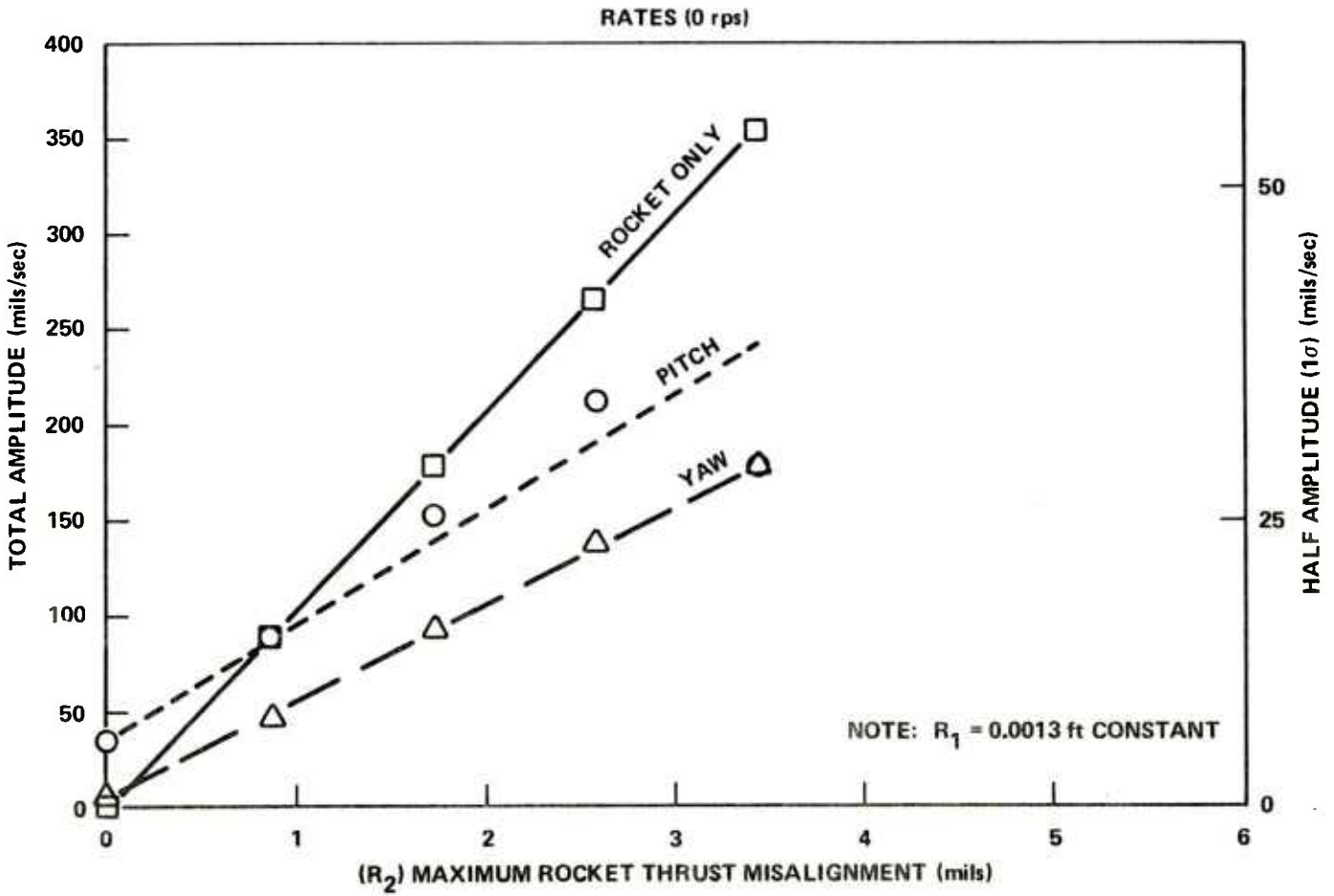

Figure 29. Rocket rate motion at tube exit versus maximum rocket thrust misalignment.

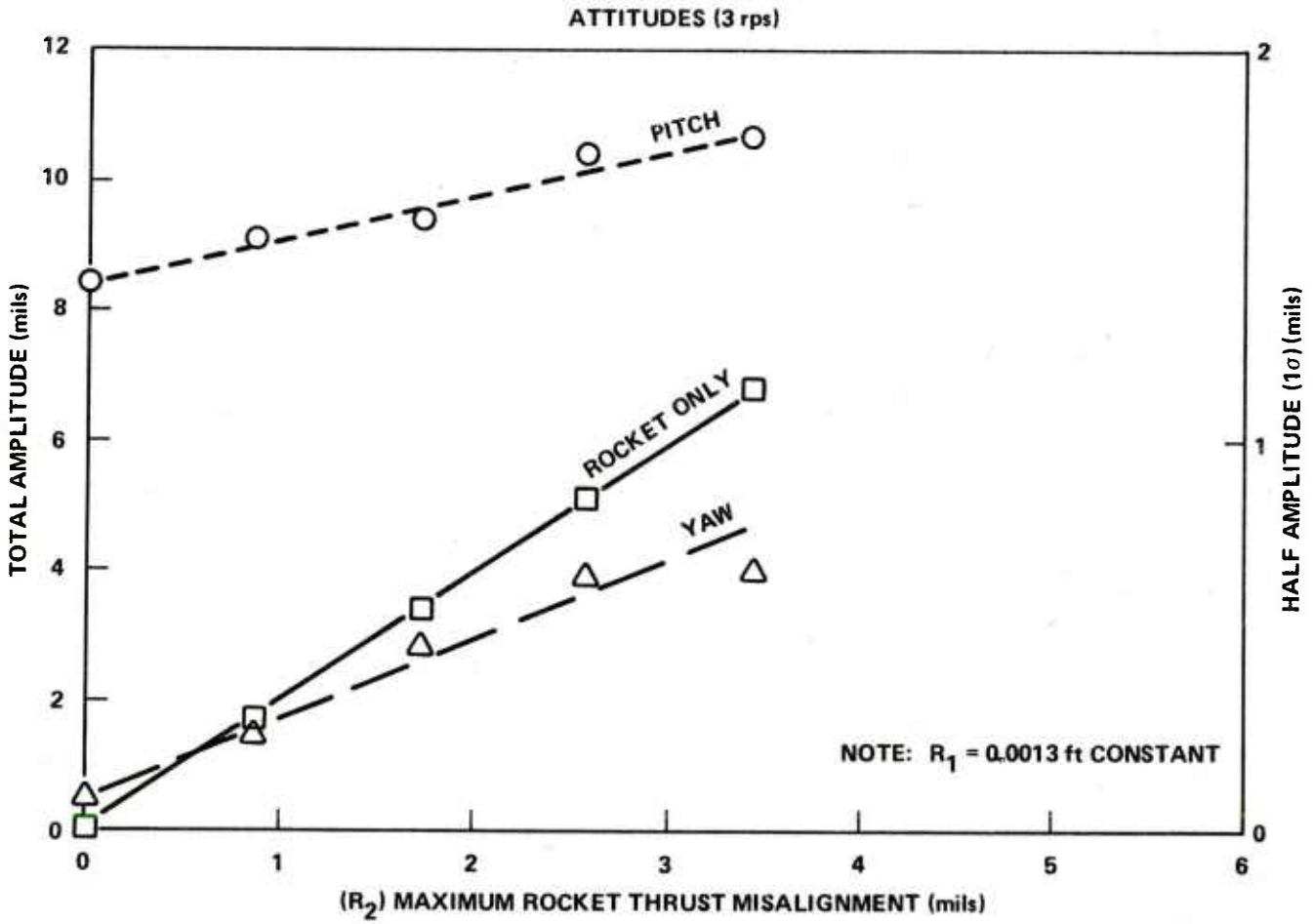

Figure 30. Rocket attitude motion at tube exit versus maximum rocket thrust misalignment.

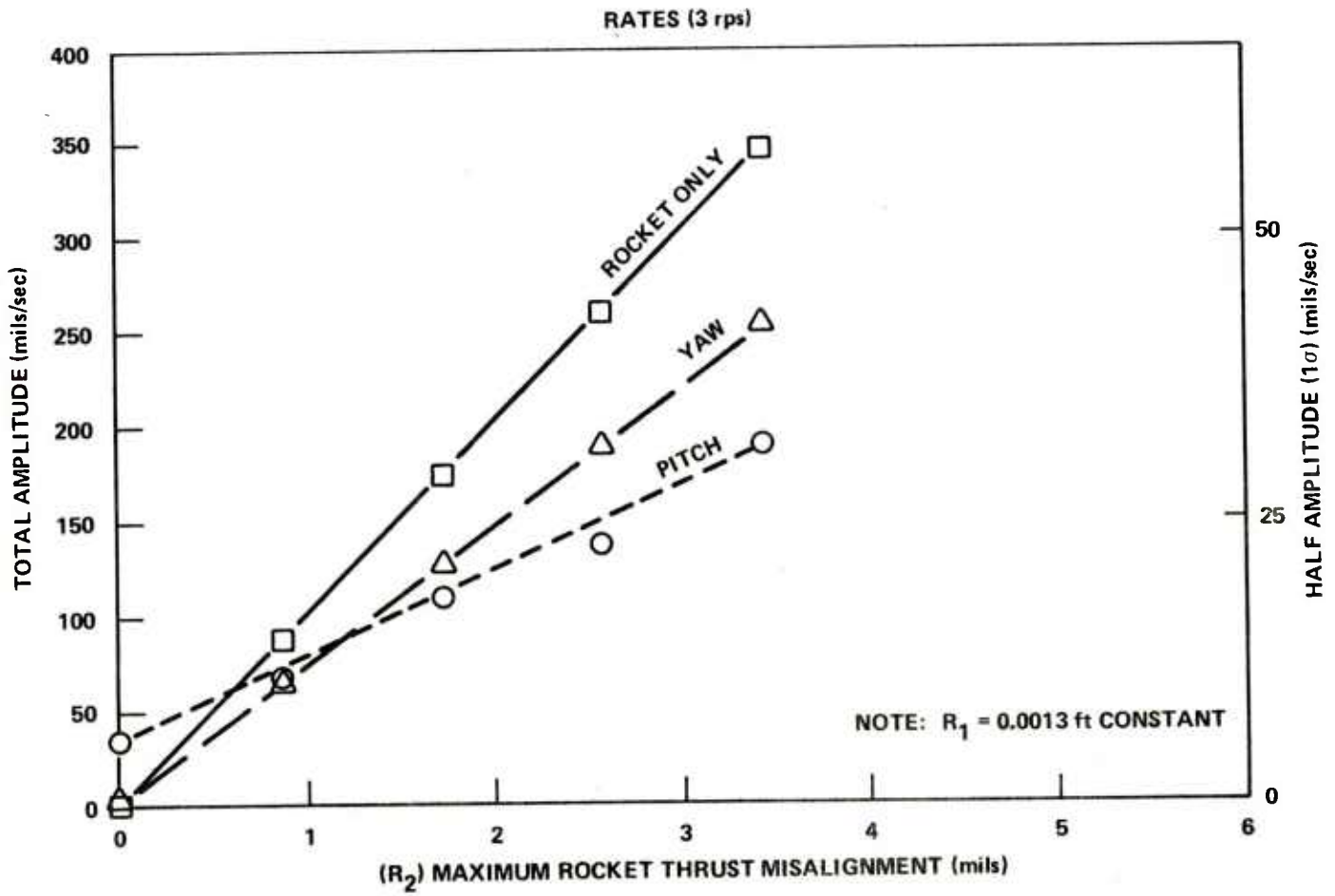

Figure 31. Rocket rate motion at tube exit versus maximum rocket thrust misalignment.

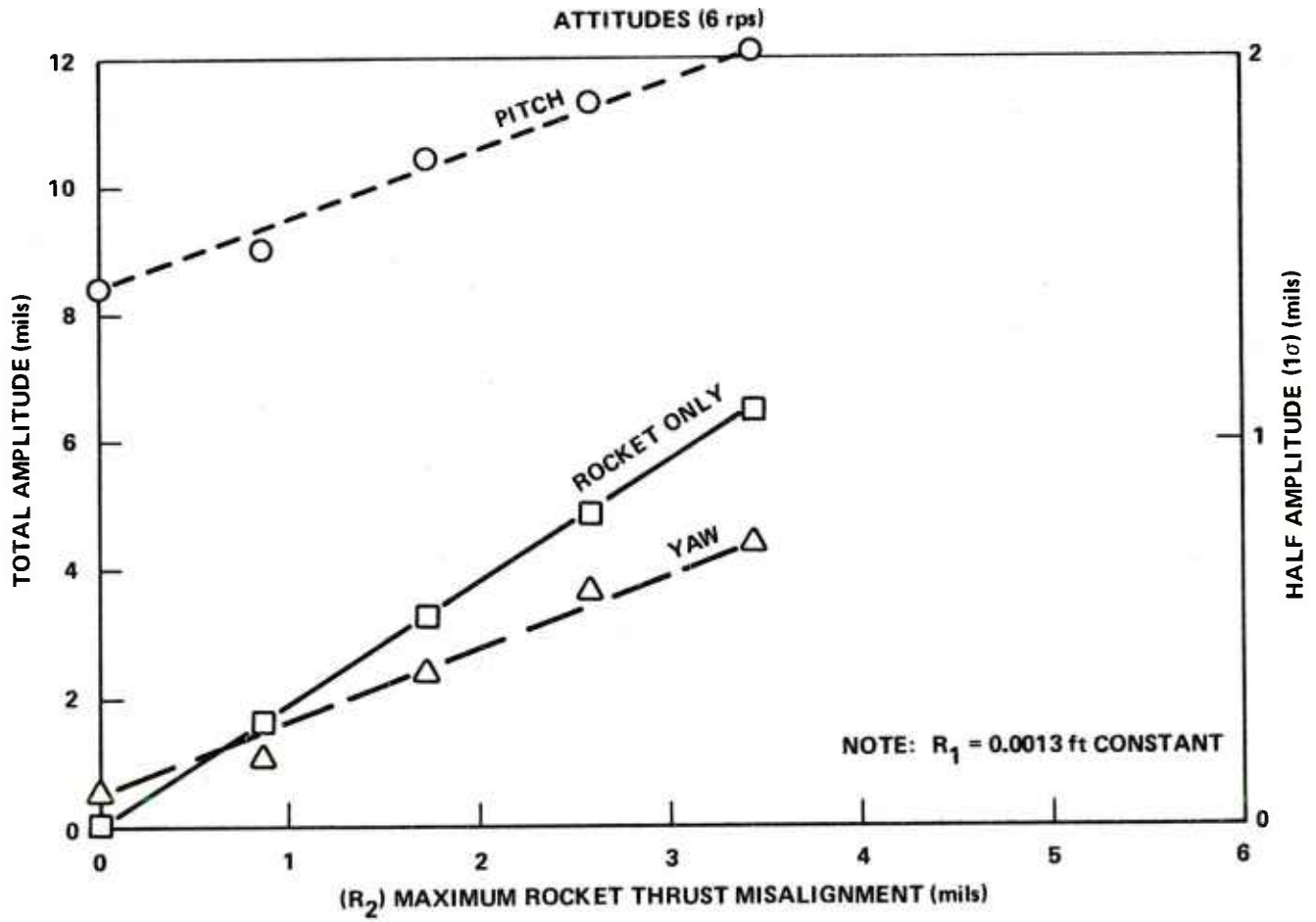

Figure 32. Rocket attitude motion at tube exit versus maximum rocket thrust misalignment.

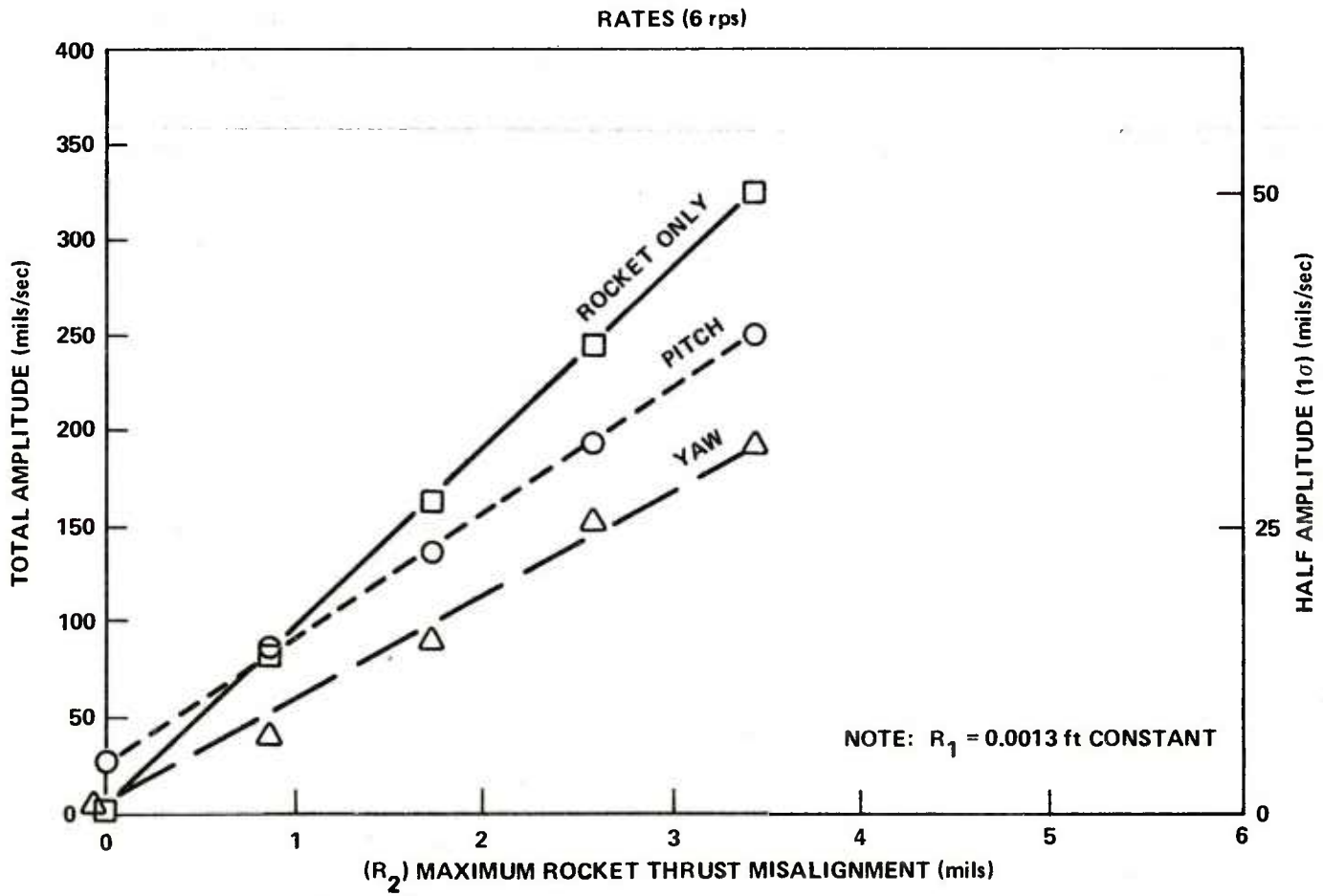

Figure 33. Rocket rate motion at tube exit versus maximum rocket thrust misalignment.

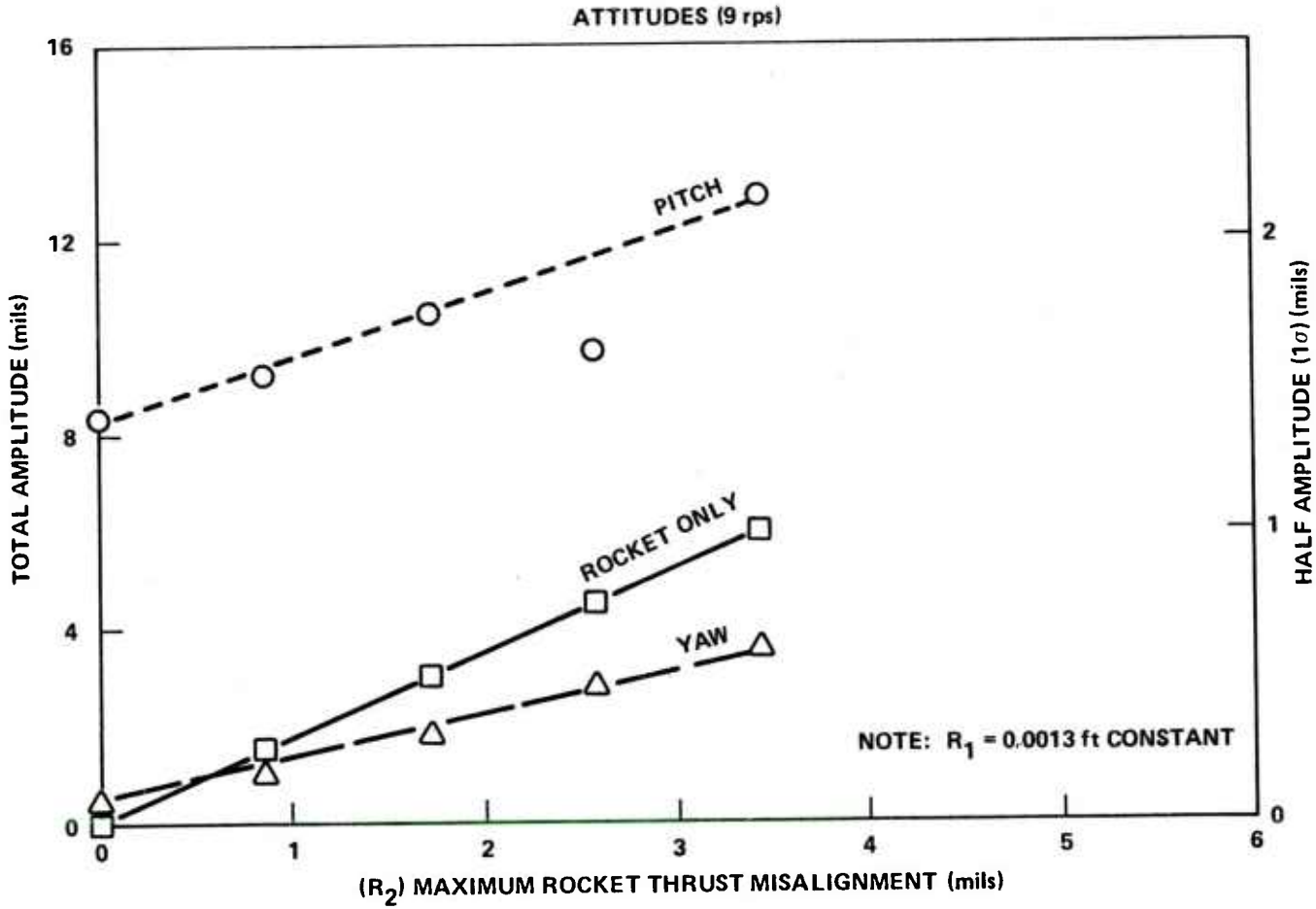

Figure 34. Rocket attitude motion at tube exit versus maximum rocket thrust misalignment.

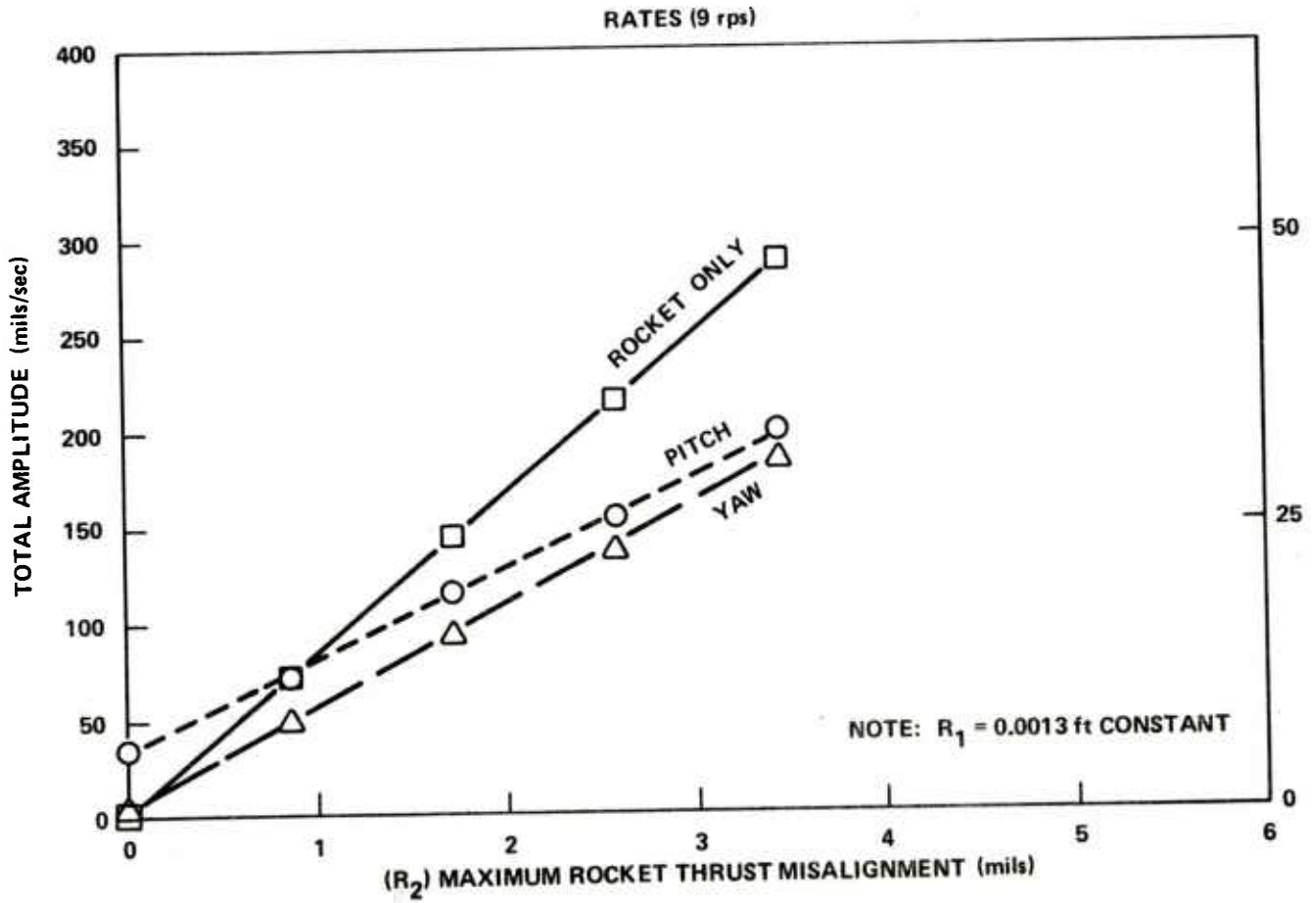

Figure 35. Rocket rate motion at tube exit versus maximum rocket thrust misalignment.

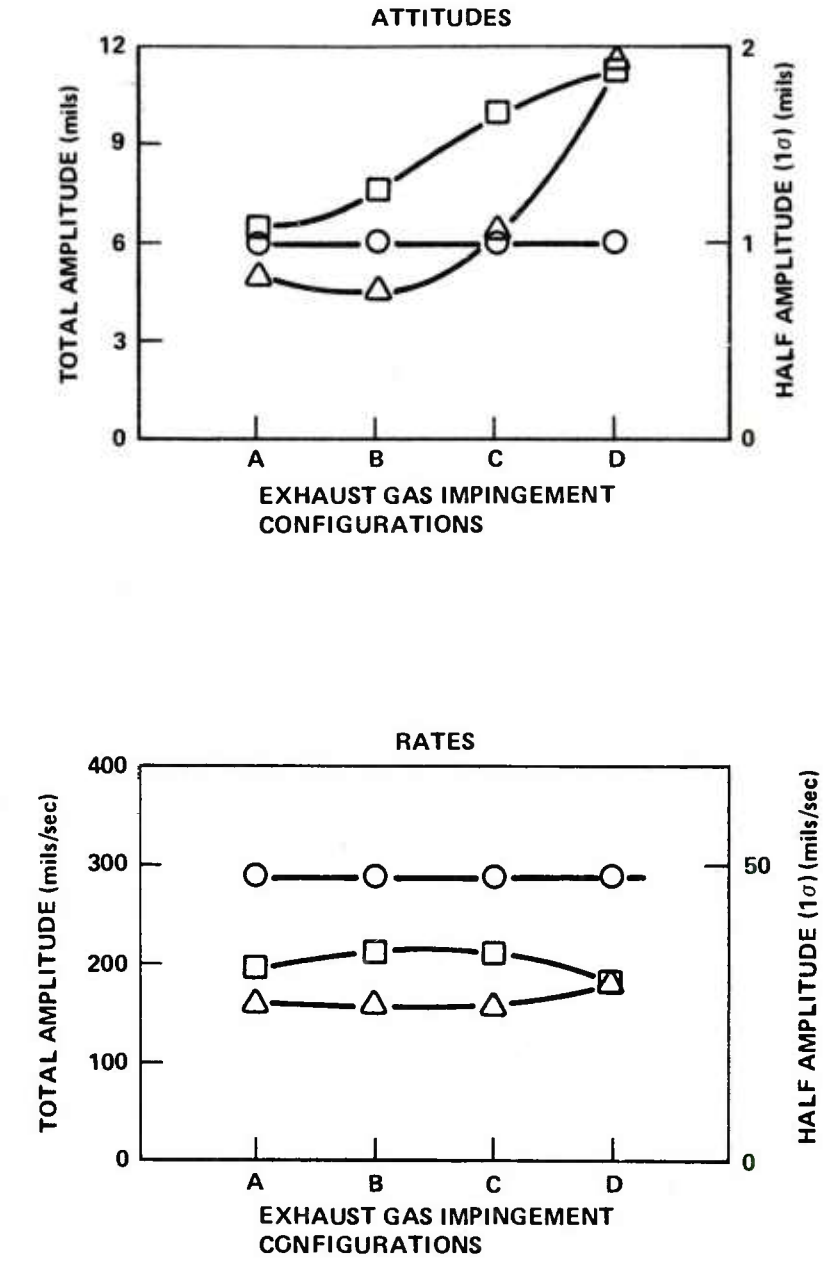

Figure 36. Rocket pitch motion at tube exit versus exhaust gas impingement configurations.

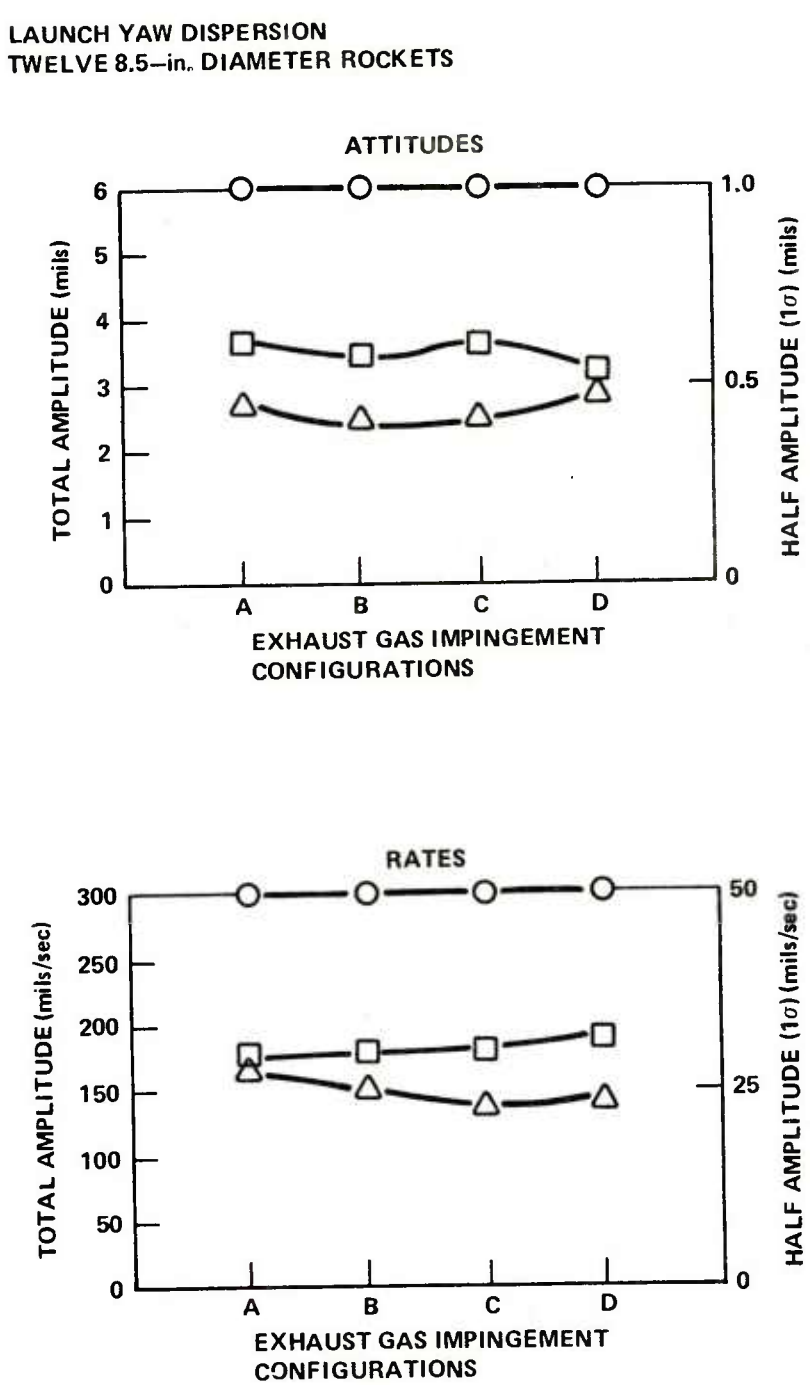

Figure 37. Rocket yaw motion at tube exit versus exhaust gas impingement configurations.

REFERENCES

1. Christensen, D. E., Multiple Rocket Launcher Characteristics and Simulation Technique, US Army Missile Command, Redstone Arsenal, Alabama, February 1976, Technical Report RL-76-11.

2. Cochran, John E., Jr., Investigation of Factors Which Contribute to Mallaunch of Free Rockets, US Army Missile Command, Redstone Arsenal, Alabama, October 1975, Technical Report RL-CR-76-4.

3. Cochran, John E., Jr., Investigation of Factors Which Contribute to Mallaunch of Free Rockets, Engineering Experiment Station, Auburn University, Auburn, Alabama, 30 January 1976.

4. Wempner, G. A. and Wilms, E. V., Multi-Rail Launcher with Six Degrees of Freedom, Final Technical Report on Contract DA-01-021-AMC-14042(Z), University of Alabama Research Institute, Huntsville, Alabama, September 1966.

5. Booker, David L., Christensen, D. E., and Rausch, R. L., Preliminary Analysis for the SAM-D Launcher, US Army Missile Command, Redstone Arsenal, Alabama, June 1971, Report No. RL-TN-71-3.

6. Campbell, B. H., Christensen, D. E., Green, P. L., and Hiatt, F. L., Progress Report, Study on Launcher/Sight Slaved, US Army Missile Command, Redstone Arsenal, Alabama, August 1969, Report No. RL-TN-69-6.

7. Christensen, D. E. and Goodson, F. D., Single Degree of Freedom Launcher Model for Lance, US Army Missile Command, Redstone Arsenal, Alabama, March 1963, Report No. RL-TN-63-3.

Appendix A. EQUATIONS OF MOTION

1. Pitch plane equations of motion

A. Case I: Rocket constrained on the launcher ($\theta = \phi$)

$$I_{L_Z}\ddot{\phi} + (d_1 + d_2 + d_7 + x)F_1 + (d_7 + x)F_2 + K(\phi - \eta) + C(\dot{\phi} - \dot{\eta}) - M_E + M_W - a_2(a_1 \cos \xi - b_1 \sin \xi)(\ddot{\eta} + \dot{\eta}^2)m_{pod} + b_2(a_1 \sin \xi + b_1 \cos \xi)(\ddot{\eta} - \dot{\eta})^2 m_{pod} = 0 \quad \text{(A-1)}$$

$$I_B \ddot{\eta} - K(\phi - \eta) - C(\dot{\phi} - \dot{\eta}) + K_B\eta + C_B\dot{\eta} - M'_E + M'_W + m_p(a_1 \sin \xi + b_1 \cos \xi)^2 (\ddot{\eta} - \dot{\eta}^2) + m_p(a_1 \cos \xi - b_1 \sin \xi)^2 (\ddot{\eta} + \dot{\eta}^2) = 0 \quad \text{(A-2)}$$

$$I_{m_z}\ddot{\theta} - d_1F_1 + d_2F_2 + (r_2 - r_1)\tau \cos \gamma - d_3F_7 = 0 \quad \text{(A-3)}$$

$$m\ddot{x} - \tau + W \sin \xi - F_7 = 0 \quad \text{(A-4)}$$

$$m(d_7 + x)\ddot{\phi} + m\, d_2\, \ddot{\theta} + m\, \phi\, \ddot{x} + 2\, m\, \dot{x}\, \dot{\phi} - m(a_1 \cos \xi - b_1 \sin \xi)\ddot{\eta} + m\, r_1\, \dot{\gamma}^2 \cos \gamma - F_1 - F_2 + W \cos \xi - \tau\, \theta = 0 \quad \text{(A-5)}$$

2. Yaw plane equations of motion

A. Case I: Rocket constrained on the launcher ($\psi = \lambda$)

$$I_{L_{y'}} \ddot{\lambda} + [-a_1 + (d_7 + d_1 + d_2 + X) \cos \xi - b_2 \sin \xi]F_3 + [-a_1 + (d_7 + x) \cos \xi - b_2 \sin \xi]F_4 + K_y \lambda + C_y \dot{\lambda} - M_{E_y} = 0 \qquad \text{(A-6)}$$

$$I_{m_y} \ddot{\psi} - d_1 F_3 + d_2 F_4 - (R_2 - R_1)\tau \sin \gamma - I_{m_x} \dot{\theta} \dot{\gamma} = 0 \qquad \text{(A-7)}$$

$$m[a_1 + b_2 \sin \xi - (d_7 + X) \cos \xi]\ddot{\lambda} - m d_2 \ddot{\psi} - 2m(\cos \xi)\dot{x} \dot{\lambda} + F_3 + F_4 + \tau \psi - m r_1 \dot{\gamma}^2 \sin \gamma - m(\cos \xi)\lambda \ddot{x} - m r_1 \ddot{\gamma} \cos \gamma = 0 \qquad \text{(A-8)}$$

Appendix B. POTENTIOMETER SETTINGS

TABLE B-1. POTENTIOMETER SETTINGS FOR THE 6-IN. DIAMETER ROCKET SIMULATION

Concepts - 6-in.-Diameter Rocket		Nominal	
Description	Potentiometer	Setting	Gain
Bias (center)	Q 02		
Amplitude (±9 V)	Q 04		
	Q 07		
	Q 09		
	Q 12		
	Q 14		
	Q 17		
	Q 19		
	Q 22		
	Q 24		
	Q 27		
	Q 29		
d_9, lateral rocket offset in the pod (max ÷ 3)	P 00	0.9999	1
$(d_1 + d_2 + d_7)$ ÷ 0.01	P 01	0.0600	1
10/mass of missile	P 02	0.1840	10
d_9 (min ÷ 3)	P 03	0.3333	1
0.01 × max flight distance	P 04	0.9000	Comp.
d_9 (intermediate ÷ 3)	P 05	0.6666	1
Adjust to balance initial conditions	P 06	0.0794	IC
(SF)	P 07	0.0100	10
$C_n \times 10^{-6}$ $C_B \times 10^{-6}$	P 08	0.0068	10
0.01 × distance of max exhaust imping.	P 09	0.2500	Comp.
(SF)	P 10	0.1000	1
$\dot{}_0$ - adjust to balance IC	P 11	0.0699	IC
(SF)	P 12	0.1000	1
(SF)	P 13	0.0400	1
0.01 × guidance length 0.01 × d_5	P 14	0.0400	Comp.
0.01 a_1	P 15	0.0600	1
$\dot{}_0$ (scales ○ to ◇) (SF)	P 16	0.5000	IC
(SF)	P 17	0.2000	1
(SF)	P 18	0.5000	10
0.01 × camera distance	P 19	0.0900	Comp.
1 - $(0.5\Delta I_{Ly}/\Delta W_{TP}) \times 0.0001 W_{TP}$; I_{Ly}(max - 20K slug-ft^2)	P 20	0.2369	1

TABLE B-1. (Continued)

Concepts – 6-in. Diameter Rocket		Nominal	
Description	Potentiometer	Setting	Gain
$1 - (0.5\Delta I_{Ly}/\Delta W_{TP}) \times 0.0001 W_{TP}$; I_{Ly}(min - 16.6 K slug-ft^2)	P 21	0.7844	1
	P 22	0.0707	1
	P 23	0.7070	1
	P 24		
(SF)	P 25	0.4000	1
$0.4 M_{rocket}$ (Coriolis term)	P 26	0.2174	10
ψ_0 scale ψ to λ (SF)	P 27	0.0500	IC
(SF)	P 28	0.5000	10
0.01 × guidance length (tipoff) tube length	P 29	0.0900	Comp.
$10^{-4} \times \tau_{max}$/thrust risetime (0.01 sec)	P 30	0.9500	100
	P 31		
	P 32		
	P 33		
$10^{-4} \times \tau_{max}$	P 34	0.9500	Comp.
$10^{-5} I_B$	P 35	0.1970	1
$10^{-6} C_B$	P 36	0.0680	1
$10^{-7} K$	P 37	0.0758	10
$10^{-7} K_B$	P 38	0.5876	1
0.01 × X start of exhaust gas impingement	P 39	0.1000	Comp.
$2 \cdot 10^{-7} K$	P 40	0.1516	10
(SF)	P 41	0.4000	1
$2 \times 10^{-6} C$	P 42	0.0130	10
(SF)	P 43	0.1000	10
$0.02 h = 0.02(a_2 \cos \xi - b_2 \sin \xi)$	P 44	0.0141	1
(SF)	P 45	0.2000	1
$0.01 I_m$	P 46	0.3700	1
$0.2 d_2$	P 47	0.1100	10
	P 48		
$5 \times 10^{-8} Ky$	P 49	0.0987	10
(SF)	P 50	0.1500	1
(SF)	P 51	0.2500	1
(SF)	P 52	0.0100	10
$5 \times 10^{-6} Cy$	P 53	0.0625	10

TABLE B-1. (Continued)

Concepts – 6-in. Diameter Rocket		Nominal	
Description	Potentiometer	Setting	Gain
	P 54		
0.5 d_1	P 55	0.2500	1
(SF)	P 56	0.2000	1
0.2 d_2	P 57	0.1100	10
0.01 I_{my}	P 58	0.3700	1
	P 59		
10^{-4} weight tipping parts	P 60	0.9100	IC
weight tipping parts per rocket removed	P 61	0.9999	10
$0.1(a_1 \sin \xi + b_1 \cos \xi) = 0.1(R_E - r_E)$	P 62	0.4949	1
0.1 a_1	P 63	0.6000	1
0.01 d_7	P 64	0.0000	1
Rise slope on F_E	P 65	0.0296	100
	P 66		
Decay slope on F_E	P 67	0.0168	100
	P 68		
0.01 · exhaust impingement max.	P 69	0.6000	Comp.
0.002 · I_m	P 70	0.0740	1
0.1 d_1	P 71	0.0500	1
(SF)	P 72	0.0400	1
0.04 d_2	P 73	0.0220	10
(SF)	P 74	0.0400	1
0.0002 W cos ξ	P 75	0.0247	1
0.002 m d_2	P 76	0.0597	1
(SF)	P 77	0.0100	10
(SF)	P 78	0.0400	10
	P 79		
0.1 d_1	P 80	0.0500	1
0.002 I_{my}	P 81	0.0740	1
0.04 d_2	P 82	0.0220	10
(SF)	P 83	0.0400	1
0.2 m	P 84	0.1087	10
0.02 m	P 85	0.1087	1
(SF)	P 86	0.1000	1

TABLE B-1. (Concluded)

Concepts – 6-in. Diameter Rocket		Nominal	
Description	Potentiometer	Setting	Gain
0.002 m d_2	P 87	0.0060	10
(SF)	P 88	0.0400	1
(SF)	P 89	0.1000	10
Initial Δ per row	P 90	0.9000	IC
Δ per row Pod Inertia	P 91	0.9985	10
Δ per row 0.1 r_E	P 92	0.2000	100
Zero magnitude	P 93	0.1000	1
	P 94	0.0600	1
$5 \times 10^{-5}(\pm I_{pod}$ loaded - 1 rocket)	P 95	0.7000	IC
(SF)	P 96	0.5000	1
50 R_2	P 97	0.5000	1
	P 98	0.7070	1
Initial magnitude	P 99	0.2000	1
Torque decay slope	P 100	0.3000	100
	P 101	0.0707	1
	P 102		
	P 103		
Maximum torque or thrust $\times 10^{-4}$	P 104	0.9500	Comp.
0.2 m	P 105	0.1087	10
0.4 m Coriolis acceleration	P 106	0.2174	10
Spin rate	P 107	0.1600	100
	P 108		
0.02 m	P 109	0.0011	100
	P 110		
	P 111		
	P 112		
	P 113		
TR-48 15		0.024	1
TR-48 16		0.740	1
TR-48 17		0.250	10
TR-48 05		0.375	1
TR-48 06		0.212	1
TR-48 35		0.621	1

TABLE B-2. POTENTIOMETER SETTINGS FOR THE 8.5-IN. DIAMETER ROCKET SIMULATION

Concepts – 8.5-in. Diameter Rocket		Nominal	
Description	Potentiometer	Setting	Gain
Bias (center)	Q 02		
Amplitude (±9 V)	Q 04		
	Q 07		
	Q 09		
	Q 12		
	Q 14		
	Q 17		
	Q 19		
	Q 22		
	Q 24		
	Q 27		
	Q 29		
d_9, lateral rocket offset in the pod (max ÷ 3)	P 00	0.9991	1
$(d_1 + d_2 + d_7) \times 0.01$	P 01	0.0800	1
50/mass of missile	P 02	0.3578	10
d_9 (min. ÷ 3)	P 03	0.3333	1
0.01 × max flight distance	P 04	0.8000	Comp.
d_9 (intermediate ÷ 3)	P 05	0.6666	1
Adjust to balance initial conditions	P 06	0.0376	IC
(SF)	P 07	0.0100	10
$C_n \times 10^{-6}$ $C_B \times 10^{-6}$	P 08	0.0068	10
0.01 × distance of max. exhaust impingement	P 09	0.3700	Comp.
(SF)	P 10	0.1000	1
$\dot{\theta}_0$ - adjust to balance IC	P 11	0.0105	IC
(SF)	P 12	0.1000	1
(SF)	P 13	0.0400	1
0.01 × guidance length 0.01 × d_5	P 14	0.0500	Comp.
0.01 a_1	P 15	0.0600	1
θ_0 (scales $\dot{\theta}$ to θ) (SF)	P 16	0.5000	IC
(SF)	P 17	0.2000	1
(SF)	P 18	0.5000	10
0.01 × camera distance	P 19	0.1300	Comp.
1.0 - $(0.5\Delta I_{Ly}/\Delta W_{TP}) \times 0.0001$; I_{Ly}(max - 20 K slug-ft^2)	P 20	0.3041	1

TABLE B-2. (Continued)

Concepts – 8.5-in. Diameter Rocket		Nominal	
Description	Potentiometer	Setting	Gain
1.0 - $(0.5\Delta I_{Ly}/\Delta W_{TP}) \times 0.0001$; I_{Ly}(min - 16.6 K slug-ft^2)	P 21	0.6559	1
	P 22	0.0707	1
	P 23	0.7070	1
	P 24		
(SF)	P 25	0.2000	1
0.4 M_{rocket} (Coriolis term)	P 26	0.5590	10
ψ_0 scale ψ to λ (SF)	P 27	0.0500	IC
(SF)	P 28	0.5000	10
0.01 × guidance length (tipoff) tube length	P 29	0.1300	Comp.
$2 \times 10^{-5} \times \tau_{max}$/thrust risetime	P 30	0.2720	100
	P 31		
	P 32		
	P 33		
$2 \times 10^{-5} \cdot \tau_{max}$	P 34	0.6800	Comp.
10^{-5} I_B	P 35	0.1970	1
10^{-6} C_B	P 36	0.0680	1
10^{-7} K	P 37	0.0758	10
10^{-7} K_B	P 38	0.5876	1
0.01 × X start of exhaust gas impingement	P 39	0.1400	Comp.
2×10^{-7} K	P 40	0.1516	10
(SF)	P 41	0.4000	1
2×10^{-6} C	P 42	0.0130	10
(SF)	P 43	0.1000	10
$0.02\ h = 0.02(a_2 \cos \xi - b_2 \sin \xi)$	P 44	0.0660	1
(SF)	P 45	0.1250	1
0.01 I_m	P 46	0.1800	1
0.2 d_2	P 47	0.1400	10
	P 48	0.1250	10
5×10^{-8} Ky	P 49	0.0987	10
(SF)	P 50	0.1500	1
(SF)	P 51	0.2500	1
(SF)	P 52	0.1000	1
5×10^{-6} Cy	P 53	0.0625	10

TABLE B-2. (Concluded)

Concepts - 8.5-in. Diameter Rocket		Nominal	
Description	Potentiometer	Setting	Gain
	P 54		
$0.5\ d_1$	P 55	0.5000	1
(SF)	P 56	0.1250	1
$0.2\ d_2$	P 57	0.1400	10
$0.01\ I_{my}$	P 58	0.1800	1
	P 59		
10^{-4} weight tipping parts	P 60	0.9999	IC
Δ weight tipping parts per rocket removed	P 61	0.2500	10
$0.1(a_1 \sin \xi + b_1 \cos \xi) = 0.1(R_E - r_E)$	P 62	0.5832	1
$0.1\ a_1$	P 63	0.6000	1
$0.01\ d_7$	P 64	0.0000	1
Rise slope on F_E	P 65	0.0812	100
	P 66		
Decay slope on F_E	P 67	0.0579	100
	P 68		
0.01 × exhaust impingement max.	P 69	0.7900	Comp.
$0.002 \cdot l_m$	P 70	0.3600	1
$0.1\ d_1$	P 71	0.1000	1
(SF)	P 72	0.2500	1
$0.04\ d_2$	P 73	0.0280	10
(SF)	P 74	0.0400	1
$0.0002\ W \cos \xi$	P 75	0.0636	1
$0.002\ m\ d_2$	P 76	0.1957	1
(SF)	P 77	0.0100	10
(SF)	P 78	0.2000	10
	P 79		
$0.1\ d_1$	P 80	0.1000	1
$0.002\ I_{my}$	P 81	0.3600	1
$0.04\ d_2$	P 82	0.0280	10
(SF)	P 83	0.2500	1
$0.2\ m$	P 84	0.2795	10
$0.02\ m$	P 85	0.2795	1
(SF)	P 86	0.1000	1

TABLE B-2. (Continued)

Concepts - 8.5-in. Diameter Rocket		Nominal	
Description	Potentiometer	Setting	Gain
0.002 m d_2	P 87	0.0196	10
(SF)	P 88	0.0400	1
(SF)	P 89	0.1000	10
Initial Δ per row	P 90	0.9000	IC
Δ per row — Pod Inertia	P 91	0.2500	10
Δ per row	P 92	0.2000	100
Zero magnitude	P 93	0.1000	1
0.01 a_1 — 0.1 r_E	P 94	0.0600	1
5×10^{-5} ($\pm 1_{pod}$ loaded - one rocket)	P 95	0.7910	IC
$\pm R_1 \times 40/0.9$ (source ± 0.9)	P 96	0.5778	1
$R_2 \times 40$	P 97	0.4400	1
	P 98	0.7070	1
Initial magnitude	P 99	0.7418	1
Torque decay slope	P 100	0.3000	100
	P 101	0.0707	1
	P 102		
	P 103		
Maximum torque or thrust · 10^{-4}	P 104	0.6800	Comp.
0.2 m	P 105	0.2795	10
0.4 m Coriolis acceleration	P 106	0.5590	10
Spin rate	P 107	0.2900	100
	P 108		
0.02 m	P 109	0.0028	100
	P 110		
	P 111		
	P 112		
	P 113		
TR-48 15		0.0480	1
TR-48 16		0.8200	1
TR-48 17		0.2500	10
TR-48 05		0.2368	1
TR-48 06		0.8130	1
TR-48 35		0.6211	1

Appendix C. RAW DATA TABLES AND PLOTS

TABLE C-1. 6-IN. ROCKET MOTION AT TUBE EXIT VERSUS SPIN RATE AT LAUNCH

$\dot{\gamma}$ (rps)	θ (mils)	ψ (mils)	$\dot{\theta}$ (mils/sec)	$\dot{\psi}$ (mils/sec)	K_B [(ft-lb)/rad]	C_B [(ft-lb-sec)/rad]
Tipoff						
0	2.1	2.7	90	140	5.88×10^6	6.4×10^4
3	2.1	2.9	76	154	5.88×10^6	6.4×10^4
6	1.7	3.9	102	160	5.88×10^6	6.4×10^4
9*	4.2	4.0	226	228	5.88×10^6	6.4×10^4
12	5.4	9.2	174	540	5.88×10^6	6.4×10^4
15	4.9	10.0	436	380	5.88×10^6	6.4×10^4
Nontipoff						
0	5.2	3.6	244	200	5.88×10^6	6.4×10^4
3	4.0	3.7	180	240	5.88×10^6	6.4×10^4
6	4.5	3.3	214	210	5.88×10^6	6.4×10^4
9*	4.6	3.6	222	180	5.88×10^6	6.4×10^4
12	3.4	3.7	142	200	5.88×10^6	6.4×10^4
15	4.0	3.5	164	120	5.88×10^6	6.4×10^4

*Nominal

Note: 6-in. diameter rockets; 42-round launcher; 7/row

F_E = 5000 lb

$\dot{\gamma}$ = spin rate at launch

f_{n_β} = 2.75 Hz

f_{n_L} = 3.7 Hz

f_{n_y} = 5 Hz (system yaw stiffness)

Firing interval = 0.5 sec

TABLE C-2. 6-IN. ROCKET MOTION AT TUBE EXIT VERSUS VEHICLE PITCH FREQUENCY ABOUT THE PIVOT

f_{n_B} (Hz)	θ (mils)	ψ (mils)	$\dot{\theta}$ (mils/sec)	$\dot{\psi}$ (mils/sec)	K_B [(ft-lb)/rad]	C_B [(ft-lb-sec)/rad]
Tipoff						
1	12.4	3.46	262	224	0.78×10^6	2.48×10^4
2	6	3.92	236	221	3.11×10^6	4.95×10^4
2.75*	4.2	4.0	226	228	5.88×10^6	6.40×10^4
3.5	4.2	4.0	204	233	9.53×10^6	8.67×10^4
5	3.75	3.92	201	220	19.44×10^6	12.38×10^4
Nontipoff						
1	13.6	3.36	230	185	0.78×10^6	2.48×10^4
2	6.8	3.48	187	182	3.11×10^6	4.95×10^4
2.75*	4.6	3.6	222	180	5.88×10^6	6.40×10^4
3.5	4.83	3.54	217	180	9.53×10^6	8.67×10^4
5	4.6	3.5	222	183	19.44×10^6	12.38×10^4

*Nominal

Note: 6-in. diameter rockets; 42-round launcher; 7/row

F_E = 5000 lb

$\dot{y}$ = 9 Hz

f_{n_B} = natural frequency of base or vehicle

f_{n_L} = 3.7 Hz

f_{n_y} = 5 Hz (system yaw stiffness)

Firing interval = 0.5 sec

TABLE C-3. 6-IN. ROCKET MOTION AT TUBE EXIT VERSUS SYSTEM YAW NATURAL FREQUENCY

f_{n_y} (Hz)	θ (mils)	ψ (mils)	$\dot{\epsilon}$ (mils/sec)	$\dot{\psi}$ (mils/sec)	K_y [(ft-lb)/rad]	C_y [(ft-lb-sec)/rad]
Tipoff						
1	4.2	13.6	223	570	0.79×10^6	0.25×10^5
2	4.2	5.2	230	179	3.15×10^6	0.50×10^5
3	4.2	4.7	252	186	7.11×10^6	0.75×10^5
4	4.2	4.4	224	176	12.63×10^6	1.00×10^5
5*	4.2	4.7	212	203	19.74×10^6	1.26×10^5
6	4.2	4.2	211	177	28.42×10^6	1.51×10^5
Nontipoff						
1	4.6	11.0	234	330	0.79×10^6	0.25×10^5
2	4.6	5.3	228	205	3.15×10^6	0.50×10^5
3	4.6	4.1	232	191	7.11×10^6	0.75×10^5
4	4.6	3.7	230	181	12.63×10^6	1.00×10^5
5*	4.6	4.0	240	180	19.74×10^6	1.26×10^5
6	4.6	3.7	241	178	28.42×10^6	1.51×10^5

*Nominal

Note: 6-in. diameter rockets; 42-round launcher; 7/row

F_E = 5000 lb

$\dot{\gamma}$ = 9 Hz

f_{n_B} = 2.75 Hz

f_{n_L} = 3.7 Hz

Firing interval = 0.5 sec

TABLE C-4. 6-IN. ROCKET MOTION AT TUBE EXIT VERSUS LAUNCHER PITCH NATURAL FREQUENCY

f_{n_L} (Hz)	θ (mils)	ψ (mils)	$\dot{\theta}$ (mils/sec)	$\dot{\psi}$ (mils/sec)	K_B [(ft-lb)/rad]	C_B [(ft-lb-sec)/rad]
Tipoff						
1.5	4.5	4.0	202	235	1.24×10^6	2.64×10^4
2.5	4.0	4.0	219	228	3.45×10^6	4.40×10^4
3.7*	3.5	4.0	202	206	7.57×10^6	6.51×10^4
5.0	3.9	4.0	241	206	13.82×10^6	8.80×10^4
Nontipoff						
1.5	7.6	3.6	275	184	1.24×10^6	2.64×10^4
2.5	5.9	3.6	245	185	3.45×10^6	4.40×10^4
3.7*	5.2	3.6	242	180	7.57×10^6	6.51×10^4
5.0	5.0	3.6	242	180	13.82×10^6	8.80×10^4

*Nominal

Note: 6-in. diameter rockets; 42-round launcher; 7/row

F_E = 5000 lb

$\dot{\gamma}$ = 9 Hz

f_{n_B} = 2.75 Hz

f_{n_L} = launcher to vehicle natural frequency (loaded)

f_{n_y} = 5 Hz

Firing interval = 0.5 sec

TABLE C-5. 6-IN. ROCKET MOTION AT TUBE EXIT VERSUS MASS OFFSET AND THRUST MISALIGNMENT

r_1 and r_2 (%)	θ (mils)	ψ (mils)	$\dot{\theta}$ (mils/sec)	$\dot{\psi}$ (mils/sec)	Max. r_1 and r_2 (mils)
Tipoff					
100*	3.7	3.7	213	230	3.4
80	3.6	3.0	202	190	2.72
60	2.4	3.0	150	163	2.04
30	2.2	2.71	100	122	1.0
0	1.3	2.16	50	96	0
Nontipoff					
100*	4.9	3.3	207	150	3.4
80	4.3	3.0	176	152	2.72
60	3.5	2.3	138	114	2.04
30	2.3	1.63	72	64	1.0
0	1.4	0.77	75	15	0

*Nominal

Note: 6-in. diameter rockets; 42-round launcher; 7/row

F_E = 5000 lb

$\dot{\gamma}$ = 9 Hz

f_{n_B} = 2.75 Hz

f_{n_L} = 3.7 Hz

f_{n_y} = 5 Hz

Firing interval = 0.5 sec

TABLE C-6. 6-IN. ROCKET MOTION AT TUBE EXIT VERSUS FIRING INTERVAL

Tipoff						
Δt (sec)	θ (mils)	$\dot{\theta}$ (mils)	ψ (mils/sec)	$\dot{\psi}$ (mils/sec)	K_B [(ft-lb)/rad]	C_B [(ft-lb-sec)/rad]
0.3	4.8	250	6.20	228	5.88×10^6	6.4×10^4
0.5*	4.1	239	3.40	228	5.88×10^6	6.4×10^4
0.7	4.2	247	2.51	228	5.88×10^6	6.4×10^4
1.0	4.4	236	2.33	228	5.88×10^6	6.4×10^4
1.5	7.7	256	2.27	228	5.88×10^6	6.4×10^4
2.0	4.7	251	2.16	228	5.88×10^6	6.4×10^4
2.5	5.9	258	2.20	228	5.88×10^6	6.4×10^4
3.0	5.0	239	2.20	228	5.88×10^6	6.4×10^4
Nontipoff						
0.3	6.0	227	4.20	180	5.88×10^6	6.4×10^4
0.5*	5.2	220	3.50	180	5.88×10^6	6.4×10^4
0.7	4.8	230	2.96	180	5.88×10^6	6.4×10^4
1.0	5.2	229	2.87	180	5.88×10^6	6.4×10^4
1.5	7.7	230	2.90	180	5.88×10^6	6.4×10^4
2.0	4.5	220	2.84	180	5.88×10^6	6.4×10^4
2.5	6.0	221	2.85	180	5.88×10^6	6.4×10^4
3.0	6.3	225	2.82	180	5.88×10^6	6.4×10^4

*Nominal

Note: 6-in. diameter rockets; 42-round launcher; 7/row

F_E = 5000 lb

$\dot{y}$ = 9 Hz

f_{n_B} = 2.75 Hz

f_{n_L} = 3.7 Hz

f_{n_y} = 5 Hz

Δt = firing interval in sec

TABLE C-7. 8.5-IN. ROCKET MOTION AT TUBE EXIT VERSUS SPIN RATE AT LAUNCH

Tipoff						
$\dot{\gamma}$ (rps)	θ (mils)	ψ (mils)	$\dot{\theta}$ (mils/sec)	$\dot{\psi}$ (mils/sec)	K_B [(ft-lb)/rad]	C_B [(ft-lb-sec)/rad]
0	3.4	1.18	72	46	5.88×10^6	6.4×10^4
3	3.8	1.60	87	80	5.88×10^6	6.4×10^4
6	4.1	4.9	92	131	5.88×10^6	6.4×10^4
9*	5.4	2.45	154	148	5.88×10^6	6.4×10^4
12	4.5	7.2	105	333	5.88×10^6	6.4×10^4
15	7.0	8.1	304	188	5.88×10^6	6.4×10^4
Nontipoff						
0	6.2	3.7	262	202	5.88×10^6	6.4×10^4
3	5.1	5.0	195	251	5.88×10^6	6.4×10^4
6	6.7	9.8	227	228	5.88×10^6	6.4×10^4
9*	7.7	3.5	228	181	5.88×10^6	6.4×10^4
12	5.2	4.3	153	193	5.88×10^6	6.4×10^4
15	5.4	2.8	170	87	5.88×10^6	6.4×10^4

*Nominal

Note: 8.5-in. diameter rockets; 12-round launcher; 6/row

F_E = 5000 lb

$\dot{\gamma}$ = spin rate at launch

f_{n_B} = 2.75 Hz

f_{n_L} = 3.5 Hz

f_{n_y} = 5 Hz

Firing interval = 1 sec

TABLE C-8. 8.5-IN. ROCKET MOTION AT TUBE EXIT VERSUS VEHICLE PITCH FREQUENCY ABOUT THE PIVOT

f_{n_B} (Hz)	θ (mils)	ψ (mils)	$\dot{\theta}$ (mils/sec)	$\dot{\psi}$ (mils/sec)	K_B [(ft-lb)/rad]	C_B [(ft-lb-sec)/rad)]
Tipoff						
1	2.7	2.45	470	148	0.78×10^6	2.48×10^4
2	5.9	2.45	170	148	3.11×10^6	4.95×10^4
2.75*	5.7	2.45	190	148	5.88×10^6	6.40×10^4
3.5	8.5	2.45	240	148	9.53×10^6	8.67×10^4
5	5.2	2.45	210	148	19.44×10^6	12.38×10^4
Nontipoff						
1	25.5	3.5	370	181	0.78×10^6	2.48×10^4
2	5.8	3.5	195	181	3.11×10^6	4.95×10^4
2.75*	6.7	3.5	205	181	5.88×10^6	6.40×10^4
3.5	6.3	3.5	195	181	9.53×10^6	8.67×10^4
5	7.2	3.5	205	181	19.44×10^6	12.38×10^4

*Nominal

Note: 8.5-in. diameter rockets; 12-round launcher; 6/row

F_E = 5000 lb

f_y = 9 Hz

f_{n_B} = natural frequency of base or vehicle

f_{n_L} = 3.5 Hz

f_{n_y} = 5 Hz

Firing interval = 1 sec

TABLE C-9. 8.5-IN. ROCKET MOTION AT TUBE EXIT VERSUS LAUNCHER PITCH NATURAL FREQUENCY

f_{n_L} (Hz)	θ (mils)	ψ (mils)	$\dot{\theta}$ (mils/sec)	$\dot{\psi}$ (mils/sec)	K_B [(ft-lb)/rad]	C_B [(ft-lb-sec)/rad]
Tipoff						
1.5	13	2.45	400	148	1.42×10^6	3.02×10^4
2.5	6.2	2.45	254	148	3.95×10^6	5.03×10^4
3.5*	6	2.45	200	148	7.74×10^6	7.04×10^4
5	6.8	2.45	220	148	15.79×10^6	10.05×10^4
Nontipoff						
1.5	10.8	3.5	210	181	1.42×10^6	3.02×10^4
2.5	6.4	3.5	270	181	3.95×10^6	5.03×10^4
3.5*	6.4	3.5	180	181	7.74×10^6	7.04×10^4
5	6.8	3.5	185	181	15.79×10^6	10.05×10^4

*Nominal

Note: 8.5-in. diameter rocket; 12-round launcher; 6/row

F_E = 5000 lb

$\dot{\gamma}$ = 9 Hz

f_{n_B} = 2.75 Hz

f_{n_L} = launcher to vehicle natural frequency (loaded)

f_{n_y} = 5 Hz

Firing interval = 1 sec

TABLE C-10. 8.5-IN. ROCKET MOTION AT TUBE EXIT VERSUS DIFFERENT EXHAUST GAS IMPINGEMENT CONFIGURATIONS

F_E Pattern	θ	ψ	$\dot{\theta}$	$\dot{\psi}$
Tipoff				
A*	6.4	2.76	162	167
B	7.55	2.50	160	153
C	9.9	2.55	158	138
D	11.3	2.90	180	143
Nontipoff				
A*	5.0	3.65	195	178
B	4.6	3.45	212	180
C	6.4	3.60	211	180
D	11.7	3.20	180	190

*Nominal

Note: 8.5-in. diameter rockets; 12-round launcher; 6/row

F_{E_A} = 5000 lb
F_{E_B} = 5500 lb
F_{E_C} = 10,500 lb
F_{E_D} = 21,000 lb

} See Figure 11

$\dot{\gamma}$ = 9 Hz

f_{n_B} = 2.75 Hz

f_{n_L} = 3.5 Hz

f_{n_y} = 5 Hz

Firing interval = 1 sec

TABLE C-11. 8.5-IN. ROCKET MOTION AT TUBE EXIT VERSUS GUIDANCE LENGTH

GL (ft)	θ (mils)	ψ (mils)	$\dot{\theta}$ (mils/sec)	$\dot{\psi}$ (mils/sec)
Tipoff				
2	14.0	7.5	357	133
3	15.0	4.6	315	145
4	13.2	3.3	235	223
5*	13.0	3.5	195	200
6	10.9	3.0	163	205
Nontipoff				
2	16.4	7.5	233	166
3	12.3	5.5	245	188
4	11.6	4.6	220	190
5*	10.2	4.0	178	190
6	9.5	3.2	131	179

*Nominal

Note: 8.5-in. diameter rockets; 12-round launcher; 6/row

F_{E_D} = 21,000 lb (max)

$\dot{\gamma}$ = 9 Hz

f_{n_B} = 2.75 Hz

f_{n_L} = 3.5 Hz

f_{n_y} = 5 Hz

Firing interval = 1 sec

TABLE C-12. 8.5-IN. ROCKET MOTION AT TUBE EXIT VERSUS THRUST MISALIGNMENT WITH 0.0013-FT CONSTANT MASS OFFSET

$(R_1 + R_2)/7$ (mils)	θ (mils)	ψ (mils)	$\dot{\theta}$ (mils/sec)	$\dot{\psi}$ (mils/sec)	r_1 (ft)	r_2 (ft)
Tipoff						
0	10	0.65	110	17.5	0	0
0.86	10	0.86	115	26.3	0.0033	0.0028
1.72	10.4	0.97	134	36.7	0.0065	0.0055
2.57	10	1.22	135	49	0.0098	0.0083
3.43*	10.6	1.29	154	58	0.0130	0.011
Nontipoff						
0	8.3	0.50	34.8	5.8	0	0
0.86	9.3	1.40	89	48	0.0033	0.0028
1.72	10	2.27	152	94	0.0065	0.0055
2.57	11.4	3.06	213	138	0.0098	0.0083
3.43*	11	3.82	178	180	0.0130	0.011
Rocket Only						
0	0	0	0	0	0	0
0.86	1.72	1.72	88.8	88.8	0.0033	0.0028
1.72	3.45	3.45	177.6	177.6	0.0065	0.0055
2.57	5.15	5.15	265.4	265.4	0.0098	0.0083
3.43*	6.88	6.88	354.2	354.2	0.0130	0.011

*Nominal

Note: 8.5-in. diameter rockets; 12-round launcher; 6/row

F_E = condition D

$\dot{y}$ = 0 Hz

f_{n_B} = 2.75 Hz

f_{n_L} = 3.5 Hz

f_{n_y} = 5 Hz

Firing interval = 1 sec

TABLE C-13. 8.5-IN. ROCKET MOTION AT TUBE EXIT VERSUS THRUST MISALIGNMENT WITH 0.0013-FT CONSTANT MASS OFFSET

$(R_1 + R_2)/7$ (mils)	θ (mils)	ψ (mils)	$\dot{\theta}$ (mils/sec)	$\dot{\psi}$ (mils/sec)	r_1 (ft)	r_2 (ft)
Tipoff						
0	9.8	0.7	110	17.5	0	0
0.86	10	0.9	120	30.2	0.0033	0.0028
1.72	10.2	1.1	135	42.5	0.0065	0.0055
2.57	10.5	1.4	130	63	0.0098	0.0083
3.43*	10.9	1.4	150	77	0.0130	0.011
Nontipoff						
0	8.4	0.53	35	5.75	0	0
0.86	9.1	1.48	67	67	0.0033	0.0028
1.72	9.4	2.85	109	128	0.0065	0.0055
2.57	10.4	3.93	137	190	0.0098	0.0083
3.43*	10.6	4.00	190	255	0.0130	0.011
Rocket Only						
0	0	0	0	0	0	0
0.86	1.7	1.7	86.8	86.8	0.0033	0.0028
1.72	3.4	3.4	173.7	173.7	0.0065	0.0055
2.57	5.1	5.1	259.5	259.5	0.0098	0.0083
3.43*	6.8	6.8	346.3	346.3	0.0130	0.011

*Nominal

Note: 8.5-in. diameter rockets; 12-round launcher; 6/row

F_E = condition D

$\dot{\gamma}$ = 3 Hz

f_{n_B} = 2.75 Hz

f_{n_L} = 3.5 Hz

f_{n_y} = 5 Hz

Firing interval = 1 sec

TABLE C-14. 8.5-IN. ROCKET MOTION AT TUBE EXIT VERSUS THRUST MISALIGNMENT WITH 0.0013-FT CONSTANT MASS OFFSET

$(R_1 + R_2)/7$ (mils)	θ (mils)	ψ (mils)	$\dot{\theta}$ (mils/sec)	$\dot{\psi}$ (mils/sec)	r_1 (ft)	r_2 (ft)
Tipoff						
0	10	0.75	105	23	0	0
0.86	10	0.65	125	25	0.0033	0.0028
1.72	10	0,95	120	33	0.0065	0.0055
2.57	10.8	1.52	153	51	0.0098	0.0083
3.43*	11.1	1.60	180	60	0.0130	0.011
Nontipoff						
0	8.4	0.55	26	5.5	0	0
0.86	9	1.07	85	41	0.0033	0.0028
1.72	10.4	2.40	136	90	0.0065	0.0055
2.57	11.3	3.66	193	153	0.0098	0.0083
3.43*	12.1	4.40	250	192	0.0130	0.011
Rocket Only						
0	0	0	0	0	0	0
0.86	1.62	1.62	81.1	81.1	0.0033	0.0028
1.72	3.25	3.25	162.2	162.2	0.0065	0.0055
2.57	4.85	4.85	242.3	242.3	0.0098	0.0083
3.43*	6.48	6.48	323.4	323.4	0.0130	0.011

*Nominal

Note: 8.5-in. diameter rockets; 12-round launcher; 6/row

F_E = condition D

$\dot{\gamma}$ = 6 Hz

f_{n_B} = 2.75 Hz

f_{n_L} = 3.5 Hz

f_{n_y} = 5 Hz

Firing interval = 1 sec

TABLE C-15. 8.5-IN. ROCKET MOTION AT TUBE EXIT VERSUS THRUST MISALIGNMENT WITH 0.0013-FT CONSTANT MASS OFFSET

$(R_1 + R_2)/7$ (mils)	θ (mils)	ψ (mils)	$\dot{\theta}$ (mils/sec)	$\dot{\psi}$ (mils/sec)	r_1 (ft)	r_2 (ft)
Tipoff						
0	10.8	0.75	146	32	0	0
0.86	9.7	0.93	126	39	0.0033	0.0028
1.72	10.1	1.11	134	44	0.0065	0.0055
2.57	10.3	1.12	132	52	0.0098	0.0083
3.43*	11.3	1.44	152	71	0.0130	0.011
Nontipoff						
0	8.3	0.50	35	5.6	0	0
0.86	9.2	1.12	73	49	0.0033	0.0028
1.72	10.5	1.82	116	94	0.0065	0.0055
2.57	9.7	2.82	154	139	0.0098	0.0083
3.43*	12.9	3.60	199	186	0.0130	0.011
Rocket Only						
0	0	0	0	0	0	0
0.86	1.51	1.51	72	72	0.0033	0.0028
1.72	3.01	3.01	144	144	0.0065	0.0055
2.57	4.50	4.50	215	215	0.0098	0.0083
3.43*	6.00	6.00	287	287	0.0130	0.011

*Nominal

Note: 8.5-in. diameter rockets; 12-round launcher; 6/row

F_E = condition D

$\dot{\gamma}$ = 9 Hz

f_{n_B} = 2.75 Hz

f_{n_L} = 3.5 Hz

f_{n_y} = 5 Hz

Firing interval = 1 sec

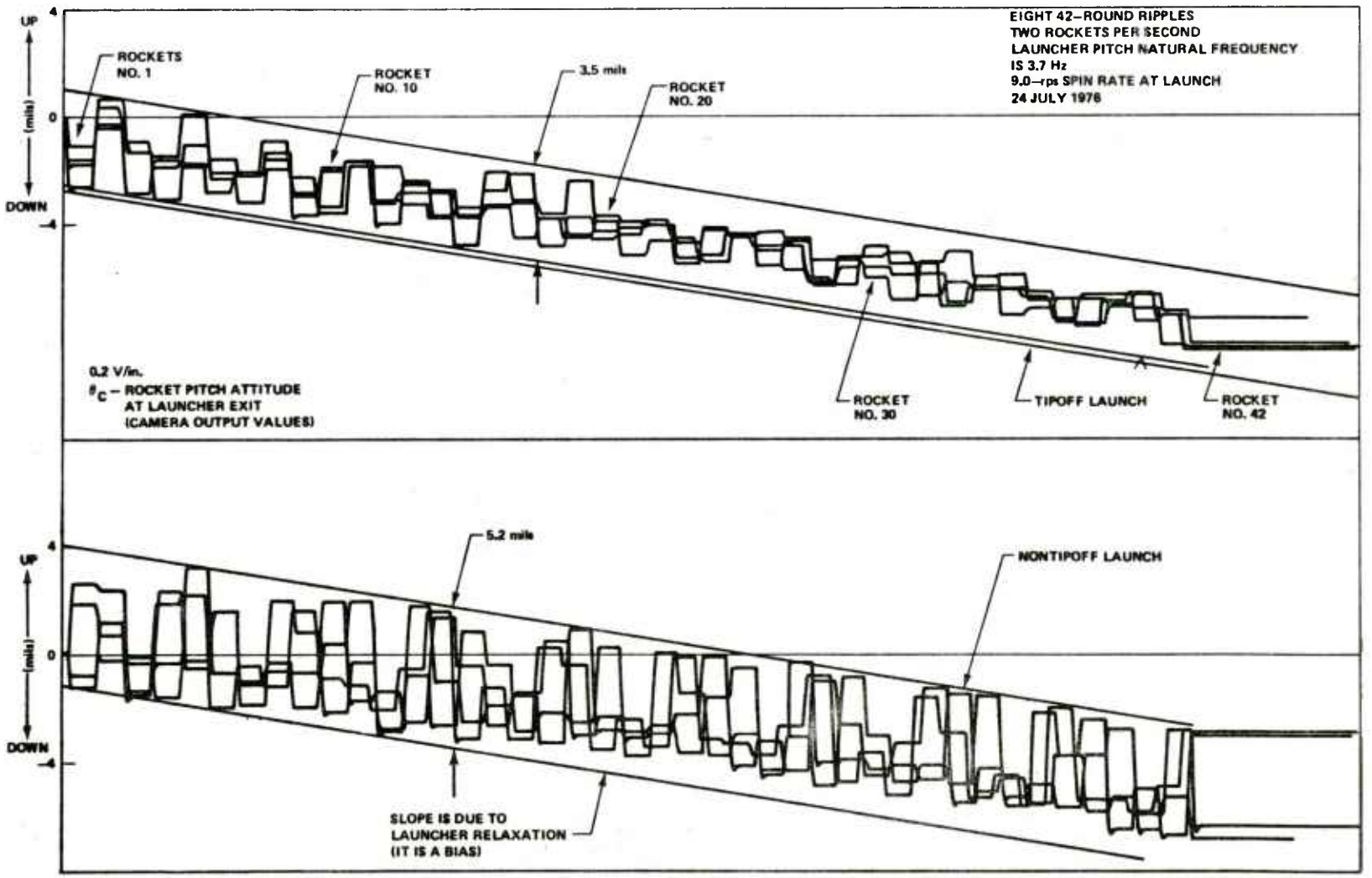
EIGHT 42–ROUND RIPPLES
TWO ROCKETS PER SECOND
LAUNCHER PITCH NATURAL FREQUENCY
IS 3.7 Hz
9.0–rps SPIN RATE AT LAUNCH
24 JULY 1976
UP
DOWN
(mils)
4
0
-4
ROCKETS NO. 1
ROCKET NO. 10
3.5 mils
ROCKET NO. 20
ROCKET NO. 30
TIPOFF LAUNCH
ROCKET NO. 42
0.2 V/in.
θ_C – ROCKET PITCH ATTITUDE AT LAUNCHER EXIT (CAMERA OUTPUT VALUES)
5.2 mils
NONTIPOFF LAUNCH
SLOPE IS DUE TO LAUNCHER RELAXATION (IT IS A BIAS)

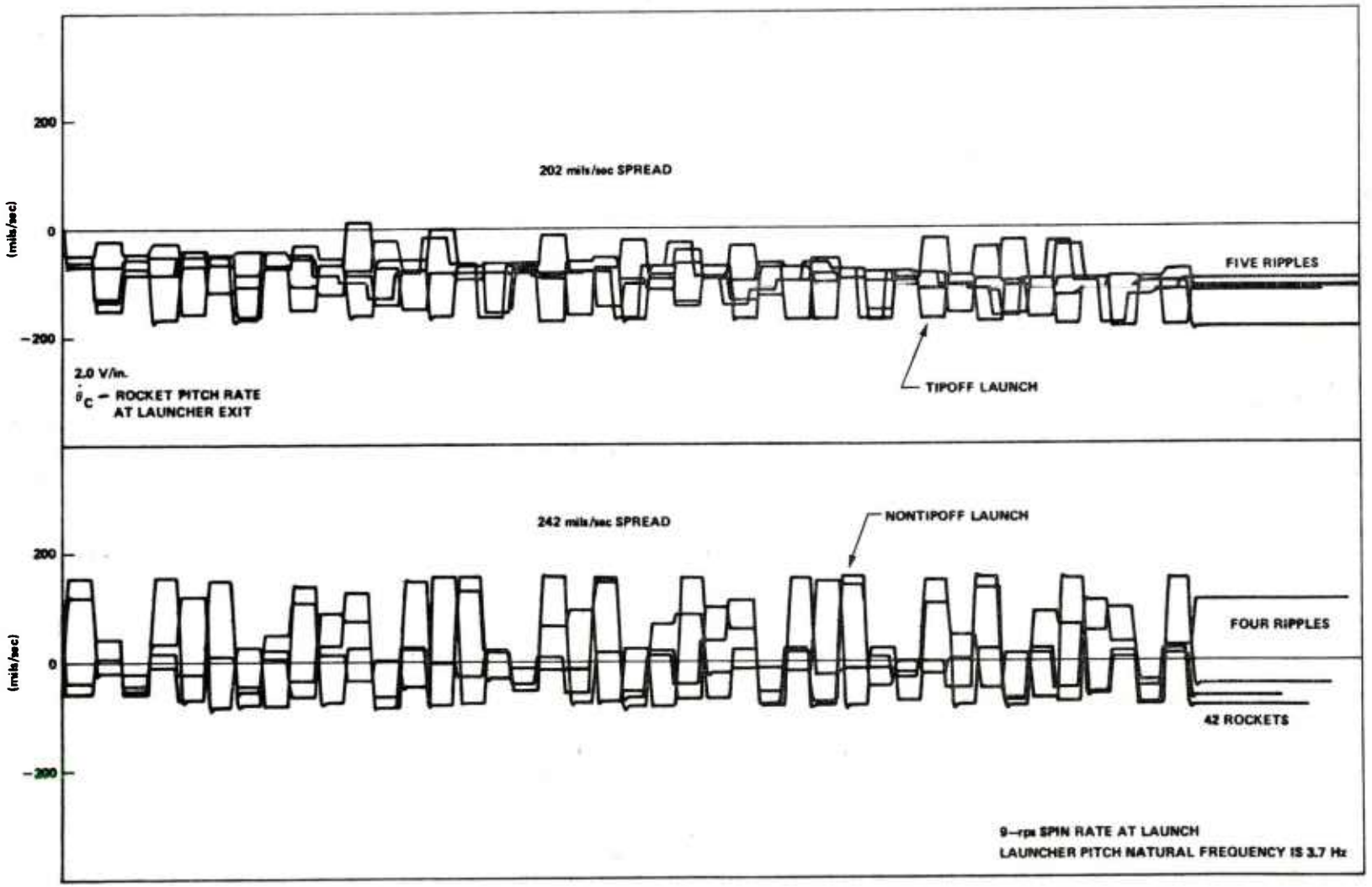
200
0
−200
(mils/sec)
202 mils/sec SPREAD
FIVE RIPPLES
2.0 V/in.
$\dot{\theta}_C$ — ROCKET PITCH RATE AT LAUNCHER EXIT
TIPOFF LAUNCH
242 mils/sec SPREAD
NONTIPOFF LAUNCH
FOUR RIPPLES
42 ROCKETS
9—rps SPIN RATE AT LAUNCH
LAUNCHER PITCH NATURAL FREQUENCY IS 3.7 Hz

Appendix D. ANALOG SCHEMATIC

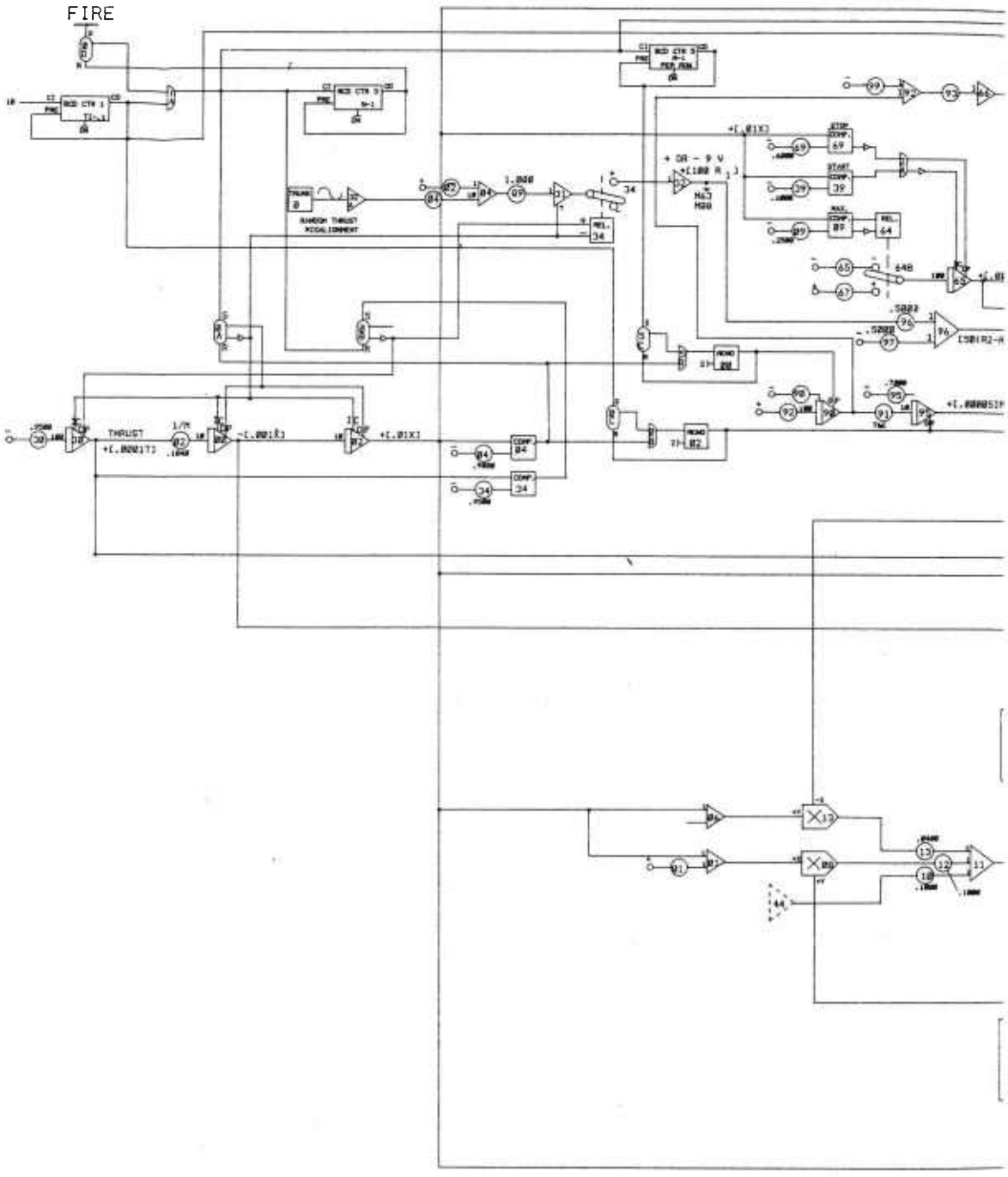
FIRE
THRUST
RANDOM THRUST
MISALIGNMENT
+ OR - 9 V
START
STOP

MULTIPLE LAUNCHING SIMULATION

REAL TIME

DRSMI-RLH 24 MAY 76

NOMINAL 42-6" DIAM BETA=1

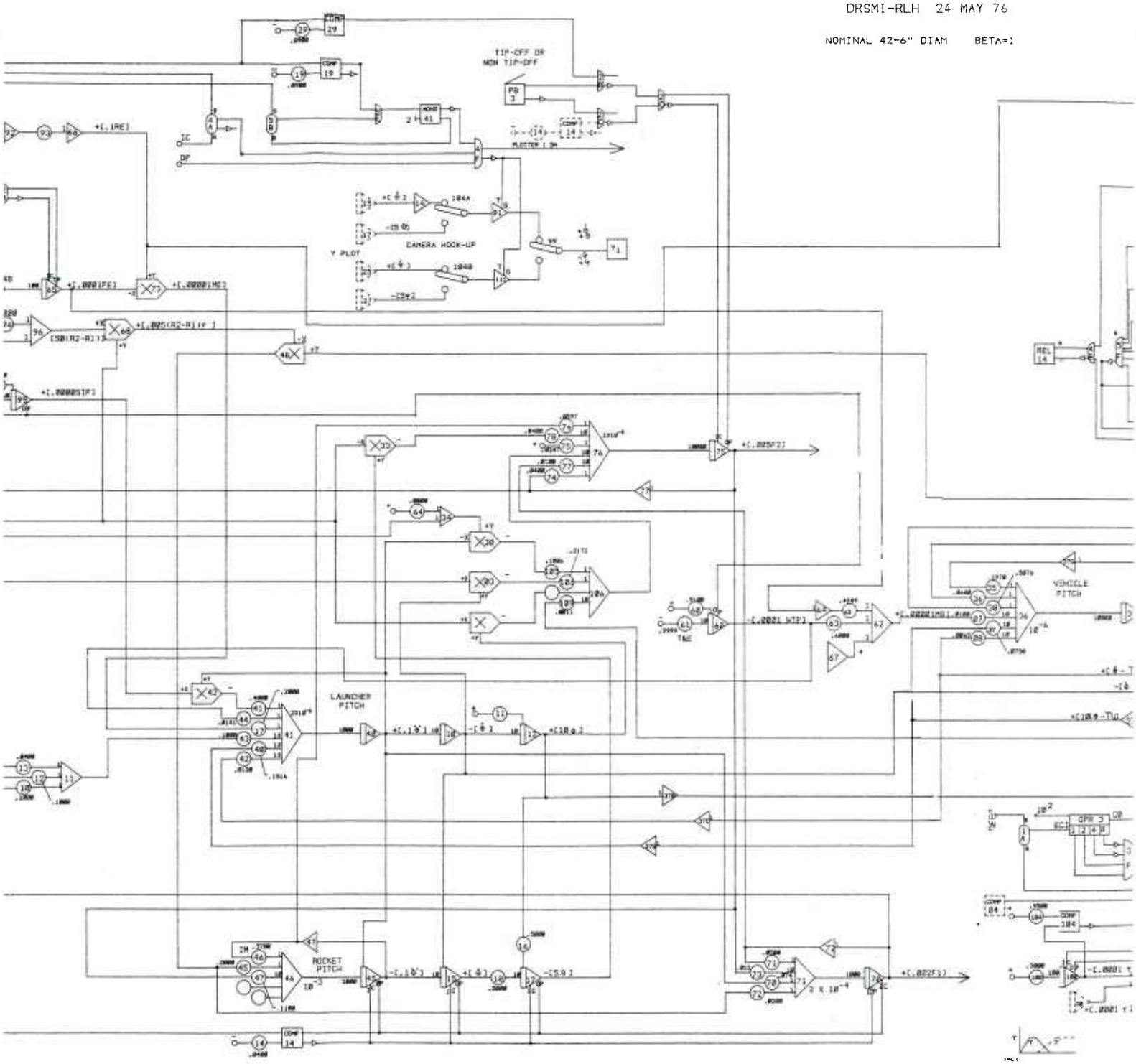

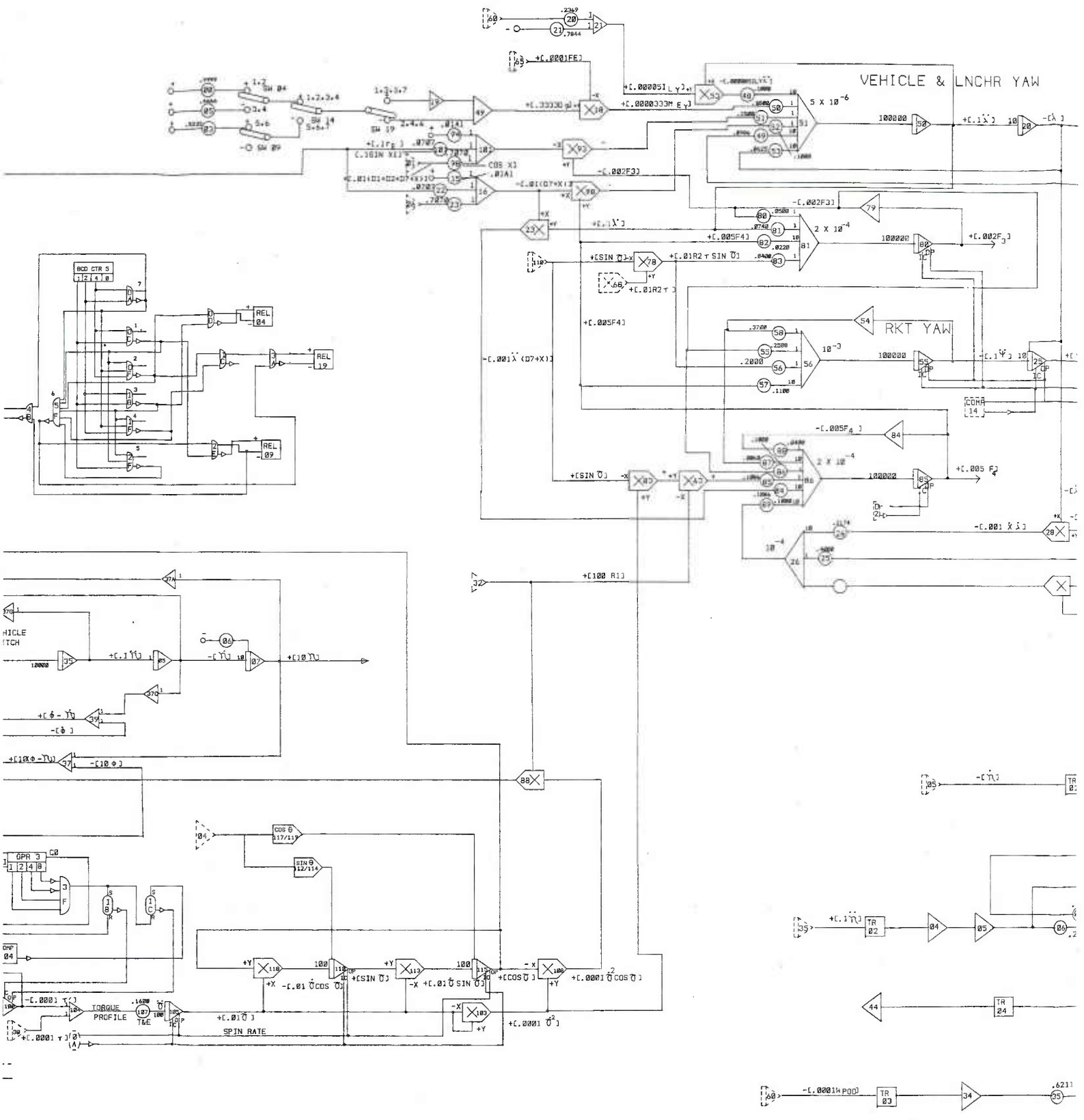
VEHICLE & LNCHR YAW
RKT YAW
BCD CTR 5
REL
SPIN RATE
TORQUE PROFILE
GPR 3
COS θ
SIN θ

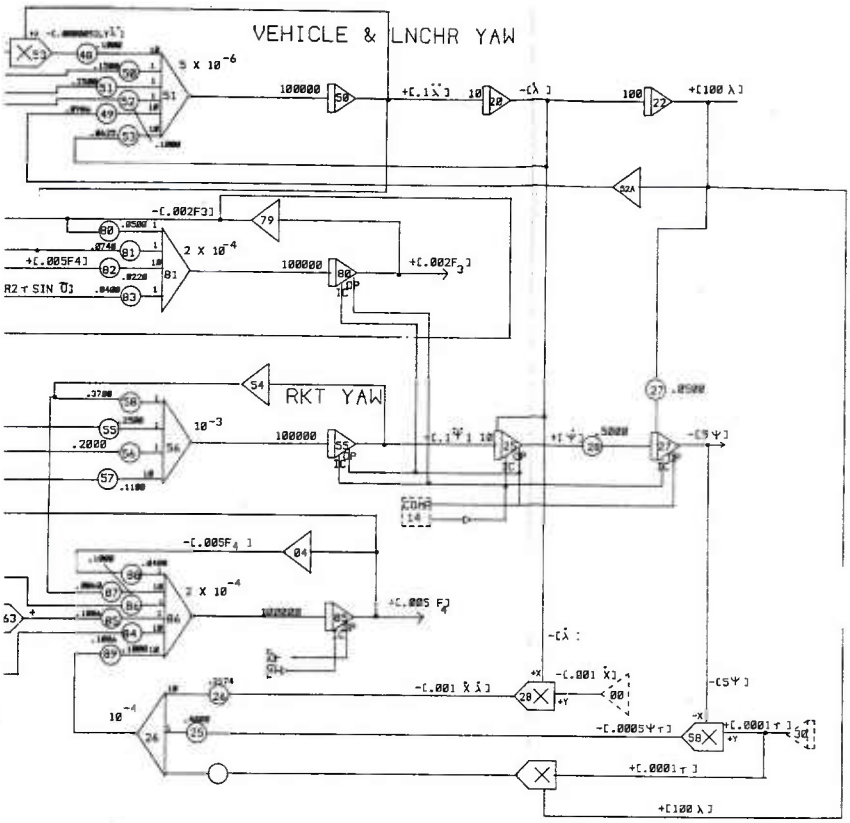

TR-48 DIAGRAM

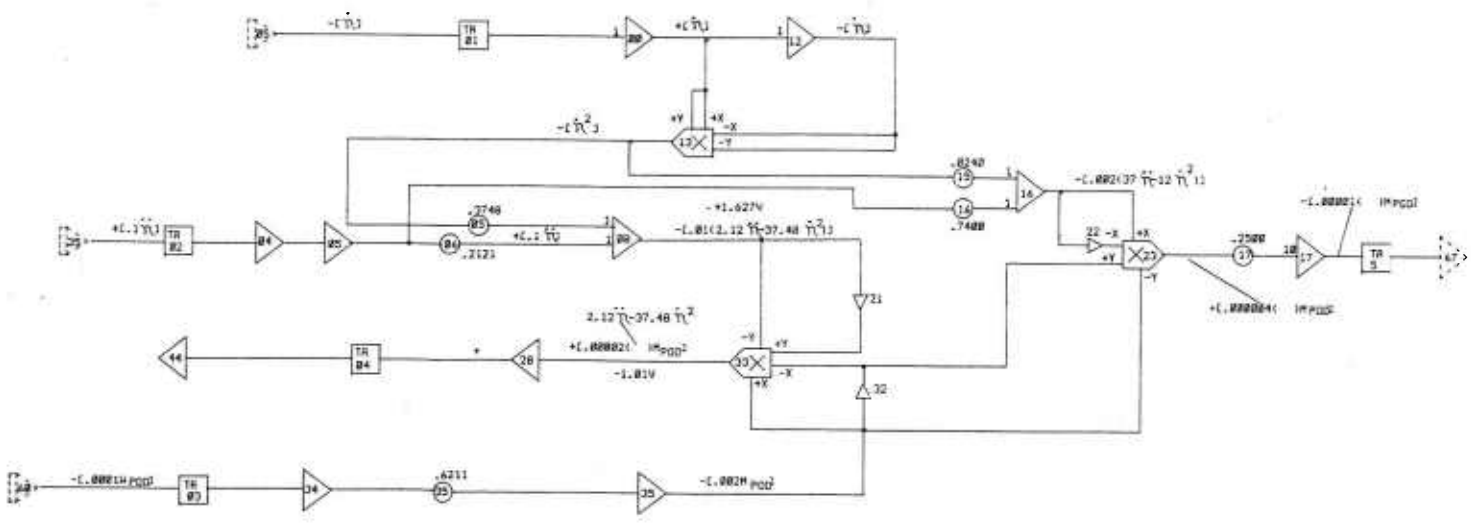

DISTRIBUTION

	No. of Copies
Defense Documentation Center Cameron Station Alexandria, Virginia 22314	12
Commander US Army Materiel Development and Readiness Command Attn: DRCRD DRCDL 5001 Eisenhower Avenue Alexandria, Virginia 22333	1 1
Commander US Army Infantry School Attn: ATSH-CD Fort Benning, Georgia 31905	1
Commander US Army Ballistic Research Laboratories Attn: AMXBR-EB Aberdeen Proving Ground, Maryland 21005	1
Headquarters Rome Air Development Center (AFSC) Attn: TLLD Griffiss Air Force Base, New York 13440	1
Commander White Sands Missile Range Attn: STEWS-AD-L White Sands Missile Range, New Mexico 88002	1
Assistant Commander US Army Armor School Attn: ATSB-CD-M Fort Knox, Kentucky 40121	1
Library US Army War College Carlisle Barracks, Pennsylvania 17103	1
Commander Edgewood Arsenal Attn: SAREA-TS-L Aberdeen Proving Ground, Maryland 21010	1

	No. of Copies
Jet Propulsion Laboratory California Institute of Technology Attn: Library/Acquisitions 111-113 4800 Oak Grove Drive Pasadena, California 91103	1
Commander US Naval Missile Center Attn: Code 5632.2 Point Mugu, California 93042	1
Commander US Army Air Defense School Attn: ATSA-CTD-MO Fort Bliss, Texas 79916	1
Technical Library Naval Ordnance Station Indian Head, Maryland 20640	1
Commander US Naval Weapons Laboratory Attn: Technical Library Dahlgren, Virginia 22448	1
Commander Rock Island Arsenal Attn: SARRI-LP-L/Technical Library Rock Island, Illinois 61201	1
Commander (Code 533) Naval Weapons Center Technical Library China Lake, California 93555	1
Commander USACACDA Fort Leavenworth, Kansas 66027	1
US Army Resarch Office Attn: Information Processing Office Box CM, Duke Station Durham, North Carolina 27706	1
Commander US Army Air Defense School Attn: ATSA-TE-CSM Fort Bliss, Texas 79916	1

	No. of Copies
Commander US Army Air Defense School Attn: ATSA-CTD-TLW Fort Bliss, Texas 79916	1
US Army Command and General Staff College Attn: ATSW-SE-L Fort Leavenworth, Kansas 66027	1
Commander US Army Aberdeen Proving Ground Attn: STEAP-TL Aberdeen Proving Ground, Maryland 21005	1
Department of the Navy Commander, Operational Test and Evaluation Force Attn: Technical Library Norfolk, Virginia 23511	1
Superior Technical Services, Inc. Attn: D. Creel 4308 Governors Drive Huntsville, Alabama 35805	1
DRCPM-LC	1
-HF	1
-ROL	1
-RK	1
-RS	1
-RSE	1
DRSMI-FR, Mr. Strickland	1
-LP, Mr. Voigt	1
DRDMI-X, Dr. McDaniel	1
-T, Dr. Kobler	1
-TL	1
-TLH	20
-TD	1
-TK	1
-C	1
-N	1
-E	1
-EA	1
-ES	1
-ET	1
-XS	1
-TBD	3
-TI (Record Set)	1
(Reference Copy)	1